

**Generation of an expression system
for human granzyme B and analysis of the
in vitro and *in vivo* efficiency**

Dissertation der Fakultät für Biologie
der Ludwig-Maximilians-Universität München
zur Erlangung des Doktorgrades der Naturwissenschaften
(Dr. rer. nat.)

vorgelegt von
Brigitte Tina Maria Doß

München 2010

Promotionsgesuch eingereicht am: 30. Juni 2010

1. Gutachter: Prof. Dr. Friederike Eckardt-Schupp

2. Gutachter: Prof. Dr. Elisabeth Weiß

Betreuer (Sondervotum): Prof. Dr. Gabriele Multhoff

Rigorosum am: 07. Dezember 2010

Ehrenwörtliche Versicherung

Ich versichere hiermit ehrenwörtlich, dass die vorgelegte Dissertation von mir selbständig und ohne unerlaubte Hilfe angefertigt ist.

München, den 30.06.2010

Brigitte Doß, Dipl.-Biochem.

Erklärung

Hiermit erkläre ich, dass die Dissertation nicht ganz oder in wesentlichen Teilen einer anderen Prüfungskommission vorgelegt ist und dass ich mich anderweitig einer Doktorprüfung ohne Erfolg nicht unterzogen habe.

München, den 30.06.2010

Brigitte Doß, Dipl.-Biochem.

**I am among those who think that science has great beauty.
A scientist in his laboratory is not only a technician:
He is also a child placed before natural phenomena which
impress him like a fairy tale.**

Marie Curie (1867 - 1934)

TABLE OF CONTENTS	5
ABBREVIATIONS	8
SUMMARY	13
ZUSAMMENFASSUNG (SUMMARY IN GERMAN)	14
1 INTRODUCTION	15
1.1. Heat Shock Protein 70 family (HSP70)	15
1.1.1 Characterization and functions	15
1.1.2 Intracellular HSP70	16
1.1.3 Extracellular HSP70	17
1.1.4 Tumor-specific Hsp70 plasma membrane localization	17
1.2 Natural killer (NK) cells	19
1.2.1 Characterization and functions	19
1.2.2 Mechanisms of target recognition	20
1.3 Granzyme B (grB)	21
1.3.1 Characterization and functions	21
1.3.2 grB mediated lysis of membrane-Hsp70 positive tumor cells	26
1.4 Aim of the study	27
2 MATERIAL AND METHODS	28
2.1 Chemicals and devices	28
2.2 Microorganisms	28
2.2.1 Bacterial strain <i>Escherichia coli</i> (<i>E. coli</i>)	28
2.2.2 Yeast strain <i>Pichia pastoris</i>	29
2.3 Cell culture and cells	29
2.3.1 Cell lines for the production of human granzyme B (grB)	30
2.3.1.1 NK cell line YT	30
2.3.1.2 Sf9 insect cells	30
2.3.1.3 Human Embryonic Kidney 293 (HEK293) cells	31
2.3.2 Target cell lines	32
2.3.2.1 Human CX+ cells	32
2.3.2.2 Human K562 cells	33
2.3.2.3 Mouse CT26 cells	33
2.3.2.4 Isolation of CD31+ endothelial mouse cells	33
2.4 Animal model	34
2.5 Molecular biology	35
2.5.1 Polymerase chain reaction (PCR)	35
2.5.2 Agarose gel electrophoresis and DNA gel extraction	36

2.5.3	Restriction digestion and ligation	37
2.5.4	Transformation of <i>E. coli</i>	37
2.5.5	Screening of clones	38
2.5.6	Plasmid purification	39
2.5.7	DNA concentration determination and sequence analysis	39
2.6	Protein biochemistry	40
2.6.1	Basic methods	40
2.6.1.1	Cell lysate	40
2.6.1.2	TCA-precipitation	40
2.6.1.3	Protein quantification assay	41
2.6.1.4	grB ELISA	42
2.6.1.5	Enzymatic activity assay	42
2.6.1.6	SDS-PAGE, silver staining and Western blot	43
2.6.2	grB purification methods	44
2.6.2.1	Nucleus protein isolation	44
2.6.2.2	Heparin affinity chromatography	45
2.6.2.3	Nickel affinity chromatography	45
2.6.2.4	Activation procedure through enterokinase (EK) digestion	46
2.6.2.5	Buffer exchange	46
2.6.2.6	Filtration	47
2.6.2.7	Storage	47
2.7	Cell biology	47
2.7.1	Transient and stably transfection of HEK293 cells	47
2.7.2	Single cell cloning	48
2.7.3	grB stability assay	48
2.7.4	Colony forming assay (CFA)	49
2.7.5	Production of spheroids	49
2.7.6	grB apoptosis assays	50
2.7.7	Flow cytometry analysis	51
2.7.7.1	Membrane-Hsp70 staining	51
2.7.7.2	Annexin-V staining	52
2.7.7.3	Caspase-3 staining	52
2.7.8	Light and immunofluorescence microscopy	53
2.8	Histopathology and immunohistochemistry	54
2.8.1	Preparation of histological paraffin sections	54
2.8.2	Hematoxylin and Eosin (HE) staining	55
2.9	Statistics	56

3 RESULTS	57
3.1 Human granzyme B (grB) production	57
3.1.1 Isolation of endogenous grB from YT cell nuclei	57
3.1.2 Purification of grB produced by <i>Pichia pastoris</i>	59
3.1.3 Purification of grB produced by Sf9/Baculovirus	59
3.1.4 Production of grB by mammalian HEK293 cells	61
3.2 Enzymatic activity and <i>in vitro</i> stability	67
3.3 Biological activity in cell culture	69
3.3.1 Apoptosis assay in a mouse cell system	69
3.3.1.1 CT26 tumor mouse cells	69
3.3.1.2 Normal mouse cells	72
3.3.2 Clonogenic survival of CT26 cells after grB treatment	74
3.3.3 Escape strategies of human K562 cells	75
3.4 Biological activity in multicellular spheroids	76
3.4.1 Growth delay and histology	76
3.4.2 Apoptosis assay	79
3.5 grB therapy for tumor bearing mice	80
3.5.1 Tumor weight	82
3.5.2 Histopathology of tumors and organs	83
4 DISCUSSION	86
4.1 Production of active granzyme B (grB) expressed in mammalian cells	86
4.2 Membrane-Hsp70 mediates perforin (PFN)-independent apoptosis of human grB in mouse cells	88
4.3 Biological activity in multicellular spheroids consisting of mouse tumor cells	90
4.4 Syngeneic tumor mouse model	91
4.5 Future prospects: grB as therapy	92
5 APPENDIX	96
6 ACKNOWLEDGEMENTS	100
7 CURRICULUM VITAE	102
8 REFERENCES	104

ABBREVIATIONS

°C	degree Celsius
µg	microgram
µl	microliter
µm	micrometer
µM	micromolar
2D	two-dimensional
3D	three-dimensional
A	adenine
Ac-IEPD- <i>p</i> NA	N-acetyl-isoleucin-glutamic acid-proline-aspartic acid- <i>p</i> -Nitroanilide
amp	ampicillin
APC	antigen-presenting cells
APS	ammonium persulfate
Asp	aspartic acid
ATCC	American Type Culture Collection
Bid	BH3 interacting domain death agonist
BiP (Grp78; HSPA5)	Binding Protein (glucose regulated protein 78; HSP70 isoform in endoplasmatic reticulum)
bps	base pairs
BSA	bovine serum albumin
C	cytosine
Ca respectively Ca ²⁺	calcium
CAD	caspase-activated deoxyribonuclease
cam	camptothecin
CD	cluster of differentiation
cDNA	complementary deoxyribonucleic acid
CFA	colony forming assay
CIP	calf intestine phosphatase
CLR	C-type lectin receptors
cmHsp70.1	monoclonal antibody clone 1 against cell membrane-Hsp70

CO ₂	carbon dioxide
CRM	cholesterol rich microdomains
ctrl	control
D	aspartic acid
DAPI	4'-6-diamidino-2-phenylindole
dH ₂ O	deionized water
DMSO	dimethylsulfoxid
DNA	deoxyribonucleic acid
DSMZ	Deutsche Sammlung von Mikroorganismen und Zellkulturen (German collection of microorganisms and cell lines)
DTT	dithiothreitol
E	glutamic acid
ECM	extracellular matrix
EC number	enzyme commission number
EDTA	ethylenediaminetetraacetate
EK	enterokinase
ER	endoplasmatic reticulum
F	phenylalanine
FACS	fluorescence-activated cell sorting
Fc region	fragment crystallizable region
FCS	fetal calf serum
FIG	figure
FITC	fluorescein isothiocyanate
FPLC	fast protein liquid chromatography
G	glycine
G	guanine
Gb3	globotriaosylceramide
Glu	glutamic acid
gr	granzyme / granzymes (protein)
grB	granzyme B (protein)
GZM	granzyme gene

GZMB	granzyme B (gene)
h	hour / hours
HE	hematoxylin and eosin
HEK293	human embryonic kidney cells 293
HEPES	4-(2-hydroxyethyl)-1-piperazineethanesulfonic acid
His	histidine
HRP	horseradish peroxidase
Hsc70 (HSPA8)	constitutively expressed isoform of heat shock protein 70
HSP	superfamily of heat shock proteins
Hsp70 (HSPA1A)	inducible isoform of heat shock protein 70
HSP70 / HSPA	superfamily of heat shock proteins 70 kDa
ICAD	inhibitor of caspase-activated deoxyribonuclease
IEPD	isoleucin-glutamic acid-proline-aspartic acid
IgG	immunoglobulin G
IL-2	interleukin 2
Ile	isoleucine
ILT	immunoglobulin-like transcripts
inact grB	inactive granzyme B
IP	intraperitoneally
IS	immunological synapse
ITAM	immunoreceptor tyrosine-based activatory motif
ITIM	immunoreceptor tyrosine-based inhibitory motif
IU	international unit
IV	intravenously
K	lysine
KIR	killer cell immunoglobulin-like receptors
L	leucine
LPS	lipopolysaccharides
M	molar
mat	mature
mg	milligram
Mg	magnesium

min	minute / minutes
MITO	mitochondria
mtHsp70 (Grp75; HSPA9)	HSP70 isoform in mitochondria (glucose regulated protein 75)
n	number (of experiments)
N	asparagines
NaCl	sodium chloride
NCR	natural cytotoxicity receptors
ng	nanogram
NK cell	Natural Killer cell
NKR	NK cell receptors
nm	nanometer
nM	nanomolar
NSCLC	non small cell lung cancer
P	proline
PBS	phosphate buffered saline
PCR	polymerase chain reaction
PE	phycoerythrin
PEG	polyethylene glycol
PFN	perforin
R	arginine
RT	room temperature
s	second / seconds
S	serine
S.D.	standard deviation
SG	serglycin
T	thymine
TAB	table
TAE buffer	TRIS-Acetate-EDTA buffer
TCA	trichloroacetic acid
TKD	Hsp70-derived peptide with the amino acid sequence TKDNNLLGRFELSG

TRIS	Tris(hydromethyl)-aminomethan
U	enzyme unit
UV	ultraviolet
v/v	volume per volume percent
w/v	weight per volume percent

SUMMARY

Generation of an expression system for human granzyme B (grB) and analysis of the *in vitro* and *in vivo* efficiency

The serine protease granzyme B (grB) was found to induce apoptosis in membrane-Hsp70 positive tumor cells via a perforin-independent pathway (Gross et al. 2003b). The goal was to produce high amounts of active human grB for *in vitro* and *in vivo* experiments. A protein expression system and a suitable purification procedure were established. After testing four different systems (Natural Killer cell line YT, *Pichia pastoris*, Sf9/Baculovirus, Human Embryonic Kidney cells HEK293), enzymatically and biologically active grB was successfully produced by a stably transfected HEK293 cell line. A purification method was established for the HEK293-derived grB, which was secreted in an inactive form containing a (His)₆ tag at the amino terminus. The purification involves (His)₆ tag-nickel affinity chromatography, removal of the (His)₆ tag, activation of grB by enterokinase (EK) digestion and affinity chromatography using a heparin column. Approximately 2 mg per liter cell culture supernatant of pure active human grB has been purified. The enzymatic activity was verified in a chromogenic substrate assay. The efficacy of grB to specifically target membrane-Hsp70 positive mouse tumor cells was proven in a 2D monolayer cell system using the murine colon carcinoma cell line CT26, which shows a stable membrane-Hsp70 expression. A significant induction of apoptosis by grB was shown for CT26 cells using caspase-3 assay and DAPI staining. In contrast, normal mouse cells, lacking membrane-Hsp70 expression were found to be resistant to grB mediated apoptosis. Also, a reduction in clonogenic cell survival of CT26 cells was observed after grB treatment. 3D tumor spheroids mimic the *in vivo* tumor tissue organization. grB has been shown to affect the integrity of the CT26 spheroid surface, induces tumor cell apoptosis and reduces the size of spheroids. The effective dose range of grB from spheroid experiments was considered in initial mouse experiments. The influence of grB on solid tumors was tested in a syngeneic BALB/c CT26 spheroid mouse model and showed good tolerability and safety. A tendency toward anti-tumoral effects of grB was visible, but needs to be confirmed by further animal experiments. Injections of active grB into patients bearing membrane-Hsp70 positive tumors might provide an innovative tumor therapy. However, leukemia appear to be unlikely to profit from this approach since leukemic blasts frequently express grB inhibitors.

ZUSAMMENFASSUNG (SUMMARY IN GERMAN)

Herstellung von humanem Granzym B (grB) mittels eines Expressionssystems und Analyse der *in vitro* und *in vivo* Effizienz

Die Serinprotease Granzym B (grB) induziert selbst in Abwesenheit von Perforin Apoptose in Tumorzellen, die das Hitzeschockprotein Hsp70 auf ihrer Zellmembran exprimieren (Gross et al. 2003b). Ziel dieser Arbeit war es, humanes grB in ausreichender Menge für *in vitro* und *in vivo* Experimente herzustellen und aufzureinigen. Nachdem vier unterschiedliche Systeme getestet wurden (NK Zelllinie YT, *Pichia pastoris*, Sf9/Baculovirus, humane HEK293 Zelllinie), konnte enzymatisch aktives sowie biologisch funktionelles grB mittels einer stabil transfizierten HEK293 Zelllinie gewonnen werden. grB wird von den HEK293 Zellen in inaktiver Form und mit N-terminalem (His)₆ tag exprimiert. Folgende Aufreinigungsschritte führten zum Erfolg: Zuerst wird grB über (His)₆ tag-Nickel-Affinitätschromatographie aufgereinigt, anschließend wird der (His)₆ tag mittels Enterokinase von grB abgespalten, was gleichzeitig zur Aktivierung von grB führt. In einem letzten Schritt wird das aktive grB über eine Heparin Säule aufgereinigt. Auf diese Weise konnten etwa 2 mg reines, aktives grB pro Liter Zellkulturüberstand von transfizierten HEK293 Zellen gewonnen werden. Durch einen Substrattest konnte die enzymatische Aktivität von grB durch Umsatz zu einem farbigen Produkt nachgewiesen werden. Die Wirksamkeit von grB wurde im 2D Zellkulturmodell mit der murinen Kolonkarzinom Mauszelllinie CT26, die Hsp70 auf der Membran exprimiert, nachgewiesen. Ich konnte zeigen, dass grB in CT26 Zellen Apoptose induziert, wohingegen normale Mauszellen, welche kein Hsp70 auf ihrer Zellmembran exprimieren, nicht in Apoptose gehen. Anhand von Koloniebildungsassays (CFA) konnte nach grB Behandlung ein signifikant vermindertes klonogenes Überleben festgestellt werden. Die Wirkung von grB wurde auch in 3D Tumorsphäroiden getestet. Diese stellen ein geeignetes Modellsystem dar, um den Aufbau von Tumorgewebe nachzuahmen. Die Behandlung mit grB beeinflusst zunächst die Integrität der Oberfläche der Sphäroide, induziert Apoptose und verringert schließlich die Sphäroidgröße. Für erste Mausexperimente wurde die Dosis, welche in den Sphäroidexperimenten wirksam war, verwendet. In einem syngenem BALB/c Tumormausmodell, in dem CT26 Tumorsphäroide eingesetzt wurden, wurde die Wirkung von grB auf solide Tumoren *in vivo* getestet. Diese Experimente haben gezeigt, dass das exogen zugegebene grB keine Nebenwirkungen in Mäusen erzeugt. Die Tendenz zu einer Tumorverkleinerung deutete sich an, muss aber noch durch weitere Mausexperimente bestätigt werden. Sollten grB Injektionen zukünftig als Therapie für Tumorpatienten angewendet werden, käme diese Therapie nur für Tumoren in Frage, die keine grB Inhibitoren exprimieren. Es hat sich gezeigt, dass Leukämien zumeist sehr schlecht auf eine grB Behandlung ansprechen, da sie häufig grB Inhibitoren produzieren.

1 INTRODUCTION

1.1 Heat Shock Protein 70 family (HSP70)

1.1.1 Characterization and functions

Heat Shock Proteins (HSP; Abbreviations for Heat Shock Protein families are written in capital letters, whereas isoforms are written in lower case letters after starting with a capital letter) were originally discovered by Ritossa in the 1960s (Ritossa 1962). He exposed salivary gland cells from *Drosophila melanogaster* to elevated temperatures and examined their chromosomes. Ritossa found an unusual "puffing pattern" that indicated the elevated transcription of a gene that codes for HSP. Apart from heat shock, other "stress stimuli" including thermal stress, physical stress (e.g. UV light, gamma-irradiation), chemical stressors (oxygen radicals, toxic chemicals, heavy metals, cytostatic drugs), as well as viral or bacterial infections, have the ability to strongly upregulate HSP.

One very important family of HSPs consists of ubiquitously-expressed highly conserved heat shock proteins: the heat shock protein 70 (HSP70) members, which were named due to their molecular size of around 70 kDa. According to the new nomenclature system, they are now called HSPA (Kampinga et al. 2009). These highly conserved components of the chaperone system exist in prokaryotic and eukaryotic cells. The best characterized HSP70 member in *E. coli* is DnaK. In human cells, more than 17 genes and 30 pseudo genes encode for HSP70 proteins (Brocchieri et al. 2008).

Together with other co-chaperones, HSP70 family members are responsible for protein folding and help to protect cells from environmental stress, which cause protein denaturation and aggregation. By temporarily binding to hydrophobic amino acids, HSP70 prevents partially-denatured proteins from aggregating, and allows them to refold. It should be noted that HSP70 family members mediate many functions under physiological conditions, such as the folding of nascent polypeptides and transport across membranes in addition to their role in stress response.

All members of the HSP70 family consist of a 44 kDa amino-terminal nucleotide binding domain (NBD) and a 28 kDa carboxy-terminal domain, which can be divided into a 15 kDa substrate binding domain (SBD) and a 10 kDa alpha helical structure domain (Patury et al. 2009).

Members of the HSP70 family are located in the cytosol, in the lumen of the endoplasmic reticulum (ER), in mitochondria, in endosomal compartments, in lysosomes, in the nucleus and in chloroplasts of plant cells. Furthermore, HSP70 is found in the intercellular space and on the plasma membrane of tumor cells.

1.1.2 Intracellular HSP70

Two major isoforms of HSP70 exist, the constitutively expressed Hsc70 (HSPA8; 73 kDa) and the stress-inducible form Hsp70 (HSPA1A; 72 kDa). They are present in the cytoplasm and in the nucleus. The constitutively expressed Hsc70 is responsible for folding and unfolding of newly synthesized proteins, protein transport processes across membranes, formation and dissociation of protein-protein complexes, as well as protein degradation under physiological conditions. However, the protective functions following stress are mainly mediated by the inducible Hsp70. In addition to its stabilizing function of hydrophobic domains of stressed proteins, it inhibits a number of steps in intrinsic and extrinsic apoptosis pathways. Intracellular Hsp70 safeguards the cell from lysosomal membrane permeabilization, activation and translocation of pro-apoptotic factors and the release of cytochrome c from mitochondria. Furthermore, intracellular Hsp70 is able to suppress cellular senescence pathways (Patury et al. 2009).

The HSP70 family member BiP (Grp78; HSPA5) is present in the endoplasmic reticulum (ER) and is responsible for the correct folding and quality control of ER proteins. The mitochondrial isoform mtHsp70 (Grp75; HSPA9) is involved in the import and export of proteins from the mitochondria (Patury et al. 2009).

Due to these widespread functions, HSP70 family members are considered central mediators of proteome homeostasis (Patury et al. 2009). Hence, it is not surprising that HSP70 members are involved in many diseases, including cancer. Cytosolic Hsp70 is overexpressed in a wide range of human cancers. This has been found to serve as a marker for poor prognosis in breast cancer, endometrial cancer, uterine cervical cancer, and transitional cell carcinoma of the bladder and overexpression correlates with an enhanced frequency of lymph node metastasis in breast and colon cancer patients (Ciocca and Calderwood 2005).

1.1.3 Extracellular HSP70

For a long time, HSP70 family members were thought to be exclusively located intracellular. However, recently it was shown that HSP70 can be released into extracellular compartments by a variety of viable cell types. HSP70 is secreted under various stress conditions, e.g. by tumor cells and antigen-presenting cells (APC). In the latter HSP70 plays a role in antigen processing and presentation (Barreto et al. 2003; DeNagel and Pierce 1992; Hartl 1996). While the mechanism of release has not been completely understood yet, it appears that the extracellular transport from tumor cells occurs via a non-classical pathway involving lysosomal endosomes (Mambula and Calderwood 2006).

1.1.4 Tumor-specific Hsp70 plasma membrane localization

Although Hsp70 does not contain a transmembrane domain in its sequence, we and others identified an unusual membrane-bound form of stress-inducible Hsp70 (72 kDa) on tumor cells (Ferrarini et al. 1992; Hantschel et al. 2000; Multhoff et al. 1995b; Tamura et al. 1993). Normal tissues were found to be negative for membrane-Hsp70 (Gastpar et al 2004) (FIG. 1). A variety of biopsies and cell lines were screened using the monoclonal antibody cmHsp70.1 (multimmune GmbH, Munich, Germany), which is highly specific for the inducible Hsp70. This antibody recognizes an 8-mer amino acid sequence, 453-461 NLLGRFEL, which is exposed to the extracellular milieu of viable tumor cells. Approximately 15 to 20% of the total cellular Hsp70 content of tumor cells is present on the cell surface (Gehrmann et al. 2008a). Hsp70 is transported to the plasma membrane through an alternative pathway, since inhibitors of the ER and Golgi transport pathway do not affect the membrane-Hsp70 expression. Co-localization of Hsp70 with the membrane protein caveolin-1, which is involved in receptor-independent endocytosis, indicates a caveolin-1 associated membrane-anchorage (Gehrmann M., *dissertation*). Recently, it was found that the tumor-specific plasma membrane localization of Hsp70 is enabled by glycosphingolipid globotriacylceramide (Gb3) in cholesterol rich microdomains (CRM) in gastrointestinal tumors (Falguieres et al. 2008; Gehrmann et al. 2008a).

Membrane-Hsp70 expression of tumors is a negative prognostic marker for patients with lower rectal carcinomas and non-small cell lung cancer (NSCLC). The overall survival of patients with membrane-Hsp70 positive tumors is significantly lower than that of their membrane-Hsp70 negative counterparts (Pfister et al. 1996). Metastases frequently express higher levels of membrane-Hsp70 compared to primary tumors (Botzler et al. 1998; Farkas et al. 2003). Membrane-Hsp70 expression on tumor cells is elevated by radiation (Gehrmann et al. 2008b), under hypoxia (Schilling et al. 2009) and by treatment with chemotherapeutics affecting the tubulin network (Gehrmann et al. 2002). These findings highlight the clinical significance of determining the membrane status of Hsp70 and the urgent medical need to specifically target Hsp70 in patients with membrane-Hsp70 positive tumors. In summary, overexpression of HSP70 family members either in the cytosol or associated to the plasma membrane seems to indicate a more aggressive and treatment-resistant type of cancer. Membrane-Hsp70 has been found to protect tumors against radiation- or chemotherapy-induced apoptosis, especially after a second treatment procedure (Gehrmann et al. 2008b). Therefore, therapies utilizing membrane-Hsp70 as a tumor-selective target structure for cytolytic attack by natural killer (NK) cells could provide an innovative strategy to treat highly aggressive tumors (Botzler et al. 1996; Multhoff et al. 1995a; Multhoff et al. 1997; Multhoff et al. 1999).

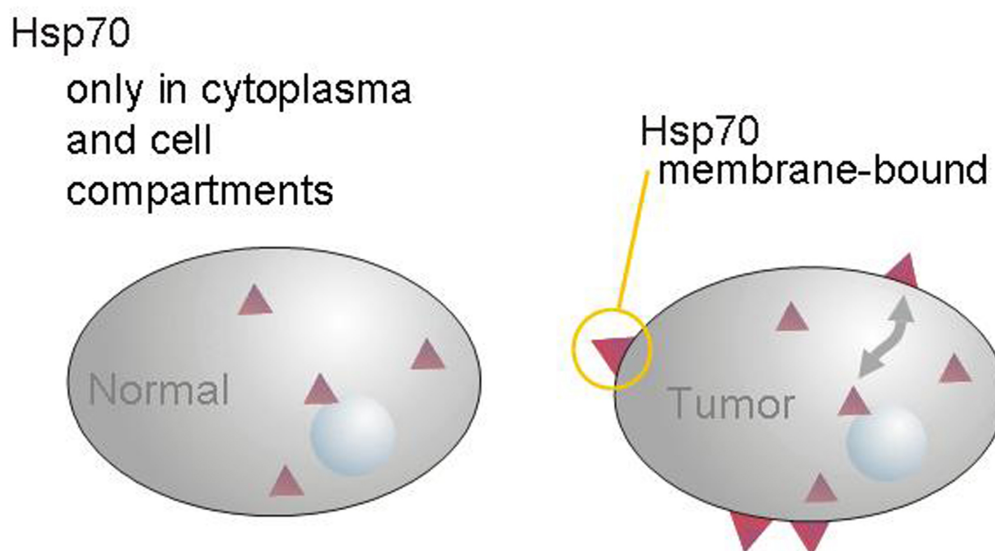


FIG. 1: Membrane-Hsp70 expression. Between 40-80% of different tumor entities express Hsp70 on their plasma membrane. In contrast normal tissues lack a membrane-Hsp70 expression. More than 1000 tumor biopsies and their corresponding normal tissue were tested in our group by flow cytometry analysis. Scheme was kindly provided by Prof. Dr. G. Multhoff and slightly modified.

1.2 Natural killer (NK) cells

1.2.1 Characterization and functions

Human Natural Killer (NK) cells are large granular lymphocytes that comprise around 15% of all lymphocytes. NK cells are important effector cells of the innate immune system, and act as the first line of defence against invading pathogens and tumor cells. NK cells kill their target cells by different routes and are able to directly lyse target cells via activating receptors. These cytotoxic capacities of NK cells are generally mediated by two pathways: the extrinsic pathway involving cell surface receptors with death ligands or the granzyme (gr)-pathway, which involves the release of cytotoxic granules. The latter pathway will be discussed in more detail later. NK cells also mediate antibody-dependent cellular cytotoxicity (ADCC) via binding of the membrane receptor CD16 to the tail region of antibodies (Fc; fragment crystallizable). Another indirect killing strategy involves attracting the attention of other immune cells by secreting immunoregulatory cytokines. These interactions trigger an antigen-specific immune response mediated by T cells (Andoniou et al. 2008).

Mature human NK cells are phenotypically defined by the expression of CD56 (neural cell adhesion molecule), and the lack of expression of CD3 and T cell receptors (Robertson and Ritz 1990). Based on the cell-surface density of CD56, two different subsets of NK cells exist that have unknown functional significance. The majority (90%) of human NK cells express low-density CD56 (CD56^{dim}), and high-density CD16 (CD16^{bright}). A minority group of NK cells expresses a high-density CD56 (CD56^{bright}) and low-density CD16 (CD16^{dim}) or lacks expression altogether. Resting cells expressing CD56^{dim} are considered to be the cytotoxic sub-population. They are mainly present in the peripheral blood, while the cytokine-producing CD56^{bright} cells are predominantly found in lymphoid organs. It has been speculated that the CD56^{bright} cells may comprise precursors of the CD56^{dim} NK cells (Poli et al. 2009).

Evidence has accumulated that NK ("Natural" Killer) cells, which are thought to kill their target without prior activation as representing innate immunity, as well as show features of adaptive immunity including memory (Sun et al. 2009).

1.2.2 Mechanisms of target recognition

The proteins encoded by the genes of the major histocompatibility complex (MHC) were expressed on the surface of cells and display antigens from the cell itself (“self”) and from invading pathogens (“non-self”) to T cell lymphocytes and NK cells. NK cells preferentially recognize and kill target cells with downregulated, lost, or altered classical and non-classical self-MHC class I molecule expression. This behaviour is termed the “missing self” theory by Kiessling (Kiessling et al. 1975a; Kiessling et al. 1975b; Ljunggren and Karre 1990). NK cells recognize and kill target cells in a complex way that involves the expression of activatory or inhibitory receptors. These multiple receptor-ligand pairs between NK and target cells are described vividly as the “NK cell zipper” (Vivier et al. 2008). Various types of NK cell receptors (NKR) play a role in these interactions. Four major human NKR-families have been identified: killer cell immunoglobulin-like receptors (KIR), immunoglobulin-like transcripts (ILT), C-type lectin receptors (CLR), and natural cytotoxicity receptors (NCR). Additional cell surface molecules (e.g. 2B4) act as co-receptors that are also involved in triggering the NK cell functions.

All inhibitory receptors (e.g. KIR-L, LAIR-1, CD94-NKG2A) share a common signaling motif in their cytoplasmic region termed immunoreceptor tyrosine-based inhibitory motif (ITIM), which starts the intracellular signaling pathway contributing to ban the NK cells from killing. Activatory and co-activatory signals are transmitted via their receptors (e.g. KIR-S, CD94-NKG2C, CD94-NKG2D) through different signaling pathways. These pathways begin with immunoreceptor tyrosine-based activatory motif (ITAM)-bearing NK receptor complexes, DAP10-associated NKG2D receptor complexes and the 2B4 receptor system. The interplay between the signals received by an NK cell is extremely dynamic and is regulated in a spatial and temporal way (Lanier 2008).

Accessorially, NK cells have other recognition strategies for “infection non-self” and “stress-induced self”. Additionally, tumor-associated molecules present positively regulating ligands.

Infiltration by NK cells may be associated with better prognosis in squamous cell lung, gastric and colorectal carcinomas (Coca et al. 1997). Tumor cells are ideal NK cell targets if their expression of MHC class I antigens are completely lost or downregulated. Additionally, tumor cells bearing a variety of altered self stress-

inducible proteins make good NK cell targets (Chang et al. 2005; Gasser et al. 2005). Our laboratory identified membrane-Hsp70 as a target recognition structure for NK cells on tumor cells (Multhoff et al. 1997).

1.3 Granzyme B (grB)

Upon activation, NK cells secrete cytotoxic granules towards the immunological synapse (IS) between the NK cell and a target cell. The granules release macromolecular complexes containing the lymphocyte serine proteases granzymes (gr) that induce apoptosis in target cells. gr are the focus of this thesis, which describes expression, purification and *in vitro* as well as *in vivo* characterization of granzyme B (grB).

1.3.1 Characterization and functions

Granzyme genes (approved gene symbol GZM) are only identified in mammals. Ten genes are known in mice (GZMA, B-G, K, M and N), while there are five genes characterized in humans (GZMA, B, H, K, M) (Pardo et al. 2009). GZM are transcribed with a signal sequence that directs their mRNA for translation to the endoplasmic reticulum (ER). In the ER, a pro-enzyme is produced that is inactive by holding an amino-terminal dipeptide. In the Golgi, gr are tagged with a mannose-6-phosphate used to target the gr to the lytic granules. Once inside the granules, gr are activated by removal of the dipeptide by the dipeptidyl peptidase I (cathepsin C) and the active gr molecule is stored on a scaffold of the chondroitin-sulfate proteoglycan serglycin (SG). Storage in this scaffolding, in combination with the acidic pH of the lytic granules, acts to minimize the proteolytic activity of gr (Chowdhury and Lieberman 2008). It is shown that grA, B, C, K and M induce apoptosis *in vitro*, but more recent results indicate that also degeneration of the extracellular matrix (ECM) and inflammation can be mediated by gr (Buzza et al. 2005). grA and grB seem to be the most frequently expressed gr and they are the best characterized gr. Knowledge about the functions of the other gr is more rudimentary (Cullen et al. 2010; Hoves et al. 2010; Pardo et al. 2009).

grB is a serine protease consisting of 227 amino acids in its active form. The substrate specificity of human grB is unusual for a serine protease, as it cleaves peptide bonds after aspartyl residues, optimally after the tetrapeptide isoleucin-glutamic acid-proline-aspartic acid (IEPD). The arginine residue R-226 in grB is the major structural element responsible for the substrate specificity (Caputo et al. 1999). This enzyme is mainly produced by activated cytotoxic T cells and NK cells. However, recent discoveries have shown that it can also be expressed under certain pro-inflammatory conditions by CD4⁺ cells, mast cells, activated macrophages, neutrophils, basophils, dendritic cells, T regulatory cells and B cells. In rare cases, grB can be found in non-immune cells in certain disease states such as solid tumor cells, smooth muscle cells, keratinocytes and chondrocytes, type II pneumocytes, sertoli cells, primary spermatocytes, granulose cells, and syncytial trophoblasts in the placenta (Boivin et al. 2009).

Soluble grB is found in the serum of normal healthy individuals at concentrations up to 15-40 pg/ml and at elevated levels in various diseases. Presently, it is unknown whether this phenomenon is caused by leakage from the IS during killing or if grB is actively released into the serum (Buzza and Bird 2006; Cullen et al. 2010; Spaeny-Dekking et al. 1998). Extracellular grB degrades and remodels the extracellular matrix (ECM) by direct cleavage of vitronectin, fibronectin and laminin. grB-mediated degradation of ECM may influence tumor metastasis and potentially enhances lymphocyte migration (Buzza et al. 2005; Pardo et al. 2007). Extracellular grB promotes inflammation by producing ECM fragments, which leads to the release of pro-inflammatory cytokines from immune cells. Nevertheless, the recent discovery that grB deficient mice demonstrate a profound resistance to LPS-induced shock provides evidence that grB also plays an important role in the regulation of inflammation (Metkar et al. 2008). In general, the existence of grB-expressing cells in the absence of the pore-forming protein perforin (PFN) gives a clue that there might be more so far unidentified roles of grB in immunity (Cullen et al. 2010). Therefore, it is not surprising that elevated levels of grB in the absence of PFN are measurable in several inflammatory diseases, including joint destruction in rheumatoid arthritis and atherosclerosis, as well as in vascular pathologies, in allergic reactions and in autoimmune diseases (Boivin et al. 2009; Cullen et al. 2010; Hagn et al. 2009).

grB must enter the cell's cytosol to induce apoptosis. Therefore, the first step is grB's uptake into the target cell. There is still a controversial debate about the exact

mechanism of grB uptake. In traditional models, the delivery of grB into the target cell is thought to be mediated by PFN (schematic FIG. 2A). PFN is a Ca^{2+} dependent, 70 kDa protein that multimerizes in the target cell plasma membrane and forms pores of 5 to 20 nm diameter (Sauer et al. 1991; Tschopp et al. 1986). Early models proposed the formation of pores in the target cell membrane so that grB could easily stream inside the target cell. Later, it was shown that grB is also been taken up in a PFN-independent manner, but without the addition of a lytic agent no apoptosis was caused in target cells (Froelich et al. 1996; Pinkoski et al. 1998).

Other models suggest a system where grB is taken up by pinocytosis or receptor-independent endocytosis (schematic FIG. 2B). Afterwards PFN is able to release grB from endosomes into the cytosol, where it initiates apoptosis (Keefe et al. 2005; Pipkin and Lieberman 2007; Shi et al. 2005). Additionally, alternative mechanisms for grB entry have been proposed (no schematic figures are shown from the following). It is assumed that a complex consisting of SG and grB and interacting PFN can incorporate into target cell membranes and delivers grB without pores (Grujic et al. 2005). It is still not clear whether grB is taken up by pinocytosis or by a receptor-mediated endocytosis mechanism. Controversy exists about the uptake via mannose-6-phosphate receptors on target cells (Dressel et al. 2004; Motyka et al. 2000; Veugelers et al. 2006). Bird et al. have speculated that the positively charged grB might leave its binding partner SG and bind to the negatively charged cell surface. The uptake would subsequently be enabled by non-selective pinocytosis (Bird et al. 2005).

Our laboratory has suggested a novel mechanism for a PFN-independent uptake of grB into membrane-Hsp70 expressing tumor cells. This mechanism leads to apoptosis without perforin or the need for other membrane permeabilizing reagents (Gross et al. 2003b) (FIG. 2C).

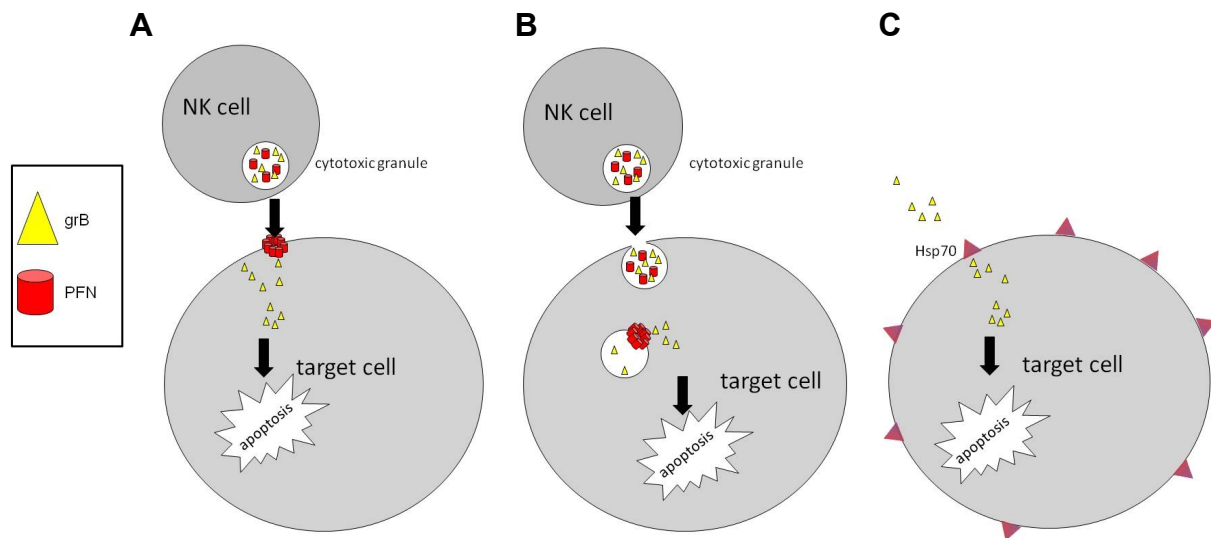


FIG. 2: Schemes for different grB uptake models. A Perforin (PFN)-pore-model. In the traditional model, perforin (PFN) builds up a pore so that grB can enter the cytosol. **B PFN-endosome-release model.** grB and PFN are taken up by endocytosis. PFN releases grB from endosomes into the cytosol, where grB induces apoptosis. **C Hsp70-grB interaction model.** grB in the absence of PFN can be taken up by membrane-Hsp70 positive tumor cells and induces apoptosis. The accurate mechanism of uptake is unknown, but it is mediated by Hsp70-grB interaction.

Apoptosis is induced as soon as grB enters the cytosol. The grB-pathway represents a pathway of apoptosis induction in addition to the extrinsic or death receptor pathway and the intrinsic or mitochondrial pathway. All three of these pathways finally converge into the same terminal pathway, starting with cleavage of caspase-3 and ending in nuclear fragmentation. The grB-pathway is split in two sub-pathways. In the first sub-pathway, the effector caspase-3 (and others e.g. caspase-7; not shown in FIG. 3) is directly activated by grB and promotes DNA fragmentation. Other substrates of the caspase pathway such as the inhibitor of caspase-activated deoxyribonuclease (ICAD) and procaspase-8 can also be directly cleaved and finally lead to DNA fragmentation (FIG. 3, arrows on top from left to right: 2, 3 and 4). In the second sub-pathway, grB starts mitochondria-dependent apoptosis through inducing permeability of the mitochondrial outer membrane starting with cleavage of Bid and Mcl-1 (FIG. 3, arrows on top from left to right: 4, 5 and 6). There are interferences between the two sub-pathways concerning caspase-8, which is able to cleave Bid and caspase-3 (FIG. 3, arrows on top from left to right: 4). Additionally, the cleavage of procaspase-9 induced by cytochrom c release triggers apoptosome formation and finally caspase-3 cleavage (FIG. 3, downstream). Accessorily, grB is able to by-pass the caspase cascade and the mitochondrial sub-pathway by directly cleaving lamin

B, which leads immediately to a loss of integrity of the nuclear membrane (FIG. 3; first arrow on top). It is controversially discussed, whether the mitochondrial sub-pathway is the main pathway in humans, which is physiologically relevant (Boivin et al. 2009; Chavez-Galan et al. 2009; MacDonald et al. 1999). However, the mitochondrial sub-pathway seems to be of minor importance in mice models (Cullen et al. 2010).

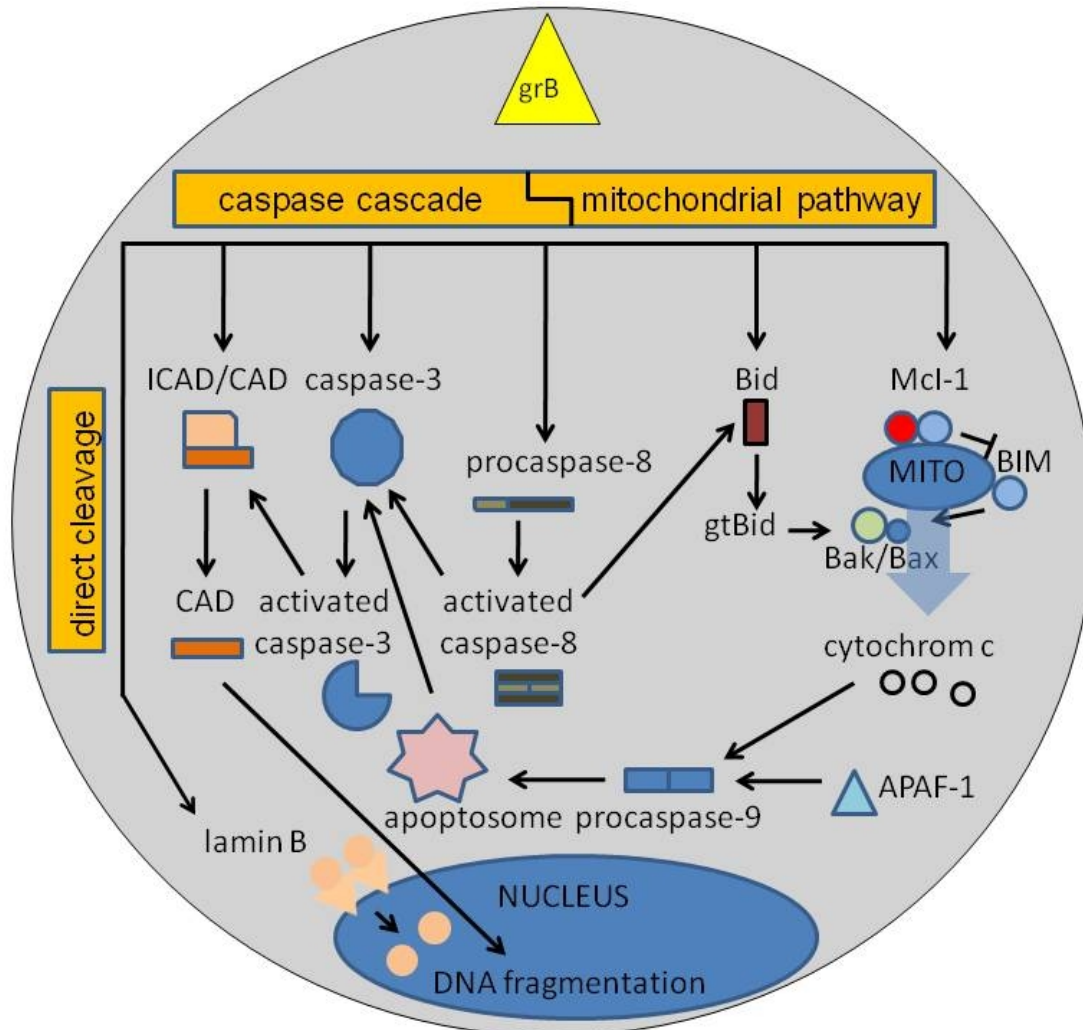


FIG. 3: grB-mediated apoptosis pathways. grB initiates apoptosis by directly cleaving caspases (mainly caspase-3 but also other caspases) or by processing caspase substrates such as the inhibitor of caspase-activated deoxyribonuclease (ICAD), which leads to CAD translocation into the nucleus, where CAD cleaves DNA (caspase cascade pathways). grB also triggers a mitochondrial apoptosis pathway, which starts with the cleavage of Bid to a truncated form (gtBid) or Mcl-1 that in the end triggers mitochondrial cytochrom c release. Cytochrom c activates procaspase-9, which leads to apoptosome formation, caspase activation and finally to apoptosis. An additional interference between the two pathways occurs after procaspase-8 cleavage. Another mode of action for inducing apoptosis by grB is its ability to cleave the nuclear membrane protein lamin B, which leads to loss of integrity of the nuclear membrane (direct cleavage; figure adapted from (Boivin et al. 2009)).

Interestingly, grB induces not only apoptosis directly through the mentioned pathways but also extracellular grB that cleaves extracellular matrix proteins might finally induce anoikis. Anoikis is a form of programmed cell death induced by loss of cell-matrix interaction (Buzza et al. 2005; Prakash et al. 2009). Additionally, grB proteolyzes extracellular proteins or cell surface receptors, like Notch1 and FGFR1, which prevents signaling needed to boost proliferation and survival. These are additional functions of grB for enhancement of apoptosis (Loeb et al. 2006).

1.3.2 grB mediated lysis of membrane-Hsp70 positive tumor cells

Our group has shown that the 14-mer peptide TKDNNLLGRFELSG (TKD), derived from the carboxy-terminal extracellular domain of Hsp70, functions as a target recognition structure for NK cells (schema shown in FIG. 4). The C-type lectin receptor CD94 is involved in NK cell interaction with the extracellular part of membrane-Hsp70. However, the mechanism how NK cells lyse membrane-Hsp70 positive tumor cells remains elusive (Gastpar et al. 2004; Gross et al. 2003a). In order to better understand this process, we looked for an interaction partner for membrane-Hsp70 from NK cells. We have shown protein-protein interaction between grB and Hsp70 and peptide-protein interaction between grB and TKD by affinity chromatography. grB, released by TKD/IL-2 activated NK cells, mediates apoptosis mainly in membrane-Hsp70 positive tumor cells. Therefore, it was proven that grB binds specifically to the cell surface of membrane-Hsp70 positive tumor cells, is taken up selectively and causes apoptosis without the need of PFN. This leads to the proposal that a novel PFN-independent grB-stimulated apoptosis pathway exists (Gross et al. 2003b). De Maio et al. have shown that Hsc70 forms a functionally stable ATP-dependent cation channel in acidic phospholipid membranes (Arispe et al. 2002; Arispe and De Maio 2000). In collaboration with De Maio, we have shown that Hsp70 forms ion channels on the cell surface of membrane-Hsp70 positive tumor cells. No channel formation has been observed in membrane-Hsp70 negative tumor cells (unpublished data). Therefore, it was assumed that Hsp70 serves as an entry port for grB into membrane-Hsp70 positive tumor target cells. Whether Hsp70 forms channels or uptake occurs through pinocytosis or receptor-dependent or -independent endocytosis has not yet been elucidated.

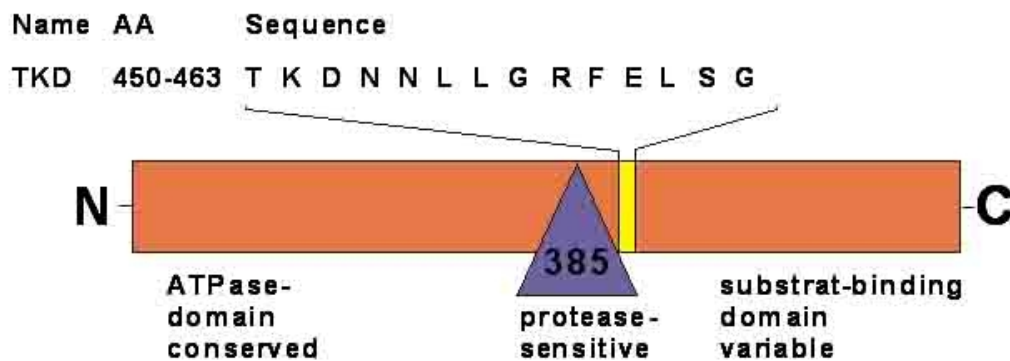


FIG. 4: The peptide TKD stimulates NK cells. Hsp70 stimulates the activity of NK cells. By protease digestion the stimulating part of Hsp70 is localized to the carboxy-terminal end of Hsp70. Finally, the 14-mer peptide TKDNNLLGRFELSG (TKD), derived from the carboxy-terminal extracellular domain of Hsp70 was found to be sufficient for NK cell activation. The schematic figure was kindly provided by Prof. Dr. G. Multhoff.

1.4 Aim of the study

This thesis is based on the finding that the specific plasma membrane localization of Hsp70 on tumor, but not on normal cells, facilitates the uptake of the human serine protease grB and initiates apoptosis in a PFN-independent manner (Gross et al. 2003b). The goal of this work was to establish a protein expression system and a suitable purification procedure, for producing high amounts of active human grB. Afterwards, the enzymatic and biological activity of human grB was tested *in vitro* in mouse tumor cells, which expose Hsp70 on their membrane. Additionally, grB was tested in a spheroid assay. These model systems are essential for a better understanding of the mode of grB action. The impact of enzymatically active human grB was tested in a syngeneic tumor mouse model. Initially, the potential side effects were studied; secondly the effects on the growth reduction of tumors in mice therapy were examined. These results will contribute to further develop the idea of a molecular therapy based on a novel PFN-independent, grB-mediated pathway leading to apoptosis in membrane-Hsp70 positive tumor cells.

2. MATERIAL AND METHODS

2.1 Chemicals and devices

Most chemicals and reagents were obtained from Sigma-Aldrich (Inc., St. Louis, MO, USA) or from Carl Roth (Carl Roth GmbH & Co.KG, Karlsruhe, Germany) unless otherwise stated. Chemicals and materials are described in detail where mentioned later on in the text for the first time. A few standard devices and consumable supplies are mentioned here.

device	company
4°C refrigerator Premium frost-free	Liebherr International AG, Bulle, Switzerland
-20°C Comfort	Liebherr
-80°C Hera Freeze HFU586 Basic	Thermo Fisher Scientific, Rockford, IL, USA
analytical scales standard A566	Ohaus corp., Pine Brook, NJ, USA
cryogenic storage system Biosafe®	Cryotherm GmbH & Co KG, Kirchen, Germany
Fresco 17 centrifuge	Heraeus/Thermo Fisher Scientific
heating plate and magnetic stirrer MR3001K	Heidolph Instruments GmbH, Schwabach, Germany
micro ultra centrifuge Discovery M120	Sorvall/Hitachi/Thermo Scientific
multifuge 3SR+Centrifuge	Heraeus/Thermo Fisher Scientific
pipettes	Eppendorf AG, Hamburg, Germany
pipettor IBS pipetboy acu	Integra Biosciences GmbH, Fernwald, Germany
scales EW620-3NM	Kern & Sohn GmbH, Balingen-Frommern, Germany
test tube shaker REAX top	Heidolph Instruments
ultrapure water system Direct-Q	Millipore corp., Billerica, MA, USA

consumable material	company
reaction tubes 0.5 ml, 1 ml, 2 ml	Eppendorf
Falcon™ tubes 15 ml, 50 ml, 250 ml	BD Biosciences
pipette tips	Eppendorf / Sarstedt AG, Nürnberg, Germany
96-well tissue culture test plates, flat bottom	TPP, Trasadingen, Switzerland
96-well tissue culture test plates, U-bottom low evaporation lid	BD Biosciences, Heidelberg, Germany
6-, 12-, 24-well tissue culture test plates, flat bottom	Corning Incorporated, Corning, NY, USA
tissue culture dishes 10 cm ²	TPP

2.2 Microorganisms

2.2.1 Bacterial strain *Escherichia coli* (*E. coli*)

Chemical competent DH5 α *E. coli* were used for transformation and plasmid amplification for cloning of grB into the vector for HEK293 transfection.

2.2.2 Yeast strain *Pichia pastoris*

The *Pichia pastoris* strain X-33 (genotype: wild-type, phenotype: Mut+ (methanol utilizing plus)) cultivated at 28-30°C was used for recombinant protein expression. Cloning for secreted expression of proteins was done by means of the EasySelect™*Pichia* expression kit (Life Technologies), according to the manufacturer's protocol. Cloning of grB was oriented on the literature, where mature grB tagged by Myc-epitope and (His)₆ tag were cloned in a pPIC9 vector (Life Technologies) and these plasmids were transformed into *Pichia pastoris* GS115 cells (Life Technologies) (Giesubel et al. 2006; Sun et al. 1999). However, we cloned mature grB with a carboxy-terminal (His)₆ tag using the pICZA vector (Life Technologies) in *Pichia pastoris* X-33. This was done by our cooperation partner K. Zettlitz from the working group of Prof. Dr. R. Kontermann (Institute for Cell Biology and Immunology, University of Stuttgart, Germany). I received the supernatants to establish a suitable purification procedure for grB and to perform tests for its enzymatic and biological activity. Therefore, the cloning, the transfection through electroporation and the production procedure are not mentioned in this study in detail.

2.3 Cell culture and cells

Cells were cultivated under sterile conditions at the appropriate temperature and CO₂ concentrations. Cell culture was performed under a laminar flow (Hera Safe KS18, Thermo Fisher Scientific).

All flasks used were obtained from Corning (T12.5, T25, T75, T162) and sterile, single-use pipettes were obtained from Sarstedt. All cell lines were screened regularly for mycoplasma contamination by an enzyme immunoassay (Roche Diagnostics GmbH, Mannheim, Germany) detecting *Mycoplasma arginini*, *Mycoplasma hyorhinis*, *Mycoplasma laidlawii*, and *Mycoplasma orale*. Only mycoplasma-free cell lines were used.

2.3.1 Cell lines for the production of human granzyme B (grB)

2.3.1.1 NK cell line YT

material / device	ingredients	company
YT cell medium	RPMI-1640 medium supplemented with 10% heat-inactivated fetal calf serum (FCS), 1 mM sodium-pyruvate, 2 mM L-glutamine, 100 IU/ml penicillin, 100 µg/ml streptomycin, 100 U/ml IL-2 (Proleukin®S)	Life Technologies Corporation, Carlsbad, CA, USA PAA laboratories GmbH, Pasching, Austria PAN Biotech GmbH, Aidenbach, Germany PAN Life Technologies Life Technologies Novartis, Basel, Switzerland

The human NK leukemia cell line YT (Yodoi et al. 1985) (ATCC 434; DSMZ GmbH, Braunschweig, Germany) was cultivated under standard conditions at 37°C, 95% humidity, 5% CO₂ in an incubator (Heraeus BBD 6220, Thermo Fisher Scientific). According to the doubling time of 40-50 h, the YT suspension cells were seeded at a low cell density of 0.1 to 0.2 x 10⁶ cells/ml three times a week.

2.3.1.2 Sf9 insect cells

material / device	ingredients	company
TNM-FH	L-glutamine, yeast extract, lactalbumin hydrolysate, 0.35 g/ml NHCO ₃ , 10% FCS	Genaxxon Bioscience, Ulm, Germany
10 µg transfection-ready cDNA		OriGene Technologies, Inc., Rockville, USA
high-titer, ready-to-use grB producing baculovirus stock		Orbigen Inc., San Diego, CA, USA

Adherent cells were grown at 27°C without the need of a humidified environment or additional CO₂ (incubator TECO20; Selutec GmbH, Hechingen, Germany). Cells were split three times a week and 4 x 10⁶ were seeded in 15 ml TNM-FH medium per T75 flask. Detachment of cells was performed through mechanically knocking against the flask.

The Sf9/baculovirus expression system for human grB was produced as follows: 10 µg human grB cDNA was ordered from OriGene as transfection-ready. Subcloning into a Baculovirus transfer vector was accomplished by Orbigen. M. Gehrmann from

our group tested three clones to find the most efficient granzyme B (grB) producing one. The production of high-titer, ready-to-use virus stock was performed by Orbigen. The transfection of Sf9 cells was performed as further explained: Sf9 cells were freshly seeded at 7×10^6 cells per T75 flask in 13 ml TNM-FH medium. Cells were put back into the incubator to adhere slightly within around 15 min. To each flask, 2 ml of high-titer baculovirus supernatant, from the stock or supernatant obtained from the last transfection was added for transfection. The cells were incubated under standard conditions for around 4 days. Transfection and grB production were successful when cells stopped dividing, lost adherence and enlarged, but did not look lysed. The supernatant containing detached cells and the attached cells were combined. Centrifugation was performed at $400 \times g$ at 4°C for 5 min. The supernatant containing virus was stored for further transfections at 4°C (it is also possible to isolate the virus and store frozen at -80°C ; for this purpose see the protocol provided by Orbigen). The cell pellet was resuspended in 30 ml of ice-cold phosphate buffered saline (PBS; Life Technologies) and centrifuged at $400 \times g$ at 4°C for 5 min. After discarding the supernatant, cells were lysed immediately (see 2.6.1.1) and purification of grB was performed.

2.3.1.3 Human Embryonic Kidney (HEK293) cells

material / device	ingredients	company
HEK293 medium (used for cell culture)	RPMI-1640 medium supplemented with 5% heat inactive FCS, 6 mM L-glutamine, 1 mM sodium-pyruvate and antibiotics (100 IU/ml penicillin and 100 µg/ml streptomycin)	
Opti-MEM® I reduced serum medium (1X) (used for production)	liquid, with L-glutamine, 2400 mg/l sodium bicarbonate, HEPES, sodium pyruvate, hypoxanthine, thymidine, trace elements, growth factors	Life Technologies

The Human Embryonic Kidney cells 293 (HEK293; ACC305; DSMZ) were cultured by trypsin/Ethylene-Diamine-Tetra-Acetic (EDTA; 0.05%/0.02% in PBS without Ca + Mg; PAN) digestion for 2 min at 37°C and seeded at 1×10^6 cells per T75 flask in 15 ml medium.

For production of inactive grB, the stably transfected HEK293 cell line (clone C10) was freshly thawed for each production cycle. 3×10^6 cells were thawed, washed and seeded into a T75 flask. Zeocin (300 µg/ml; Life Technologies) selection was started immediately and proceeded for the next 2 passages. Cells were expanded to 20 T162 flasks within approximately 9 days. As soon as there were enough cells, grB production was started: Cells were grown to 80% confluency (normally on day 2 after passaging) and the medium was removed. The cell layer was washed with PBS and 25 ml of OptiMEM (Life Technologies) without any additives as carefully added to each T162 flask. Every 3-4 days (4 times) the grB containing supernatant was collected and fresh medium was added to the cells. In total 2 l of supernatant were gained from one production cycle.

2.3.2 Target cell lines

Tumor cell lines and the endothelial cells were cultured under standard conditions at 37°C, 95% humidity, 5% CO₂ in an incubator.

2.3.2.1 Human CX+ cells

material / device	ingredients	company
CX+ medium	RPML-1640 medium supplemented with 5% heat inactive FCS, 6 mM L-glutamine, 1 mM sodium-pyruvate and antibiotics (100 IU/ml penicillin and 100 µg/ml streptomycin)	

The human tumor subline CX+ was derived by fluorescence activated cell sorting (FACS) of the CX-2 colon carcinoma cell line (Nr. 300160; CLS Cell Lines Services, Eppelheim, Germany) (Ovejera et al. 1978) using the Hsp70-specific monoclonal antibody cmHsp70.1 (Multhoff 1997) (multimmune GmbH, Munich, Germany). CX+ cells were kept in culture under exponential growth conditions by regular cell passaging. Every 3-4 days, cells were trypsinated for 1 min and 0.5×10^6 cells were cultured per T25 culture flasks.

2.3.2.2 Human K562 cells

material / device	ingredients	company
K562 cell medium	RPMI-1640 medium supplemented with 10% heat inactive FCS, 6 mM L-glutamine, 1 mM sodium-pyruvate and antibiotics (100 IU/ml penicillin and 100 µg/ml streptomycin)	

The human myelogenous cell line K562 was purchased from ATCC (CCL243, Rockville, MD) and the suspension cells were diluted 5×10^4 per ml into new medium two times a week to keep them under exponential growth conditions.

2.3.2.3 Mouse CT26 cells

material / device	ingredients	company
CT26 medium	RPMI-1640 medium supplemented with 5% fetal calf serum, 6 mM L-glutamine, 1mM pyruvate, 100 IU/ml penicillin and 100 µg/ml streptomycin, non-essential amino acids (100 x solution) and 50 µM β-mercaptoethanol	PAA Life Technologies

The murine colon adenocarcinoma cell line CT26 (CT26.WT, ATCC CRL-2638) (Wang et al. 1995) is derived from a carcinogen-induced, undifferentiated tumor from a BALB/c mouse. Cells were cultured twice a week by trypsin/EDTA digestion (30 s at 37°C) and seeded at 1×10^6 cells per T75 flask in 20 ml medium. Cells were used until passage 50.

2.3.2.4 Isolation of CD31+ endothelial mouse cells

Isolation of CD31+ endothelial mouse cells was kindly performed by our lab member W. Sievert and cells were provided for my experiments.

To obtain CD31 positive cells, the subcutis from the back of two BALB/c mice was removed aseptically and rinsed 3 times with PBS on ice. Then the subcutis was disintegrated into 1 mm pieces with a scalpel and digested in 10 ml of collagenase A

(Roche Diagnostics) dissolved in HBSS (Life Technologies)/10 % FCS at 37°C under rotation for 45 min. This pre-digested cell-clump was passed through a needle (18G) 10 times to dissociate any pieces. The single cell suspension was filtered through a 70 µm mesh and washed twice with HBSS/10% FCS (500 x g, 10 min). The cells were resuspended in 6 ml of HBSS/10% FCS and incubated with 10 µl of magnetic dynabeads (Life Technologies) coated with CD31 antibody (BD Biosciences) at RT for 20 min. The cells with bound beads were washed 5 times with HBSS/10% FCS using the magnet DynaMag™-15 for selection (Life Technologies). CD31 positive cells were seeded in 3 ml of endothelial cell growth medium (PromoCell GmbH, Heidelberg, Germany) in a gelatin coated T12.5 culture flask. Cells were cultured twice a week by trypsin/EDTA digestion for 1 min at 37°C and seeded at 3×10^5 cells per T75 flask in 20 ml of medium. Cells for experiments were cultured at least two passages after magnetic separation and only cells up to passage 4 were used.

2.4 Animal model

Female BALB/c mice were obtained from an animal breeding colony (Charles River Laboratories, Inc., Wilmington, MA, USA) and maintained in pathogen-free, individually ventilated cages (Tecniplast, Hohenpeissenberg, Germany). Animals were fed a sterilized, laboratory rodent diet (Meika, Großaitingen, Germany) and were used for experiments between 10 and 12 weeks of age. All animal experiments were approved by the “Regierung von Oberbayern” and were performed in accordance with institutional guidelines.

For a syngeneic mouse model, spheroids from the BALB/c-derived CT26 cell line (see 2.3.2.3 and 2.7.5) were used for tumor growth. A single seven day old CT26 spheroid per mouse was injected intraperitoneally (IP), while the animal was manually restrained. Weighing of the mice was performed at every step and mice were identified by ear punch. On day 6 after spheroid injection, the grB treatment started. 3 groups of 5 animals were used for each experiment. The first group was the control group, which was not treated at all. The second and the third groups were treated with inactive grB or active grB, respectively the same concentration and volume. In the first experiment, mice received 20 µg per g body weight inactive or active grB on days 6 and 7. In the second experiment, grB was given on days 6, 7,

13 and 14 to double the overall dose. The rest of the experiment was performed as stated above. Mice were monitored for one hour after each injection for irregularities. On day 21 after spheroid injection mice were anesthetized. For anesthesia a freshly prepared xylazine (4 mg/ml; stock 20 mg/ml, 2% Xylazin Rompun, Bayer Healthcare, Animal Health Division Monheim, Germany) plus ketamine (80 mg/ml; stock 100 mg/ml, 10% Ketamin Intervet/Schering-Plough Animal Health, Boxmeer, The Netherlands) mixture was used. 40 µl per 20 g of the xylazine-ketamin mix was injected IP. A blood sample was taken from the anaesthetized mice from the orbital sinus or plexus via a microhematocrit tube. After 30 min of blood clotting, blood was centrifuged (750 x g, RT, 10 min), the serum aliquoted and frozen at -80°C. Mice were sacrificed by cervical dislocation and the tumor, liver, kidney, lung, heart and spleen were resected. Tumors were weighted. Tumors and organs were immediately fixed in 3.7% formalin (1:10 dilution of 37% formaldehyde in PBS) to obtain paraffin slides for pathohistology.

2.5 Molecular biology

2.5.1 Polymerase chain reaction (PCR)

material / device	ingredients	company
cDNA of human pre-pro-GZMB (pCMV6-XL4)	cDNA template in the cloning vector pCMV6-XL4	OriGene Technologies, Inc., Rockville, USA
dNTPs, 10 mM		Fermentas, Burlington, USA
PCR cycler RoboCycler 96		Stratagene, La Jolla, USA
cloning primers	see below	Thermo Fisher Scientific
Taq buffer with (NH ₄) ₂ SO ₄ , 10 x		Fermentas
Taq DNA-polymerase (1 U/µl)		Fermentas

The cDNA fragment encoding granzyme B (gene symbol GZMB) was amplified by PCR using the following oligonucleotides as primers: Agel-GZMB-back (5' TTT ACC GGT ATC ATC GGG GGA CAT GAG 3') for producing mature grB respectively using Agel-(His)₆-EK-GZMB-back (5' TTT ACC GGT CAT CAT CAT CAT CAT GAC GAC GAC GAC AAA ATC 3') for inactive and tagged grB and for both GZMB-Stop-EcoRI-forward (5' CCG GAA TTC TTA GTA GCG TTT CAT GGT TTT C 3').

The PCR reaction mix was prepared as:

cDNA template	0.5 µl
10 x Taq buffer with (NH ₄) ₂ SO ₄	5 µl
MgCl ₂	4 µl
forward primer (10 pmol/µl)	1 µl
reverse primer (10 pmol/µl)	1 µl
dNTPs	2.5 µl
Taq DNA-Polymerase	1.25 µl
sterile dH ₂ O	ad 50 µl

The amplification was performed using the following PCR program:

pre-cycle	5 min 94 °C
denaturation	1 min 94 °C
annealing	1 min 55 °C
elongation	1 min 72 °C
cycles	30x
post-cycle	5 min 72 °C
end	hold on 4 °C

2.5.2 Agarose gel electrophoresis and DNA gel extraction

material / device	ingredients	company
DNA loading buffer, 5 x	1 ml TAE buffer, 50x; 2.5 ml glycerol; 0.02% (w/v) bromphenol blue; ad 10 ml H ₂ O	
ethidium bromide		Roth
Gene Ruler™ DNA Ladder		Fermentas
NucleoSpin Extract II, PCR Clean-up Gel extraction kit		Macherey-Nagel GmbH & Co. KG, Düren, Germany
ready agarose precast gel system		BioRad, Hercules, CA, USA
TAE buffer	40 mM TRIS, 8 mM sodium acetate, 1 mM EDTA (pH 7.8)	
transilluminator, gel documentation system Felix		Biostep, Jahnsdorf, Germany

Analysis and purification of DNA (amplified or digested DNA) was performed by horizontal agarose gel electrophoresis. DNA samples were mixed with 5 x DNA loading buffer and separated using a 1% agarose gel containing 1 µg/ml ethidium bromide in TAE buffer. Samples were run at 85 V for 60 min. Relevant DNA bands were excised under UV light and extracted with a DNA gel extraction kit, according to the manufacturer's protocol. DNA was eluted in 30 µl of sterile dH₂O.

2.5.3 Restriction digestion and ligation

material / device	ingredients	company
Agel 10 U / μ l		Fermentas
alkaline calf intestine phosphatase (CIP) (5 U/ μ l)		Fermentas
buffer 0		Fermentas
EcoRI 10 U / μ l		Fermentas
ligase buffer (10 x)		Fermentas
NucleoSpin Extract II, PCR Clean-up Gel extraction kit		Macherey-Nagel
pSECTagA vector (5.2 kb)		Life Technologies
pSECTagAL1 modified vector	pSECTagA vector with an additional Agel in its cloning site	modifications by AG Kontermann, Stuttgart, Germany
T4 DNA ligase (5 U/ μ l)		Fermentas

Ten μ g vector DNA or the total amount of DNA extracted from agarose gels were digested in a total volume of 50 μ l. Restriction enzymes (20 U/reaction) and the corresponding buffers were added. The incubation was performed for 3 h. For buffer exchange, the PCR Clean-up Gel extraction kit was used. To avoid vector religation, digested vector DNA was dephosphorylated after restriction digestion by adding 1 U CIP to the reaction mix and incubating at 37°C for 1 h. Ligation was performed at RT for 1 h with 1 μ l of T4 DNA ligase and 2 μ l of ligase buffer (10 x) in a total volume of 20 μ l. Different concentrations of the linearized and dephosphorylated vector and insert were assembled to find the best ratio for ligation. As a control for religation the linear, dephosphorylated vector without insert was used.

2.5.4 Transformation of *E. coli*

material / device	ingredients	company
LB medium (low salt)	10 g pepton, 5 g NaCl, 5 g Yeast Extract (< 90 mM salt), ad 1l (pH 7.5), autoclave	
LB _{amp} plate	LB medium (low salt) + 2% agar, 100 μ g/ml ampicillin	
petri dishes		Thermo Fisher Scientific

100 μ l of chemical competent DH5 α *E. coli* cells and 10 μ l of the ligation preparation were mixed on ice and incubated for 15 min. Then the mixture was placed for 45 s in a 42°C tempered water bath and thereafter another 1 min on ice. Next, 1 ml of low salt LB-medium was added and cells were incubated at 37°C for 1 h while shaking.

The cells were centrifuged (17,000 x g, 4°C, 1 min) and the supernatant was discarded. Cells were resuspended in the remaining medium and plated on an LB_{amp} plate, which was incubated at 37°C overnight.

2.5.5 Screening of clones

material / device	ingredients	company
mastermix (20 µl per tube)	10 µl Red Taq, 9.2 µl dH ₂ O, 0.4 µl of each primer (50 pmol/µl)	
REDTaq™ Ready Mix		Sigma
pSECTagA sequencing primer pET-Seq1	5' - TAA TAC GAC TCA CTA TAG G - 3'	Thermo Fisher Scientific
pSECTagA sequencing primer pSec-Seq2	5' - TAG AAG GCA CAG TCG AGG - 3'	Thermo Fisher Scientific

The single clones, which were grown overnight on the amp selection plate were tested for the grB insert. For this, the clones were screened by PCR (see 2.5.1) with the above mentioned primers, which start amplifying outside of the multiple cloning site (marked in the vector sequence in the appendix). A mastermix was prepared on ice and for each clone tested, 20 µl thereof was preloaded in PCR-tubes. The single colonies were picked with a sterile toothpick, dipped into its PCR-tube and simultaneously streaked out on a masterplate, which was cultured at 37°C overnight. The PCR was performed as mentioned in 2.5.1. and analyzed on an agarose-gel. Positive clones were identified by bands of the predicted insert size. As a negative control, the empty vector was used.

2.5.6 Plasmid purification

material / device	ingredients	company
incubator with shaker HAT Multitron 2		Infors AG, Basel, Switzerland
Nucleo Bond® Xtra Midi		Macherey-Nagel

A clone streaked out on the masterplate and validated by the analytical agarose-gel, was used to inoculate an overnight culture in 100 ml of LB medium including 100 µg/ml ampicillin and 1% glucose. Plasmids were extracted using a commercial

purification kit following the manufacturer's instructions. The purified plasmid was resuspended in 100 µl of sterile water.

2.5.7 DNA concentration determination and sequence analysis

material / device	ingredients	company
spectrophotometer GeneQuant		GE Healthcare, Little Chalfont, UK

DNA absorbance was measured photometrically at the wavelengths 260 nm and 280 nm with the spectrophotometer. The purity was determined by the ration $OD_{260/280}$. The concentration was calculated by the formula:

$$c_{DNA} [\mu\text{g}/\mu\text{l}] = OD_{260} * \text{dilution factor} * 0.05$$

Sequences were validated by GATC Biotech AG (Konstanz, Germany) using the sequencing primers (mentioned in 2.5.5).

2.6 Protein biochemistry

2.6.1 Basic methods

2.6.1.1 Cell lysate

material / device	ingredients	company
insect cell lysis buffer	50 mM TRIS, 150 mM NaCl, 1% Nonidet P40 (pH 7.8)	
PMSF dissolved in ethanol (100 mM stock solution)		
protease inhibitor cocktail (25 x stock solution)		Roche Diagnostics
TRIS-buffered saline (TBS)	1 mM TRIS, 0.9 % (w/v) NaCl (pH 8.5)	
TBST	TBS with 1% (v/v) Triton X-100 (TBST)	

This protocol was utilized to produce cell lysates e.g. for Western blot applications. Fresh 1 mM PMSF and protease inhibitors (from frozen stocks at -20°C) were added to TBST, which was stored at 4°C for several months. Cell pellets were resuspended in 100 μl of TBST for each 1×10^6 cells. Lysis was performed in TBST buffer on ice for 45 min, while vortexing every 10 min. Insoluble material was pelleted at 17,000 x g at 4°C for 10 min and the protein containing supernatant was stored at -80°C for further experiments.

In order to perform lysis of Sf9 and YT cells for purification of grB other protocols were used. These methods are mentioned below for Sf9 cells and for the YT lysate in the corresponding section 2.6.2.1. Sf9 cells were lysed by resuspending the cell pellet in 1 ml of insect cell lysis buffer for each 4×10^6 cells and incubation on ice for 45 min, mixing cautiously every 10 min. The insoluble material was pelleted at 10,000 x g at 4°C for 30 min and the grB containing supernatant was saved for the further purification.

2.6.1.2 TCA-precipitation

Protein precipitation by trichloroacetic acid (TCA) was used to concentrate cell culture supernatant for grB detection in Western blots. Therefore, 40% TCA solution was mixed 1:1 with cell culture supernatant and then incubated 20 min on ice. Centrifugation was performed at 17,000 x g at 4°C for 20 min and supernatant was

discarded. Pellets were washed twice with 500 μ l of acetone and centrifuged for 15 min. Pellets were resuspended in 1 x reducing sample buffer. When the pellet turned yellow, TAE-buffer was added to neutralize TCA leftovers until the solution became blue again.

2.6.1.3 Protein quantification assay

material / device	ingredients	company
BCA protein assay kit	BSA standard (2 mg/ml), solution A, solution B	Pierce/Thermo Fisher Scientific
Bio-RAD protein assay, dye reagent concentrate		Bio-RAD, Hercules, USA
BSA standard (2 mg/ml)		Pierce/Thermo Fisher Scientific
plate reader EL808		BioTek, Bad Friedrichshall, Germany

Protein quantification was either performed by BCA assay or by Bradford assay. Standards and samples were measured in duplicate in a 96-well plate.

The BCA assay was executed using a BCA protein assay kit. Colorimetric detection of proteins is based on the biuret reaction (copper reduction by means of peptide bindings in alkaline milieu), linked to the stable, sensitive chelating reagent bicinchoninacid. For quantification of protein different concentrations of BSA, diluted in the same buffer as the samples, act as a standard. This assay is quite insensitive to detergents. The plate was incubated at 37°C for 2 h and the absorbance was measured at 550 nm.

The protein determination by the Bradford assay was performed with a purchased dye reagent concentrate according to the manufacturer's instructions. The principle of this assay is that proteins form a complex with the dye coomassie brilliant blue G-250 in acid milieu. Therefore, a quantitative, colorimetric detection of this complex was performed at around 595 nm. For quantification, a standard curve of different BSA concentrations was measured simultaneously. Absorbance was measured at RT at 570 nm after 5 min incubation.

2.6.1.4 grB ELISA

grB from different lots and expression systems was quantified by standard ELISA technique. grB ELISA was performed following the instructions of the grB ELISA kit (Gene-Probe, Inc., San Diego, CA, USA). Briefly, grB antibody-coated 96-well plates were incubated with 100 μ l of samples or standard solutions at different concentrations in combination with the secondary capture antibody, for 3 h at room temperature. After two washing steps, freshly prepared avidin-peroxidase was added for 30 min and afterwards substrate solution for another 12-15 min. Sulfuric acid was added to stop the reaction. Plates were measured at 450 nm and at the reference wavelength 650 nm using the plate reader.

2.6.1.5 Enzymatic activity assay

material / device	ingredients	company
substrate reaction buffer	10 mM HEPES, 140 mM NaCl, 2.5 mM CaCl ₂ (pH 7.4 at RT)	
Ac-IEPD-pNA	substrate VIII	Merck KGaA, Darmstadt, Germany

The colorimetric grB substrate Ac-IEPD-pNA (Ac-Ile-Glu-Thr-Asp-p-Nitroanilide,) was dissolved in DMSO. For qualitative measurements (e. g. to identify the grB containing fractions from the heparin purification step), 5 μ l of sample were incubated with 200 μ M of chromogenic substrate in reaction buffer in a total volume of 100 μ l (for the stability assay 30 μ l of sample in 100 μ l were used). For determining specific activity, different concentrations of purified grB were measured (Dalken et al. 2006). The absorption of the cleaved substrate was measured in a 96-well plate at the wavelength 405 nm using the reader after incubation at 37°C for 60 min.

2.6.1.6 SDS-PAGE, silver staining and Western blot

material / device	ingredients	company
Amersham Hyperfilm™ ECL High Performance chemiluminescence film		GE Healthcare
blotting buffer	20% methanol, 25 mM TRIS, 190 mM glycine, 0.1% SDS (w/v)	
chemicals for fixation and development		Tetenal, Norderstedt, Germany
ECL detection kit		GE Healthcare
electrophoresis buffer	25 mM TRIS, 190 mM glycine	
electrophoresis system Hoefer Pharmacia Biotech SE 250		GE Healthcare
full range rainbow recombinant protein molecular weight marker		GE healthcare
grB antibody, monoclonal (1:2000)	clone 2C5, mouse IgG2a	BD Biosciences
nitrocellulose membrane filter paper sandwich		Life Technologies
PI-9 antibody (polyclonal goat anti-SERPINB9) (1:500)		Everest Biotech Ltd., Oxfordshire, UK
reducing sample buffer, 4 x	100 mM DTT, 5% SDS, 10% glycerol, 0.06 M TRIS, 0.2 mg/ml bromphenol blue (pH 6.8)	
resolving gel	10%/15% acrylamide solution, 0.38 M TRIS (pH 8.8), 0.1% (w/v) SDS, 0.1% (w/v) APS, 0.0004 % (v/v) TEMED	
Roti®-Black P silver staining kit		Roth
secondary mouse anti-IgG horseradish peroxidase antibody (1:2000)		Dianova, Hamburg, Germany
semi-dry blotting system Hoefer Semiphor		GE Healthcare
skim milk, 5%	5% skim milk powder in TPBS	Heirler Cenovis GmbH, Radolfzell, Germany
stacking gel	5% acrylamide solution (37.5:1 acrylamide : N,N-methylenbisacrylamide), 0.13 M TRIS (pH 6.8), 0.1% (w/v) SDS, 0.1% (w/v) APS, 0.001% (v/v) TEMED	
TPBS	PBS with 0.1% Tween 20	Tween 20 from Merck
X-Omat M-35 Developer		Eastman Kodak, Rochester, NY, USA

The stacking and resolving gels were polymerized in a gel caster. Protein samples were mixed with reducing sample buffer and heated for 5 min to 95°C according to the literature (Laemmli 1970). Proteins were separated by their molecular weight using SDS-PAGE at a 10% or a 15% polyacrylamide slab gel in a gel electrophoresis chamber. 200 ng of pure protein per lane (except of the elution fractions, there volumes of approximately 200 ng of grB in the highest fractions were loaded), 10 µg

of cell lysate or 5 μ l of marker (0.5 μ l of marker for silver staining) were applied. Subsequently, the gels were either silver-stained following the manufacturer's instructions to visualize protein bands or further blotted on a nitrocellulose membrane. Blotting was performed with 50 V and 0.8 mA pro cm^2 for 30 min for grB (31 kDa) and 45 min for larger proteins. Blots were blocked with 5% skim milk in TPBS at RT for 1 h. Membranes were incubated with the primary antibody at the above mentioned dilutions in 5% skim milk at RT for 1 h. Afterwards, blots were washed with TPBS and incubated with the secondary antibody coupled with horseradish peroxidase (HRP), for 1 h at RT. Bands were visualized using the ECL kit. Blots were exposed on a chemiluminescence film for normally 5 s for grB detection or and 3 min for Protease Inhibitor-9 (PI-9) detection. Western blot quantification was performed with ImageJ (National Institute of Health, Bethesda, MA, USA).

2.6.2 grB purification methods

2.6.2.1 Nucleus protein isolation

material / device	ingredients	company
YT lysis buffer I	0.5% (v/v) Nonidet P40, 25 mM KCl, 5 mM MgCl_2 , 10 mM TRIS (pH 8.0)	
YT lysis buffer II	YT lysis buffer I, 1% (v/v) Triton X-100	
YT nuclear protein extraction buffer	0.5% (v/v) Nonidet P40, 5 mM EDTA, 10 mM TRIS (pH 8.0 at 4°C)	

For grB purification, YT cell culture was expanded to harvest around 2×10^7 cells at each timepoint. The pellet was washed twice with PBS and stored as a dry pellet at -80°C until around 2×10^8 cells were collected. The pellet was resuspended in 20 ml of ice-cold YT lysis buffer per 2×10^8 cells and incubated for 30 min on ice. Centrifugation was performed at $1,000 \times g$ at 4°C for 5 min. Supernatant was then removed. The pellet was resuspended in YT lysis buffer II. Then the centrifugation step was repeated, supernatant was removed and the pellet was resuspended in buffer II and incubated on ice for 10 min. After a next centrifugation step, the supernatant was removed and the pellet was resuspended in 5 ml of nuclear protein extraction buffer. The next centrifugation step was performed in the micro ultra

centrifuge (50,000 x g, 4°C, 30 min). The supernatant containing nuclear proteins was saved and further purified for grB.

2.6.2.2 Heparin affinity chromatography

material / device	ingredients	company
Äkta prime		GE Healthcare
heparin buffer A	10 mM TRIS, 0.1 M NaCl, (pH 8.0 at 4°C)	
heparin buffer B	10 mM TRIS, 1 M NaCl, (pH 8.0 at 4°C)	
HiTrap™Heparin HP (1 ml/5 ml)	heparin sepharose high performance	GE Healthcare

The heparin binding capacity is around 3 mg protein per ml material. Therefore, the volume of the heparin column was chosen after estimating the amount of grB in the sample. Heparin affinity chromatography was performed at 4°C using an Äkta purifier at a flow rate of 1 ml/min for columns containing 1 ml of heparin sepharose and a flow rate of 2.5 ml/min for 5 ml columns. The run was monitored by the software Äkta View (GE Healthcare). The heparin column was equilibrated with heparin buffer A. The grB containing sample was loaded onto the column and washed with buffer A. When the base line was reached again (280 nm absorption), elution was started. grB was eluted with gradually increasing concentrations of buffer B to 100%. 20 fractions of 2 ml each were collected for 1 ml columns and 20 fractions of 4 ml each were collected for 5 ml columns. The protein content of the different fractions was determined and their grB concentration was ascertained by grB ELISA (2.6.1.4) and Western blot analysis (2.6.1.6). The purity was analyzed by silver-stained SDS-PAGE (2.6.1.6).

2.6.2.3 Nickel affinity chromatography

material / device	ingredients	company
his buffer A	20 mM TRIS, 20 mM imidazole, 500 mM NaCl (pH 8.0 at 4°C)	
his buffer B	20 mM TRIS, 500 mM imidazole, 500 mM NaCl (pH 8.0 at 4°C)	
HisTrap™FF (1 ml)	nickel sepharose G fast flow	GE Healthcare

For (His)₆ tagged proteins, a nickel column (HisTrapTMFF) was used for the first purification step. The binding capacity of the nickel sepharose G fast flow is 40 mg protein per ml material, so that columns containing 1 ml of material were sufficient for my purpose. Nickel affinity chromatography was performed by Äkta purifier of a flow rate of 1 ml/min at 4°C. The HisTrapTMFF column was equilibrated with his buffer A. The grB sample was mixed with 20 mM imidazole loaded onto the column and washed with buffer A until the base line (280 nm absorption) was reached again. grB was eluted with gradually increasing concentrations of his buffer B to 100% within 20 ml, while 20 fractions of 1 ml each were collected. Protein content of the different fractions was determined and their grB concentration was ascertained by grB ELISA (2.6.1.4) and Western blot analysis (2.6.1.6). The purity was analyzed by silver-stained SDS-PAGE (2.6.1.6).

2.6.2.4 Activation procedure through enterokinase (EK) digestion

material / device	ingredients	company
enterokinase (EK) bovine, recombinant expressed in <i>E. coli</i> ; 28 kDa		Sigma
EK buffer	500 mM TRIS, 2 mM CaCl ₂ (pH 8 at RT) plus 1% Tween-20; (buffer was produced without Tween-20, which was added not until finishing the concentration step)	

Inactive grB, derived from transfected HEK293 cells, was concentrated to 1.5 mg/ml, while the buffer was exchanged to EK buffer (2.6.2.5). 0.02 U of recombinant bovine EK was added per mg protein and this mix was incubated at RT on a rotator for 16 h.

2.6.2.5 Buffer exchange

material / devices	ingredients	company
disposable PD-10 desalting columns IMPROVED		GE Healthcare
Amicon Ultra-15 centrifugal filter units	MWCO 10000	Millipore

These two methods for buffer exchange were performed as described in the manufacturer's instructions. Buffer exchange via PD-10 columns was the method of choice if the volume was less than 10 ml and an enhancement of volume of at least 1.4-fold was acceptable. Amicon Ultra-15 centrifugal filter units were chosen to exchange buffer and simultaneously concentrate protein.

2.6.2.6 Filtration

material / devices	ingredients	company
SFCA filter unit 500 ml 75 mm diameter (0.45 µm pore size)		Nalgene/Thermo Fisher Scientific
Supor® membrane (0.2 µm pore size)	sterile filter	PALL Corporation, Port Washington, NY, USA

Culture supernatant was centrifuged (500 x g, 4°C, 10 min) and filtered through a low protein binding SFCA filter unit (0.45 µm) before chromatography steps. For sterile filtration of proteins, the low protein binding Supor® membrane (0.2 µm) syringe filter was used.

2.6.2.7 Storage

Every purification procedure was performed as fast as possible to quickly freeze purified grB and preserve degradation. Sterile filtered grB in PBS was shock frosted in liquid nitrogen and stored at -80°C. A new aliquot was carefully thawed on ice for each usage in experiment. No freeze-thaw cycles were performed.

2.7 Cell biology

2.7.1 Transient and stable transfection of HEK293 cells

For transient grB transfection, 1×10^6 HEK293 cells were seeded in 2 ml of medium per well of a 6-well plate. On the next day, 166 µl of OptiMEM was combined with 6.66 µl of lipofectamine™2000 (Life Technologies) and this solution A was incubated at RT for 5 min. Solution B was prepared from 166 µl of OptiMEM and 2.66 µg of the

plasmid. Solution A and B were mixed gently and the emerging solution C was incubated at RT for 20 min. While solution C was incubating, cells were prepared: The medium was removed and 1.33 ml of OptiMEM was added per well. Next, solution C was added dropwise and the cells were further incubated under standard conditions. On the next day, the supernatant was removed, centrifuged and transferred to a reaction tube. The supernatant was screened by Western blot for secreted grB. Also, cell lysates and precipitated cell culture supernatants were tested.

For producing stable cell lines, the transfection was performed as stated above. 24 h after the transfection, cells were diluted. For this, cells were trypsinated and all cells were seeded into a 10 cm² tissue culture dish in 8 ml of HEK293 medium. On the next day, 300 µg/ml zeocin was added to start the selection process. Medium containing 300 µg/ml zeocin was exchanged regularly. After 1.5 to 2 weeks, non-transfected cells died off and stably transfected cells were expanded. After expansion, 3 x 10⁶ cells per cryovial (TPP) were frozen in a Nalgene™Cryo 1°C freezing container (Thermo Fisher Scientific) in 10% DMSO, 50% FCS, 40% RPMI-1640. Frozen cells were stored in the gas phase above liquid nitrogen.

2.7.2 Single cell cloning

Single cell cloning was performed to find the best grB producing clone of transfected HEK293 cells. Cells were diluted to 2 cells per ml and 200 µl of this cell suspension was pipetted in each well of a 96-well U-bottom plate (on average 0.4 cells per well). After two weeks, clones were transferred to fresh wells of a 96-well flat-bottomed plate and gradually expanded.

2.7.3 grB stability assay

2 x 10⁴ CT26 cells were seeded into half of the wells of a 96-well flat-bottom plate. The other wells were blocked with CT26 medium. After 24 h, the medium was removed and the wells were washed with PBS. For testing the stability of grB under cell culture conditions, 200 µl of grB (4 µg/ml) in RPMI-1640 without phenol red (Life

Technologies) was applied to half of the wells with cells and to half of the wells without cells. To the remaining wells, RPMI-160 without phenol red and without grB was added. At different timepoints, the medium was removed, centrifuged, aliquoted and frozen at -80 °C.

2.7.4 Colony forming assay (CFA)

1.5 x 10² CT26 cells per well were seeded in 0.5 ml of medium in 24-well plates. The outer wells were filled with PBS. After 24 h, the old medium was removed and cells were treated with grB diluted in CT26 medium in triplatt for each treatment condition (0.04, 0.1, 0.2, 0.4, 0.6, 0.8, or 1 µg/ml). After seven days, colonies were fixed and stained. The medium was removed from the dishes and wells were washed with 1 ml of PBS. Colonies were fixed with methanol (-20°C) for 5 min. The fixative was removed and colonies were stained with 1 ml of 0.1% crystal violet for 2 min. The plates were rinsed with tap water and dried. Colonies consisting of more than 50 cells were counted. The plating efficiency (PE) was determined as the number of counted colonies divided by the number of seeded cells. The survival fraction was calculated as the PE of treated colonies divided by the PE of untreated colonies.

2.7.5 Production of spheroids

High affinity plates (Corning Costar 96-well EIA/RIA, Thermo Fisher Scientific) were coated with sterile 1% agarose (Sigma) dissolved in RPMI-1640 without phenol red. 5 x 10³ cells in 200 µl of CT26 medium were pipetted into each well.

For *in vitro* experiments, the spheroids were grown under standard conditions for 4 days. Then, the spheroids were transferred to a fresh uncoated plate to avoid effects of agarose coating during the treatment. This procedure consists of isolating single spheroids of the same size and placing each in a 1.5 ml reaction tube filled with 1 ml of PBS for washing. The tubes were closed and mixed by rotation. After this washing procedure, the spheroids were transferred to a 96-well U-bottom plate filled with 100 µl of RPMI-1640 per well. Treatment was performed in 200 µl of RPMI-1640 as described in the corresponding section (2.7.6).

For *in vivo* experiments, the spheroids were grown for 7 days. After that time, the spheroids were pipetted into a 50 ml tube filled with 30 ml RPMI plus 10% FCS and the closed falcon was turned over to wash the spheroids. Each spheroid was aspirated in 0.2-0.3 ml 5% FCS-containing RPMI-1640 using a 1 ml syringe (luer-lok™ tip, BD; sterican® 0.7 x 30 mm, B.Braun Melsungen AG, Melsungen, Germany). A single spheroid per BALB/c mouse was injected IP.

2.7.6 grB apoptosis assays

material	ingredients	company
camptothecin (cam)	powder was dissolved in DMSO for a 10 mM stock solution	Sigma
PE-conjugated monoclonal active caspase-3 antibody apoptosis kit I		BD Biosciences
Vectashield	mounting medium containing DAPI	Vector Laboratories Inc., Burlingame, CA, USA

For monolayer apoptosis assays analyzed by FACS cytometry, 5×10^5 CT26 mouse tumor cells or CD31 positive cells obtained from BALB/c mice were seeded into 6-well plates in 3 ml of RPMI-1640 mixed at the appropriate concentrations of grB and camptothecin (cam; 4 μ g/ml or 10 μ M, end concentration respectively) as a positive control for apoptosis induction, or PBS alone as negative control. Cells were incubated at 37°C for an additional 4 to 48 h. After the various timepoints, fractions of apoptotic cells were determined by annexin-V staining (see 2.7.7.2) or caspase-3 staining for flow cytometry analysis (see 2.7.7.3). Simultaneously, an Hsp70/PI-staining was performed for each sample as stated in 2.7.7.1.

For monolayer apoptosis assays analyzed by DAPI and caspase-3 fluorescence microscopy, 0.25×10^6 cells in 1.5 ml of CT26 medium were seeded into 2-well chamber slides (Thermo Fisher Scientific). After 24 h incubation, the medium was changed to RPMI-1640 without additives as a negative control or to RPMI-1640 with grB (4 μ g/ml), or cam (4 μ g/ml). After an additional 48 h incubation period, the detached cells in the supernatants and the attached cells on the chamber slides were washed with PBS once and stained separately with active caspase-3-PE antibody. Contrary to the FACS analysis for caspase-3, a PE-coupled antibody was used for fluorescence microscopy, since FITC-labeled caspase-3 bleaches out faster than PE.

Chamber slides as well as detached cells were covered in mounting medium containing DAPI and analyzed by bright field and by fluorescence microscopy.

Apoptosis was induced in spheroids in the following way: After transferring the spheroids to a fresh 96-well U-bottom plate, different concentrations of grB (4, 10, 20, 40, and 80 µg/ml), 4 µg/ml cam, or PBS were added to the spheroids. Medium was added to a total volume of 200 µl. Every third day, spheroids were treated by replacing half of the medium with fresh medium containing additives. 48 h after treatment 10 spheroids were picked and their 3D-tissue structure was disrupted with trypsin/EDTA for 15 min at 37°C and pipetting up and down. Cells were counted and caspase-3 staining and flow cytometry analysis were performed as described in 2.7.7.3.

2.7.7 Flow cytometry analysis

Cells were analyzed by flow cytometry on a FACS Calibur instrument endowed with Cell Quest Pro Version 6.0 software (BD Biosciences).

2.7.7.1 Membrane-Hsp70 staining

material	ingredients	company
cmHsp70.1-FITC/isotype mouse IgG1-FITC		multimmune GmbH, Munich, Germany/ BD Biosciences
FACS buffer	10% FCS in PBS	
MHC class I/isotype mouse IgG1-FITC		Sigma-Aldrich/BD Biosciences
MHC class I H2Dd/isotype mouse IgG2a-FITC		abcam plc, Cambridge, UK/abcam
propidium iodide (PI)	100 µg/ml stock solution (100 x) in PBS	

For the cmHsp70.1-FITC staining, it is important to use the correct antibody dilution as mentioned for each individual lot. The FITC-conjugated mouse IgG1 was used as an isotype matched control antibody. As positive control for adjusting the right settings, MHC class I-FITC (5 µl) was used for human cell lines and MHC class I H2Dd (0.2 µg) was used for cells derived from BALB/c mice together with appropriate isotype controls. The staining should be performed with 1 x 10⁵ cells in a 1.5 ml tube. Cells were washed once with 1 ml of FACS buffer. After centrifugation (500 x g, 4°C,

5 min), the supernatant was removed completely. Antibody was administered to the pellet and mixed. Staining was performed on ice, in the dark for 30 min. After washing the cell pellet with 1 ml FACS buffer, the pellet was resuspended in 500 μ l of FACS buffer and transferred to a FACS tube (5 ml polystyrene round-bottom tube Falcon, BD Biosciences). To differentiate between dead and viable cells, PI was added and FACS analysis was performed immediately. The percentage of positively stained cells was calculated as the number of specifically-stained, propidium iodide (PI)-negative, viable cells minus the number of cells stained with an isotype-matched control.

2.7.7.2 Annexin-V staining

material	ingredients	company
Annexin-V-FLUOS		Roche
annexin buffer	10 mM HEPES, 140 mM NaCl, 2.5 mM CaCl ₂ (pH 7.4)	
annexin solution	10 μ l Annexin-V-FLUOS in 1 ml annexin buffer	

2 x 10⁵ cells were washed subsequently in PBS and in annexin buffer (500 x g, RT, 5 min). The pellet was stained using 100 μ l of annexin solution at RT in the dark for 15 min. 400 μ l of annexin buffer and 5 μ l of PI were added and flow cytometry analysis was performed immediately. Annexin/PI double staining represents late apoptotic and necrotic cells, while annexin only stained cells represent early apoptotic cells.

2.7.7.3 Caspase-3 staining

material	ingredients	company
FITC-conjugated monoclonal active caspase-3 antibody apoptosis kit I	see components below	BD Biosciences
FITC conjugated monoclonal rabbit anti-active caspase-3 antibody		BD Biosciences
Cytofix/Cytoperm™ solution	neutral pH-buffered saline, saponin, 4% (w/v) paraformaldehyde	BD Biosciences
Perm/Wash™ buffer	FCS, sodium azide, saponin	BD Biosciences

The principle of this assay is based on a quantitative FACS measurement of active caspase-3, a key protease that is activated during the early stages of apoptosis. A FITC-conjugated monoclonal active caspase-3 antibody apoptosis kit was used. The provided antibody recognizes human and mouse active caspase-3. Briefly, the procedure was performed as stated below: Cells were trypsinated and combined with detached cells from the supernatant. Cells were washed twice with PBS and subsequently incubated 20 min on ice in 100 μ l of Cytotfix/Cytoperm solution. After fixation, cells were washed twice with 100 μ l of Perm/Wash. Active caspase-3 antibody was added (20 μ l of Perm/Wash plus 4 μ l of caspase-3-FITC per tube) and incubation was performed at RT in the dark for 30 min. 1 ml of Perm/Wash was then added and cells were washed by centrifugation. For FACS analysis, the pellet was resuspended in 500 μ l of Perm/Wash.

2.7.8 Light and immunofluorescence microscopy

Cell culture, monolayer experiments and determination of spheroids' diameter were analyzed using a Zeiss Axiovert 3500 light microscope equipped with 10 x, 20 x and 32 x objectives. Pictures were taken with the camera FinePix S1 Pro; Carl Zeiss, MicroImaging GmbH, Oberkochen, Germany). For fluorescence microscopy, samples were analyzed using a Zeiss Axioscop 2 plus microscope equipped with 10 x, 20 x, and 100 x objective (Achromplan oil) and standard filters. Multiplicative shading corrections were performed using the software Axiovision version 4.7.1 (Zeiss) and photographs were taken using the Axio Cam MRc5 camera (Zeiss). The same microscope was used in the bright field modus for analyzing hematoxylin and eosin (HE) stained tissue paraffin slides. Image procession was performed with the software Photoshop version CS3 (Adobe Systems Inc., San Jose, CA, USA).

2.8 Histopathology and immunohistochemistry

2.8.1 Preparation of histological paraffin sections

material / devices	ingredients	company
automated alcohol series Shandon Excelsior ES		Thermo Fisher Scientific
disposable embedding base molds (15 x 15 mm)		Thermo Fisher Scientific
cytotation pen		DakoCytotation
glass slides superfrost ultra plus		Thermo Fisher Scientific
hematoxylin		Mayer's haematoxylin, pharmacy of hospital rechts der Isar, Munich, Germany
microtom Microm HM355S		Microm; now: Thermo Fisher Scientific
microtome blade R35		PFM, Cologne, Germany
stretching table medite OTS 40		Medite, Burgdorf, Germany
tissue block system TB588		Microm; now: Thermo Fisher Scientific
tissue cool plate COP20		Medite, Burgdorf, Germany
tissue flotation bath medite TFB 35		Medite, Burgdorf, Germany
tissue processing cassettes		Roth

The mouse tumor and organs were fixed in 3.7% PBS-buffered formalin for approximately one week, dehydrated and embedded in paraffin. Afterwards, the fixed tissue was cut in pieces and placed in a tissue processing cassette and transferred through baths of rising ethanol to remove the water. This was followed by the hydrophobic clearing agent xylene to remove the alcohol, and finally molten paraffin, the infiltration agent, which replaces the xylene. This was performed by a robot (Shandon Excelsior ES) at the Institute of Pathology of the Hospital rechts der Isar.

The protocol for embedding and deparaffinizing spheroids was modified and adapted to the special need of these very small tissue parts. Fixed spheroids were transferred to glass slides into an area marked by the fatty cytotation pen. For better visibility the spheroids were prestained with 200 µl of freshly filtered hematoxylin for 1 min. The remaining liquid was pipetted off the slide and the spheroid was washed with PBS for 5 min. Next, an alcohol series was performed in ascending order: 50%, 70%, 96%, and 100% ethanol, and finally 100% xylene. Thereby, the higher concentrated ethanol and xylene did not need to be pipetted off because they evaporated under the chemical hood. I took special care that the spheroids did not dry out. Immediately after the xylene was nearly evaporated, the spheroid was pipetted into a reaction

tube, which was filled with hot, liquid paraffin. The content was completely filled into an embedding form and incubated another 10 min on a heating plate, before it was covered and cooled down.

Paraffin blocks were pre-cooled at -15°C (lung 4°C) and consecutive slices were performed at $2.5\ \mu\text{m}$ thickness for spheroids, mouse organs (liver, kidney, lung, heart, spleen) and mouse tumors. For the mouse organs consecutive slices from two different areas at a distance of $100\ \mu\text{m}$ were performed. Slices were placed in a 45°C preheated water bath for stretching, placed on glass slides and for 10 min on a pre-heated stretching table. Slides were incubated at 60°C in the incubator for 1 h and then stored at RT.

2.8.2 Hematoxylin and Eosin (HE) staining

Formalin-fixed, paraffin-embedded sections on glass slides were stained with Eosin (Eosin y-solution 0.5% aqueous, Merck) and Hematoxylin (HE). HE staining was performed for mouse organs, mouse tumors and CT26 spheroids according to the following standard protocol.

step	solution	period
1.	xylene (A 1)	30 min
2.	xylene (A 2)	30 min
3.	ethanol 100% (1)	10 min
4.	ethanol 100% (2)	10 min
5.	ethanol 96% (1)	5 min
6.	ethanol 96% (2)	5 min
7.	ethanol 70%	5 min
8.	ethanol 50%	5 min
9.	dH ₂ O	5 min
10.	Hematoxylin	1 min
11.	warm tap H ₂ O (not dH ₂ O)	10 min running water
12.	eosin Y-solution 0.5% aqueous (Merck) + 2 drops glacial acetic acid per 200 ml	2 min
13.	dH ₂ O	5 min
14.	ethanol 50%	5 min
15.	ethanol 70%	5 min
16.	ethanol 96%	5 min
17.	ethanol 100%	5 min
18.	xylene (B)	5 min
19.	mounting with Eukitt (O. Kindler, Freiburg, Germany) and covering with a cover slip (24 x 60 mm; Menzel, Braunschweig, Germany / Thermo Fisher Scientific	

2.9 Statistics

Error bars represent the standard deviations (S.D.) of the number (n) of experiments as indicated. The significance of the data was determined by the student's t-test or the paired student's t-test using SigmaPlot (Erkrath, Germany). The following p -values were used as limits for significance levels: $*p \leq 0.05$ (5%); $**p \leq 0.01$ (1%); $***p \leq 0.001$ (0.1%).

3 RESULTS

3.1 Human granzyme B (grB) production

In this study, I established a method for expressing and purifying enzymatically and biologically active granzyme B (grB) sufficient for animal studies. The HEK293 expression system was chosen after testing four different systems. The advantages and disadvantages of each system are described shortly for all systems and with detailed data for the HEK293 system.

3.1.1 Isolation of endogenous grB from YT cell nuclei

grB is not only present in the cytotoxic granules of the NK leukemia cell line YT, but also in the nuclei. Human grB derived from YT cell nuclei is perforin-free (Trapani et al. 1994; Trapani et al. 1996). Therefore, I isolated the nuclei of YT cells and extracted proteins with high salt buffer. DNA was pelleted using a micro ultra centrifuge and grB was further purified by heparin affinity chromatography via the FPLC purification system Äkta prime. Immobilized heparin exhibits a high affinity for grB that also naturally interacts with cell surface heparan sulphate (Veugelers et al. 2006). Herewith, 20 fractions of 2 ml were eluted with gradually increasing NaCl concentrations. The protein content of the different fractions was determined and the grB concentration was measured by ELISA and Western blot analysis. The grB-containing fractions were determined to be 9 and 10 and correspond to NaCl concentrations of 660 to 800 mM (see FIG. 5). By using this method approximately 0.8 mg endogenous grB was purified from 2×10^8 YT cells which were cultured in 0.5 l of medium. The purity of grB as determined by silver-stained SDS-PAGE analysis was about 70% (data not shown). In Western blot analysis grB antibody detected besides grB (31 kDa) another band at 67 kDa (FIG. 5). A band of this size was identified by Sun et al. as a complex consisting of the grB inhibitor Protease Inhibitor-9 (PI-9/Serpin B9) complexed with grB. Detailed analyses have shown that the grB inhibitor co-purifies with grB (Sun et al. 1996). It is proposed that the inhibitor inactivates the grB not stored in cytotoxic granules in order to mediate self-protection in YT cells. This 42 kDa inhibitor is covalently bound to grB and the 67 kDa grB-PI-9-complex is stable in SDS-PAGE. The grB-PI-9-complex was affirmed in my

purification by visualization by an antibody against PI-9 (data not shown). In the consulted literature about grB in NK cell nuclei, a protein band at the identical molecular weight of the grB-PI-9-complex is also present in Western blot analysis; however, this band was not commented as the inhibitor (Trapani et al. 1994).

Despite the presence of the inhibitor, some enzymatic activity was seen in a qualitative enzymatic assay using the chromogenic substrate N-acetyl-Ile-Glu-Thr-Asp-*p*-nitroanilide (Ac-IEPD-*p*NA). The cleavage of this substrate results in an increase in the absorption at a wavelength of 405 nm. However, apoptosis induction could not be detected by annexin-V assay in membrane-Hsp70 expressing human cell lines after 4 and 24 h treatment with grB at concentrations of 100 ng/ml to 10 µg/ml (assay described in 2.7.7.2 and 3.1.3). In contrast, the positive control topoisomerase I inhibitor camptothecin (cam) was able to induce apoptosis (data not shown). A concentration of 40 µg/ml grB was required to induce apoptosis. Experiments were not continued at this high concentration because 40 µg/ml grB exceed the concentrations used in literature for perforin-dependent and perforin-independent apoptosis assays (Azuma et al. 2007; Giesubel et al. 2006; Gross et al. 2003b; Kurschus et al. 2004).

These data reveal that only a small part of the isolated grB is biologically active. Most likely, the small amount of grB inhibitor drastically affects the biological activity of grB (FIG. 5).

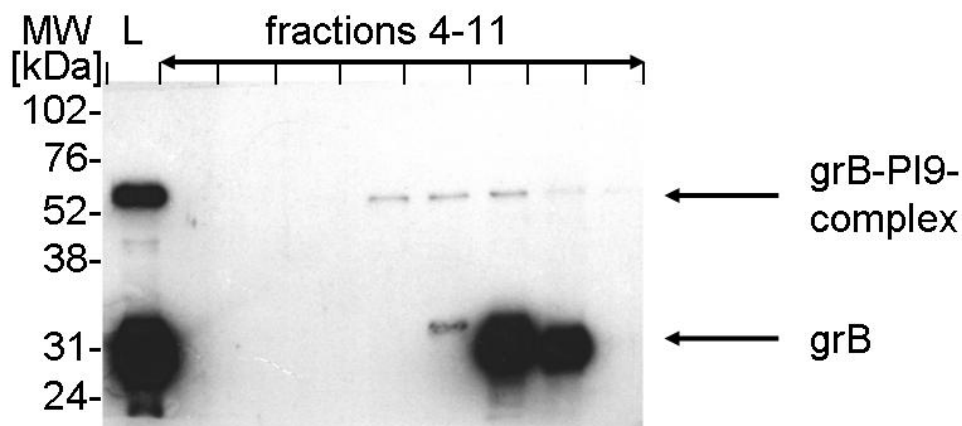


FIG. 5: Purification of grB from nuclei of YT cells. Western blot analysis of a representative purification. The purification process involves a heparin column. 1 µg lysate (L) and 1 µl of the fractions 4-11 (around 200 ng in fraction 9) from 20 fractions of 2 ml total volume each were analyzed, shown from left to the right. For this Western blot, a grB-specific antibody was used and the blot was developed 5 min to visualize the grB-PI-9-contamination. grB protein is visible at around 31 kDa, whereas the covalent grB-PI-9-complex has a size of 67 kDa. The grB-containing fractions were determined to be 9 and 10 and correspond to NaCl concentrations of 660 to 800 mM.

3.1.2 Purification of grB produced by *Pichia pastoris*

Pichia pastoris is regarded as an established eukaryotic cell system for the production of a number of recombinant proteins. The system allows post-translational modifications, which are needed by higher eukaryotic cells such as proteolytic processing, disulfide bond formation, folding, and glycosylation. It was chosen because it is faster, easier, and less expensive to use than expression systems derived from higher eukaryotes such as insect and mammalian tissue culture cell systems. Usually, the yields are higher compared to other systems. The system was established by our cooperation partner (K. Zettlitz, laboratory of Prof. Dr. R. Kontermann, Institute for Cell Biology and Immunology, University of Stuttgart, Germany). I obtained supernatants derived from *Pichia pastoris* secreting (His)₆-tagged mature grB for purification. The mature form of grB comprises 227 amino acids (EC number 3.4.21.79) starting with Ile-21 (Trapani et al. 1988). The signal peptide (pre-sequence: amino acids 1-18) and the prodomain (pro-sequence: amino acids 19-20) were effectively deleted on DNA level. After heparin affinity purification, only 0.3 mg grB could be obtained from 0.5 l of culture supernatant. This was very low compared to a single purification process in YT cells. The enzymatic activity was proven by a qualitative substrate assay using the colorimetric substrate Ac-IEPD- ρ NA. The grB produced by *Pichia pastoris* did not induce apoptosis in membrane-Hsp70 expressing human cell lines (measured by annexin-V assay; data not shown). The molecular weight was about 35 kDa, whereas the molecular weight of YT cell-derived grB shown in SDS-PAGE was only 31 kDa. Therefore, it was assumed that the missing apoptosis induction was due to a different glycosylation pattern. Regarding the low yield and the lack of function, a different expression system was tested.

3.1.3 Purification of grB produced by Sf9/Baculovirus

Sf9 cells are derived from pupal ovarian tissue of the Fall armyworm *Spodoptera frugiperda*. Sf9 cells are easily infected with recombinant baculovirus and consequently comprise a suitable eukaryotic expression system for eukaryotic proteins that require post-translational modifications. The transfection of Sf9 cells

with grB-producing Baculovirus and the lysis of the cells were performed as explained in 2.3.1.2 and 2.6.1.1. It has to be noted that it is important to use lysis buffer without protease inhibitors. My previous experiments indicated that protease inhibitors negatively affect the enzymatic activity of grB (data not shown). 3×10^7 transfected cells were harvested and lysed. grB was further purified from the supernatant by heparin affinity chromatography via the FPLC purification system Äkta prime. Herewith, 20 fractions of 2 ml were eluted with gradually increasing salt concentrations. The protein content was determined for each fraction separately. The grB concentration was confirmed by grB ELISA and Western blot analysis. Ultimately, around 0.3 mg of recombinant grB with a purity of 70% were obtained from 3×10^7 cells. The enzymatic activity was shown using a qualitative assay measuring the cleavage of the colorimetric substrate Ac-IEPD-*p*NA. Apoptosis was measured by annexin-V/propidium iodide (PI) staining using flow cytometry analysis. Whereas annexin-V binds to phosphatidylserine exposed on the outer membrane leaflet of apoptotic cells, PI staining is a marker for late apoptotic and necrotic cells. The membrane-Hsp70 positive (> 80%) human colon carcinoma cell line CX+ was incubated with 2-20 μ g/ml grB for 24 h. As a positive control 4 μ g/ml of cam were used and as a negative control (ctrl), PBS was added in identical amounts. Trypsinated and detached cells in the supernatant were collected, pooled and stained with annexin-V/PI. The amount of annexin-V positive cells not stained by PI marks the cells in early apoptosis (FIG. 6; black bars: early apoptotic cells). The induction of cell death was determined by an increase in annexin-V positive cells plus annexin-V/PI double-positive cells (FIG. 6, grey bars: early apoptotic and late apoptotic/necrotic cells).

These cell death measurements gave no hint for any biological activity targeting membrane-Hsp70 positive cells (FIG. 6; compare the first two bars of the negative control (ctrl) with the middle two bars of grB; $n = 4$). In contrast, the positive control cam was able to induce significant cell death (FIG. 6; two bars on the right side; $p^* = 0.02$; $p^{**} = 0.003$). Since neither early nor late apoptosis could be induced by grB derived from Sf9 cells, this expression system was not further developed.

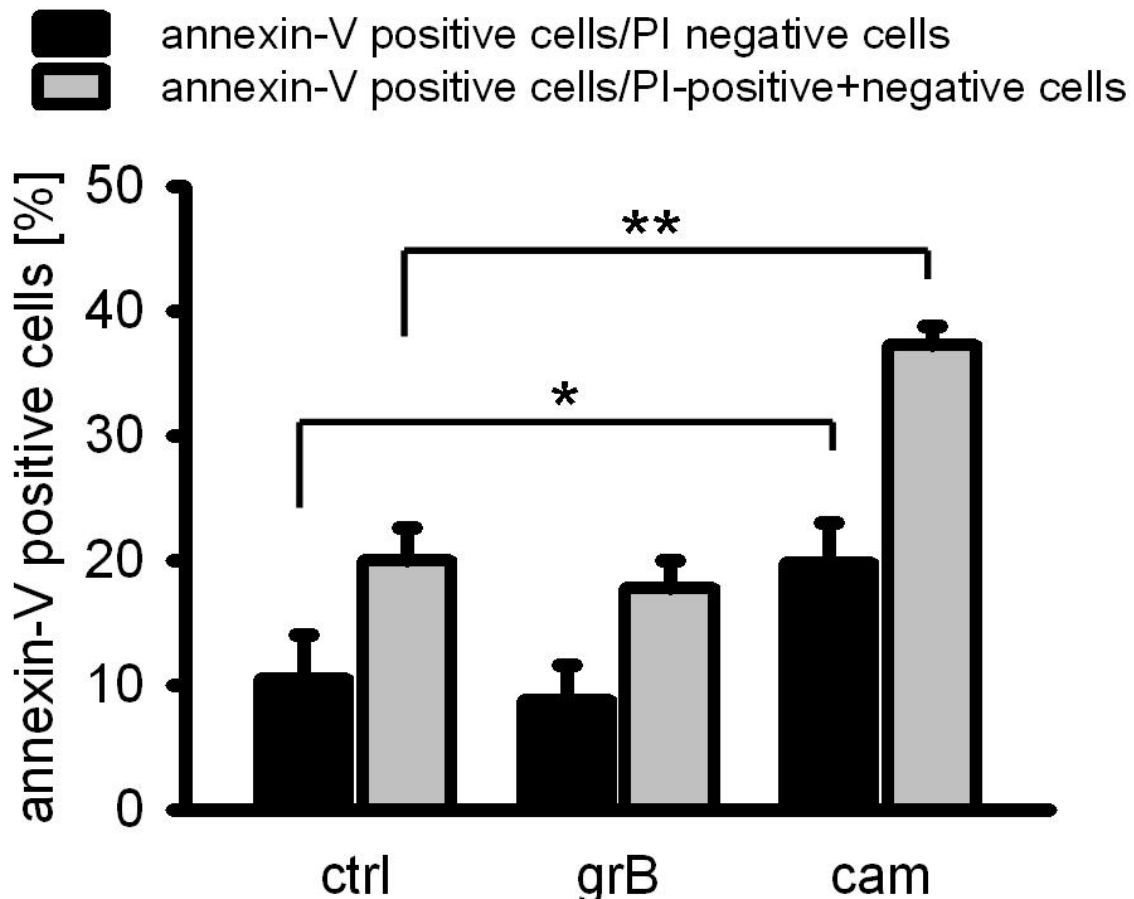


FIG. 6: Sf9/Baculovirus-derived grB tested on CX+ cells for apoptosis induction. The membrane-Hsp70 expressing tumor cell line CX+ (> 80%) was used to test the ability of Sf9/Baculovirus-derived grB to induce apoptosis. Cells were treated for 24 h with PBS (ctrl), with different concentrations of grB (grB) and with 4 $\mu\text{g/ml}$ cam as positive control (cam). In the first experiment, 2 $\mu\text{g/ml}$ grB was used, which was raised to 4 $\mu\text{g/ml}$ grB in the second experiment and to 20 $\mu\text{g/ml}$ grB in the third and fourth experiment. The experiments were pooled due to the fact that apoptosis was not even induced at the highest concentration. Here, the mean \pm S.D. of the four independent experiments is shown. Bars represent significance between cam and the corresponding ctrl ($p^* = 0.02$; $p^{**} = 0.003$).

3.1.4 Production of grB by mammalian HEK293 cells

Finally, a human embryonic kidney (HEK293) cell expression system was tested. I performed the cloning and transfection in the laboratory of Prof. Dr. R. Kontermann (Institute of Cell Biology and Immunology of the University of Stuttgart).

A modified pSECTagA vector (pSECTagAL1; 5.2 kb) with a cleavage site for the restriction enzyme AgeI in its multiple cloning site was used to express active grB. As active grB might harm the HEK293 cells, an alternative cloning strategy to produce inactive grB was pursued. Active mature and inactive GZMB (approved gene symbol

for granzyme B) were amplified by PCR from the template of human pre-pro-GZMB (cDNA) cloned into a pCMV6-XL4 cloning vector. For amplification of the sequence for active mature GZMB without the signal sequence for secretion (gene sequence coding for amino acids 1-18) and the inactivating prodomain (gene sequence coding for amino acids 19-20) the primers Agel-GZMB-back (5' TTT ACC GGT ATC ATC GGG GGA CAT GAG 3') and GZMB-Stop-EcoRI-forward (5' CCG GAA TTC TTA GTA GCG TTT CAT GGT TTT C 3') were used (FIG. 7; primers in upper row). To generate inactive GZMB the coding sequence for a (His)₆ tag was placed after the cutting site for Agel and the GZMB gene was modified by replacing the pre-pro-peptide with the coding sequence for an EK cleavage site between the mature GZMB and the sequence coding for the (His)₆ tag by PCR (FIG. 8B). Therefore, the primers Agel-(His)₆-EK-GZMB-back (5' TTT ACC GGT CAT CAT CAT CAT CAT GAC GAC GAC AAA ATC 3') and GZMB-Stop-EcoRI-forward were used (FIG. 7; primers in lower row).

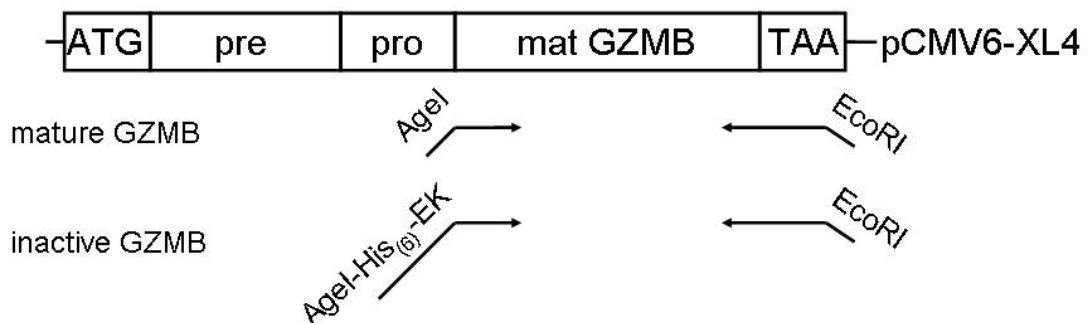


FIG. 7: Scheme of the PCR for the mature and the inactive grB gene construct. For PCR, primers (back) were designed that insert an Agel cleavage site on the 5' end of the construct and delete the sequence coding for the pro-pro-peptide. For the construct used for inactive GZMB between the cutting site for Agel and the sequence for mature GZMB (cDNA) an additional sequence for a (His)₆ tag and for an EK cutting site were included due to the primer sequence. For both constructs, the forward primer was designed for annealing at the end of the mature GZMB, including the TAA-Stop sequence and additionally inserting a cleavage site for the restriction enzyme EcoRI .

Both PCR products, the mature GZMB and the inactive GZMB, were digested with Agel and EcoRI and inserted into the respective restriction sites of the modified pSECTagA vector resulting in the plasmids pSECTagAgel-GZMB (5794 base pairs (bps); FIG. 8A) and pSECTagAgel-(His)₆-EK-GZMB (5827 bps; FIG. 8B). After ligation, the plasmids were transformed into *E. coli* and the amplified plasmids were

extracted. The purified plasmids were resuspended in sterile water and the sequence was validated. In both strategies, the in-frame fusion after the Ig κ -chain leader sequence enabling secretion of heterologous proteins was confirmed. The mature GZMB was correctly inserted, but the inactive GZMB contained a mutation of the base 390. In the base triplett AAG, the G was replaced by an A representing a silent mutation (lysine \diamond lysine). The plasmid map and the entire sequence of pSECTagAgeI-(His)₆-EK-GZMB are shown in the appendix.

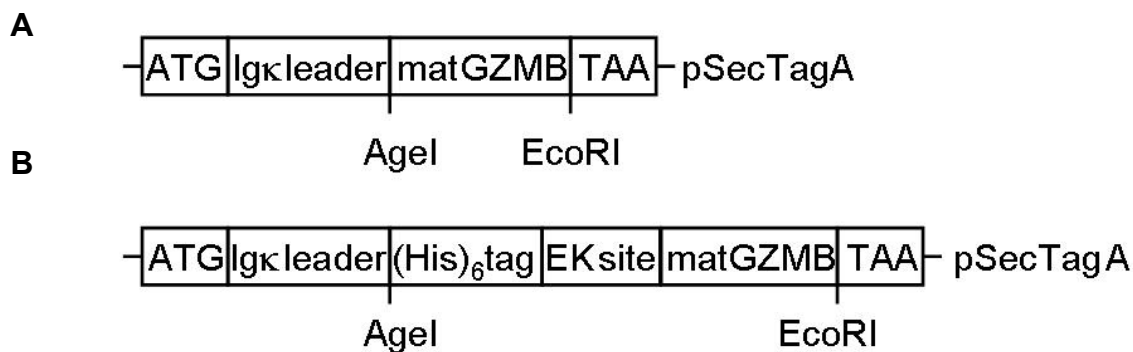


FIG. 8: Schematic representation of the constructed vectors used to clone mature and inactive grB. ATG represents the start codon and the Ig κ leader tags the mRNA for becoming a secreted protein. The inserts were each cloned into an additive AgeI site and the existing EcoRI site of the multiple cloning site of the pSecTagA vector. **A** The mature GZMB was cloned into the vector to express the coding sequence of 227 amino acids starting with Ile-21. **B** The inactive GZMB was cloned into the vector to express a (His)₆ tag, the enterokinase (EK) site and the mature grB.

First, I tried to establish the HEK293 cell system for producing active recombinant human grB. After successful cloning and transient transfection, active grB was expressed by HEK293 cells and was detectable in the TCA-precipitated supernatant. Next, a stable transfection was performed (data not shown). However, under these conditions HEK293 cells were harmed by the active grB. HEK293 cells lost their adherence and underwent apoptosis. The yields decreased even more when HEK293 cells were cultivated in the FCS free producing medium OptiMEM.

Therefore, the strategy was to produce inactive grB, which would not harm the producing cells. HEK293 cells were transiently transfected with pSECTag-AgeI-(His)₆-EK-grB. The presence of inactive recombinant human grB in the cell culture supernatant of transiently transfected HEK293 cells was tested by Western blot analysis. After the transient production was proven successfully (data not shown), the transfection procedure was performed by selection of stably transfected cells via 300

$\mu\text{g/ml}$ zeocin. Those stably transfected cells secreted $(\text{His})_6\text{-EK-grB}$ into the cell culture supernatant. The expressed protein consisted of the mature grB amino acid sequence, starting with IIGGH and ending with MKRY. Amino-terminally a $(\text{His})_6$ tag was expressed and the mature grB was inactive by the sequence DDDDK forming a new inactivating prodomain which could be cleaved by enterokinase (schematic protein shown in FIG. 9).

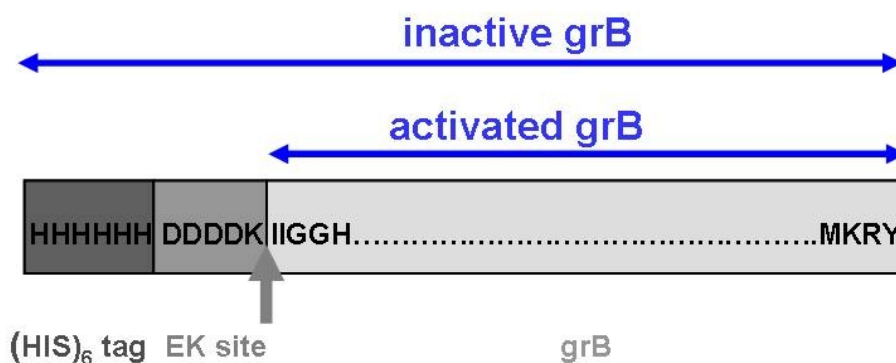


FIG. 9: Inactive grB expressed by HEK293 cells. The HEK293-derived grB was expressed in its inactive form by the amino acid sequence DDDDK representing an EK cutting site. A $(\text{His})_6$ tag (HHHHHH) was expressed amino-terminally to the EK cutting site and thus gets cut off during EK activation. The activated grB represents the mature grB starting with the amino acid sequence IIGGH and ending with MKRY without any further modifications.

Single cell cloning was performed in two 96-well plates to isolate the best producing clone and to establish a monoclonal production cell line. After selection, nine clones grew and were subsequently expanded. The C10 clone (nomenclature based on wells in a 96-well plate) was chosen as the best producing clone (data not shown). For grB production, the cells were expanded to 20 T162 flasks at a confluency of 80%. The cells were cultured for 2 weeks and the supernatant of 500 ml was collected every 3-4 days. After centrifugation ($500 \times g$, 4°C , 10 min) and filtration to remove detached cells, the supernatant was immediately applied to a nickel column. After washing, the bound $(\text{His})_6\text{-EK-grB}$ was eluted with increasing concentrations of imidazole ranging from 20 to 500 mM. 20 fractions at a volume of 1 ml each were collected. Fractions 8-12, which refer to imidazole concentrations of 168 to 308 mM were found to contain $(\text{His})_6\text{-EK-grB}$. The presence of grB was proven by SDS-PAGE with subsequent silver staining or Western blot analysis as shown (FIG. 10A+B). Before the next step, the grB-containing fractions from the four consecutively purified cell culture supernatants were pooled (pool 1). The buffer was substituted with EK

buffer and the grB was concentrated to a final concentration of 1.5 mg/ml. The EK digestion was performed removing the inactivation site and the (His)₆ tag so that grB became activated. The efficiency of the EK digestion was tested by silver staining (FIG. 10C) and Western blot analysis (FIG. 10D). Lane -EK shows grB before digestion (MW ~34 kDa), lane +EK shows digested activated grB, which results in a lower molecular weight (MW ~31 kDa).

Pool 1 containing activated grB (pool 1; +EK) was administered to a heparin column because the highly positively charged grB has a strong affinity for the negatively charged heparin column. Elution was performed using a gradient of 0.1 to 1.5 M NaCl and 20 fractions of 2 ml each were collected. Activated grB was detected in fractions 9 and 10 at NaCl concentrations of 660 to 800 mM and pooled (FIG. 10C+D, pool2a). After changing the buffer to PBS and sterile filtration, aliquots were frozen at -80°C (FIG. 10C+D, lane pool2b).

TAB.1 shows the results of six grB preparations. Starting with two liters of supernatant, 8.0 ± 1.9 mg grB was purified after the nickel column purification (TAB.1, column 1). Following the EK digestion and heparin column, 4.9 ± 2.0 mg grB was obtained (TAB.1, column 2). After buffer exchange to PBS and sterile filtration, 4.0 ± 1.6 mg highly pure grB (> 95 %) was obtained (TAB.1, pure grB).

These preparations yielded sufficient amounts of grB to perform *in vitro* and *in vivo* experiments.

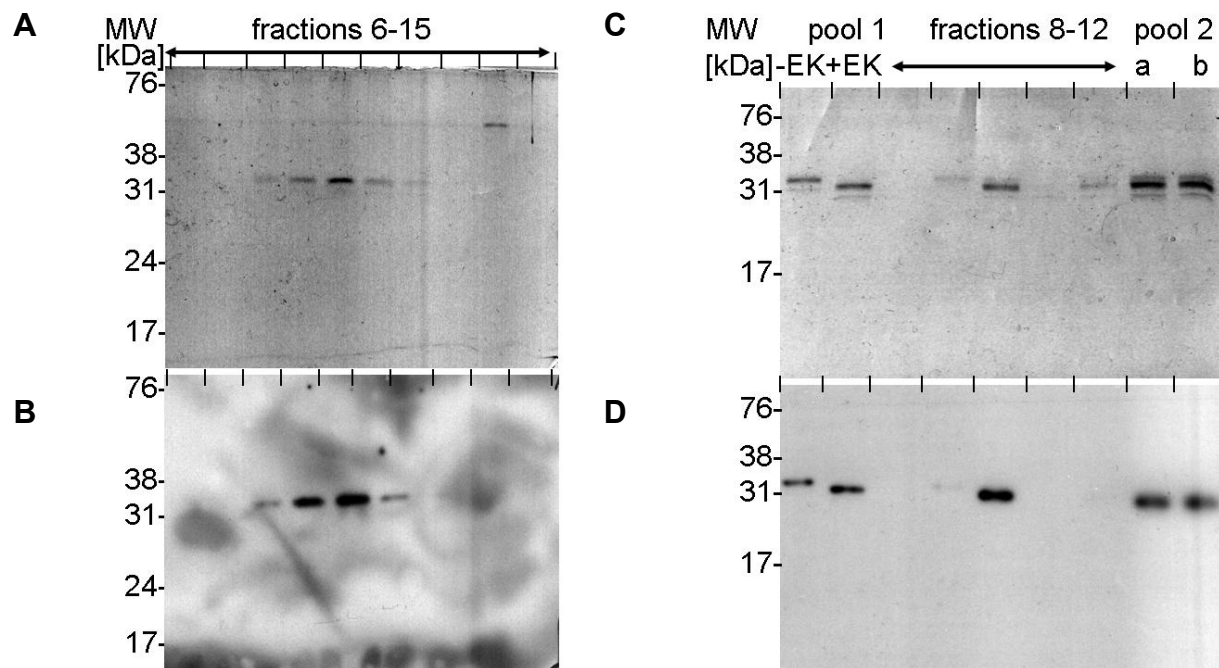


FIG. 10: Purification of human grB expressed in HEK293 cells.

Silver-stained SDS-PAGE and Western blots analyses are shown for a representative purification.

A-B Illustrate the first step of the purification process using a nickel column for (His)₆ tag purification. Fractions 6-15 were analyzed by SDS-PAGE, shown from left to right. Equal volumes of each fraction were applied (200 ng in fraction with the highest concentration). The grB-containing fractions were determined to be 8-12 and pooled. **A** Silver-stained SDS-PAGE gel. **B** Western blot using the grB-specific antibody 2C5.

C-D Represent the further steps of the purification process and show from left to the right: Pool of the grB-containing fractions from the (His)₆ tag purification (Pool 1 -EK; 200 ng protein was applied); EK digestion (Pool 1 +EK; 200 ng protein was applied); fractions 8-12 from heparin affinity chromatography (fractions 8-12; equal volumes of each fraction were applied; 200 ng in fraction with the highest concentration). Fractions 9 and 10 were chosen as grB-containing fractions and pooled (Pool 2a; 200 ng protein was applied). In the end, buffer was exchanged to PBS and the grB was sterile filtered (Pool 2b; 200 ng protein was applied) and stored at -80°C.

C Silver-stained SDS-PAGE gel. **D** Western blot using the grB-specific antibody 2C5.

TAB.1 Amount of grB produced by HEK293 cells after different purification steps from 2 liters of supernatant (comparison of 6 different preparations).

PURIFICATION STEP	1	2	3	4	5	6	MEAN ± S.D.
column 1	7.0 mg	9.0 mg	6.0 mg	5.8 mg	10.0 mg	10.0 mg	8.0 ± 1.9 mg
column 2	3.2 mg	5.5 mg	3.3 mg	3.7 mg	5.3 mg	8.4 mg	4.9 ± 2.0 mg
pure grB	2.5 mg	4.8 mg	2.2 mg	3.4 mg	4.4 mg	6.6 mg	4.0 ± 1.6 mg

3.2 Enzymatic activity and *in vitro* stability

The enzymatic activity of various lots of activated grB purified from HEK293 cells was proven in a substrate Ac-IETD-pNA assay. By increasing the concentration of grB up to 6.2 $\mu\text{g/ml}$, the absorption at 405 nm increased from the base line 0.037 ± 0.001 up to 0.430 ± 0.016 (FIG. 11). The graph shows mean values of three independent grB purification procedures. The enzymatic activity of HEK293 cell-derived grB was greater than that of same amounts of grB derived from YT cells, Sf9/Baculovirus transfection and *Pichia pastoris* expression (data not shown). Due to the high conformity of the results, high activity and the high yields, grB purified from the HEK293 expression system was used for all further experiments.

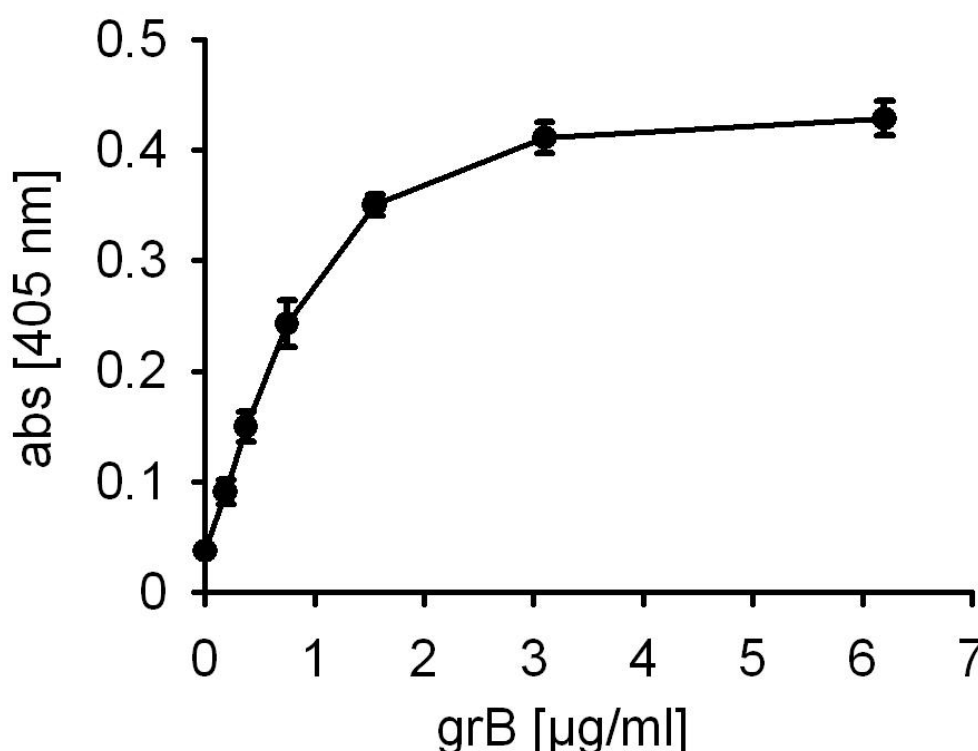


FIG. 11: Enzymatic activity of recombinant human grB. grB at the indicated concentrations was incubated with chromogenic substrate (200 μM Ac-IETD-pNA) at 37°C for 60 min. Absorption was measured at 405 nm. Results are derived from 3 independent purifications. Mean values \pm S.D. are shown.

Before starting further *in vitro* experiments, it was important to determine the stability of grB under cell culture conditions. Therefore, 4 $\mu\text{g/ml}$ grB was added to cell culture and to pure medium. Incubation was performed under cell culture conditions (37°C; 5% CO₂; 95% humidity) and enzymatic activity was measured in the supernatant

after different timepoints (FIG. 12). In cell-conditioned supernatant the enzymatic activity of active grB steadily decreased from day 0 to day 9 from 100% to $36 \pm 8\%$ (FIG. 12). Approximately on day 6, the activity fell below the value of 50%. These data were confirmed by ELISA. A decline of grB to 50% of the starting concentration was measurable within 12 days (data not shown). As a result of these data, grB was re-newed every 3 days in cell culture experiments ($> 50\%$ activity).

The absence of cells did not affect the activity of grB, compared to the data obtained by cell-conditioned supernatant (data not shown). grB that was thawed and stored at 4°C instead of incubated at 37°C showed only a decrease of 10% activity within 10 days (data not shown).

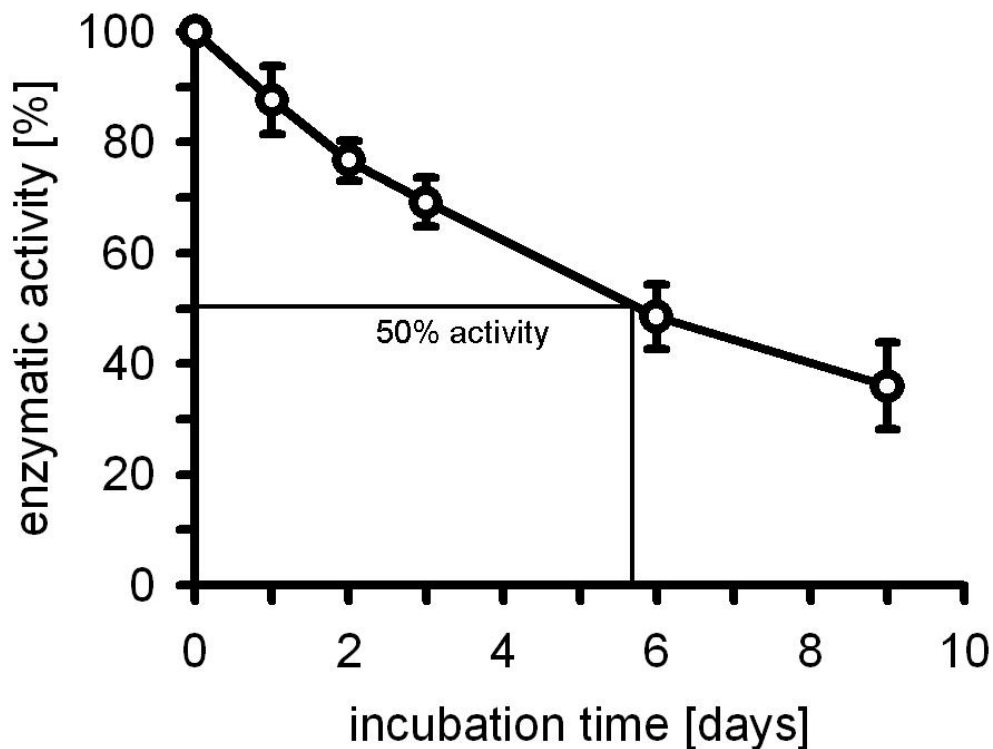


FIG. 12: Stability of grB (4 $\mu\text{g}/\text{ml}$) under cell culture conditions. The enzymatic activity of grB, which was incubated together with cells under cell culture conditions, was measured with the chromogenic substrate Ac-IEPD-*p*NA at day 1 to day 9. 30 μl of supernatant were added to 100 μl of total volume to process 200 μM substrate. Mean values of 3 independent experiments \pm S.D. are shown.

3.3 Biological activity in cell culture

3.3.1 Apoptosis assay in a mouse cell system

3.3.1.1 CT26 tumor mouse cells

HEK293-derived inactive grB, which was purified and activated by EK digestion, shows high enzymatic activity and perforin-independent apoptotic activity in human membrane-Hsp70 bearing cancer cells (annexin-V assay (2.7.7.2) and caspase assay (2.7.7.3); data not shown). Gross et al. have already shown that grB alone, without any perforin, shows apoptotic activity specifically towards human cancer cells expressing Hsp70 on their plasma membrane (Gross et al. 2003b).

As a next step to further develop a grB-based therapy, it is necessary to test the activity of grB in a syngeneic tumor mouse model. Therefore, human grB was tested against mouse tumor cells, which express Hsp70 on their membrane. The membrane-Hsp70 positive colon adenocarcinoma cell line CT26 (50-60 %), derived from BALB/c mice was tested for its sensitivity to human grB. CT26 cells were incubated with grB (4 µg/ml) for different periods of time. As a positive control, cells were incubated with cam (4 µg/ml) and as a negative control (ctrl), PBS was added. 12 h (black bars), 24 h (grey bars), and 48 h (white bars) after treatment, adherent and non-adherent cells were pooled and the percentage of caspase-3 positive cells was determined by flow cytometry analysis (FIG. 13A). The percentage of active caspase-3 positive cells indicating early apoptosis increased from $3 \pm 0\%$ to $22 \pm 9\%$ after 12 h, to $39 \pm 17\%$ after 24 h, and to $54 \pm 8\%$ after 48 h grB treatment (FIG. 13A, left and middle groups of bars). The apoptotic effect was comparable after treatment with cam (FIG. 13A, middle and right group of bars). The data represent the mean of three to ten independent experiments \pm S.D. Values which are significantly different between ctrl and grB treatment are indicated with asterisks (***) $p = 0.0001$; ** $p = 0.009$).

Light microscopical analyses 48 h after treatment with 4 µg/ml grB show that the cells change their morphology in cell culture (FIG. 13B, compare ctrl (top) with the grB-treated cells (middle)). Loss of adherence is shown by a round-shaped appearance (FIG. 13B, middle). Similar effects were observed by cam treatment (FIG. 13B, bottom). The pictures illustrate representative views of one out of three experiments. The data were confirmed by fluorescence microscopy analyses of CT26 cells (FIG. 13C). Cells were grown in chamber slides for 24 h and then treated with 4 µg/ml grB

(middle column), 4 µg/ml cam (right column) or were kept untreated (ctrl, left column) for 48 h. Analysis was performed for adherent cells in chamber slides (FIG. 13C, top row), and for detached cells collected from the supernatant (FIG. 13C, bottom row). Cells were stained with a PE-labeled antibody against caspase-3 (red staining) for 30 min, and mounted with Vectashield containing DAPI (blue staining). Representative pictures are shown in FIG. 13C. Adherent control cells (upper left panel) show typical nuclear blue staining with dotted intensive blue staining due to the structural organization of the nucleus. Cell nuclei have a regular round ellipsoid form with a sharp border. The differences between the cells are small. No red staining of caspase-3 expression is detectable. There were only a few cells present in the supernatant of control cells (FIG. 13C, bottom left). These cells are not healthy and show characteristics such as decreased size of their nuclei and a homogenous blue staining. grB-treated cells (FIG. 13C, middle row) tend to undergo apoptosis characterized by decreased size of their nuclei, irregular border shape, and a nearly homogenous blue staining due to the loss of the structural organization of the nucleus, which leads to nucleus fragmentation. The slight red staining indicates the activation of caspase-3 in adherent cells (FIG. 13C, middle row, upper panel) and is much more pronounced in the detached cells (FIG. 13C, middle row, bottom panel). Cam-treated cells show similar characteristics as grB-treated cells (FIG. 13C, right column of panels).

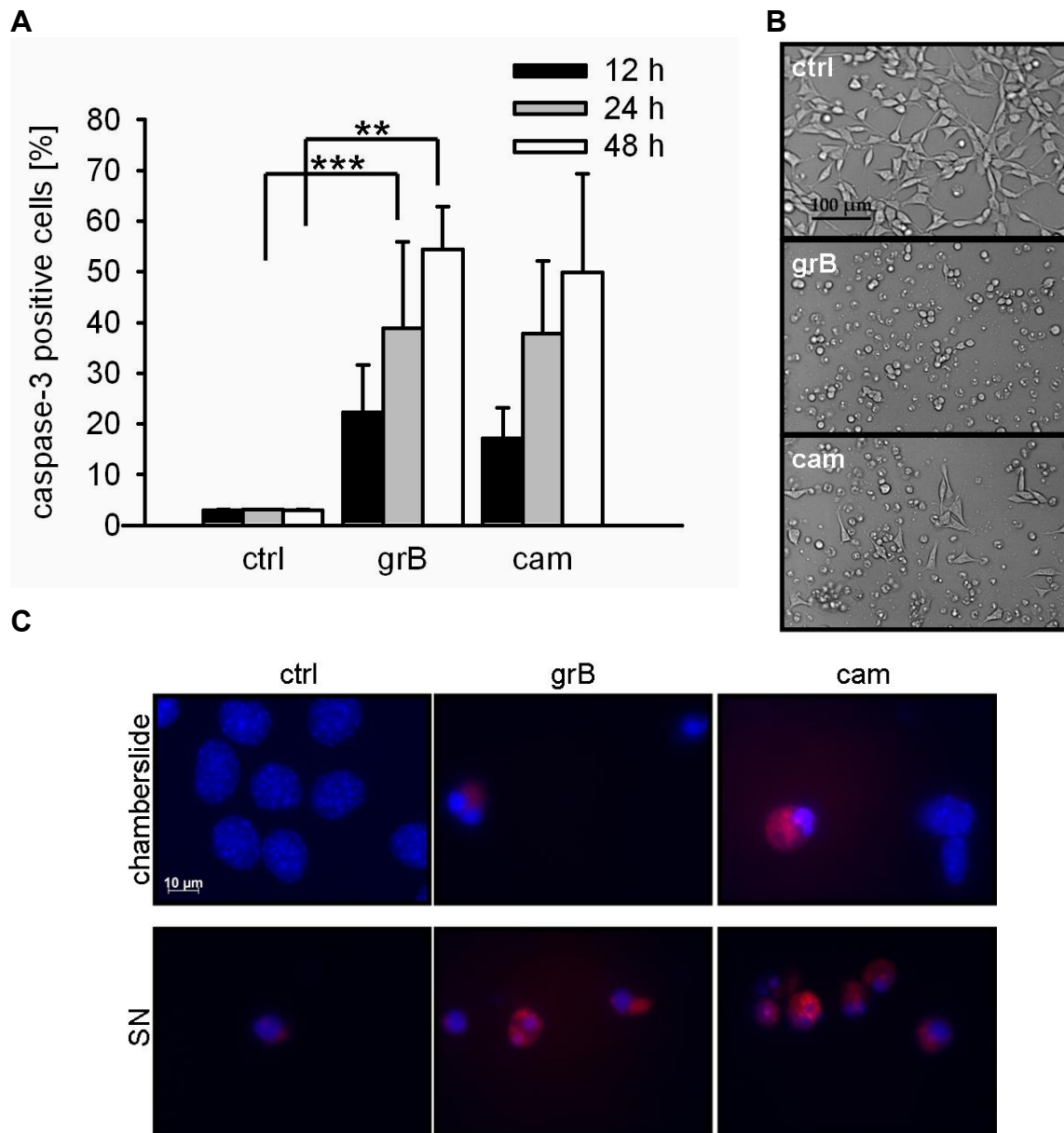


FIG. 13: Induction of apoptosis in murine CT26 tumor cells by recombinant human grB. CT26 cells were treated with PBS (ctrl) as negative control, with 4 μ g/ml grB (grB) and with 4 μ g/ml camptothecin (cam) as positive control at timepoints as indicated. **A** For caspase-3 staining, cells were collected 12 h (black bars), 24 h (grey bars) or 48 h after treatment (white bars) and stained with a fluorescence labeled antibody. The fraction of active caspase-3 positive cells was determined by flow cytometry analysis. The data represent the mean of 3-10 independent experiments \pm S.D. Bars represent significance between grB and the corresponding ctrl ($p^{***} = 0.0001$; $p^{**} = 0.009$). **B** Light microscopical bright field analysis of adherent growing CT26 cells treated 48 h either with PBS (ctrl), 4 μ g/ml grB or 4 μ g/ml cam. Pictures are representative for independent experiments with similar results ($n = 3$, objective 20 x, scale bar 100 μ m). **C** Fluorescence microscopical analysis of CT26 cells. Cells were grown in chamber slides for 24 h and treated with human grB, cam or left untreated (ctrl) for 48 h. Detached cells were collected and are shown in the lower row. The blue pattern shows nuclear staining with DAPI and the red staining highlights active caspase-3. Pictures show typical results of independent experiments ($n = 3$, objective 100 x, scale bar 10 μ m).

The induction of late apoptosis/necrosis (PI positive cells [%]) 12 h, 24 h and 48 h after treatment with 4 $\mu\text{g/ml}$ grB or cam was measured by flow cytometry analysis. In FIG. 14A the mean values of four independent experiments \pm S.D. are illustrated. FIG. 14A shows that both, grB and cam, induce cell death but cam to a higher extent than grB. The opposite effect was detected after determination of cell numbers. While untreated cells show an increase in cell numbers at each timepoint, grB- and cam-treated cells start to diminish from 12 h onwards (FIG. 14B mean values \pm S.D. of independent experiments after 12 h (n = 5), 24 h (n = 9) and 48 h (n = 4) treatment).

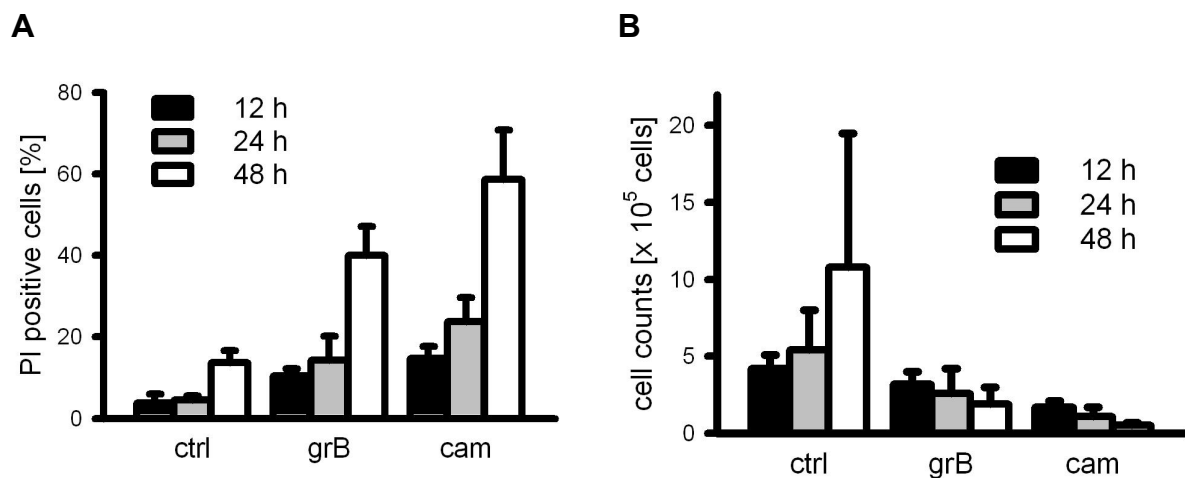


FIG. 14: Changes in the amounts of PI positive cells and cell numbers after incubation with PBS (ctrl), grB and cam. CT26 cells were treated with PBS as a negative control (ctrl), 4 $\mu\text{g/ml}$ grB (grB) or 4 $\mu\text{g/ml}$ cam as positive control at the timepoints indicated. Cells were collected 12 h (black bars), 24 h (grey bars) or 48 h after treatment (white bars), counted and stained by PI. **A** The fraction of PI positive cells was determined by flow cytometry analysis. The data represent the mean of 4 independent experiments \pm S.D. **B** Cell numbers were determined by manually counting cells in a Neubauer counting chamber by light microscopy. The data represent the mean of 4-9 independent experiments \pm S.D.

3.3.1.2 Normal mouse cells

To exclude that grB has a negative effect on normal cells that lack the membrane expression of Hsp70, CD31 positive endothelial cells were tested. The CD31 positive cells investigated were derived from BALB/c mice after sorting by magnetic beads. These cells were chosen because they come into direct contact with grB after intravenous (IV) injection. No notable staining with cmHsp70.1 monoclonal antibody was detected by flow cytometry (data not shown). CD31 positive cells from BALB/c

mice (normal) and CT26 tumor cells (tumor) were treated with either PBS or 4 $\mu\text{g/ml}$ active grB. Microscopical analyses showed that in contrast to CT26 cells, the CD31 positive mouse endothelial cells retain their adherence and regular morphology even 48 h after treatment with 4 $\mu\text{g/ml}$ grB (compare grB-treated cells from FIG. 15B with FIG. 13B). Cells in supernatant and adherent cells were collected 24 h after treatment and stained for active caspase-3 with a FITC labeled antibody. The fraction of cells positive for active caspase-3 was determined by flow cytometry (FIG. 15A). After incubation with grB (4 $\mu\text{g/ml}$), the percentage of caspase-3 expressing normal mouse cells remained nearly unchanged ($3 \pm 0\%$ to $7 \pm 6\%$) (FIG. 15A, left side). The fraction of caspase-3 positive tumor cells with an initial value of $3 \pm 1\%$ increased to $35 \pm 11\%$ following grB treatment (4 $\mu\text{g/ml}$) (FIG. 15A; right side). The data represent the mean values of six independent experiments \pm S.D. Significant differences were shown between grB and PBS treatment of CT26 tumor cells ($p^{***} = 0.001$). In contrast to tumor cells, endothelial cells showed no statistically significant change in the amount of active caspase-3 positive cells ($p = 0.2$). Most importantly, I could show a significant difference in grB-mediated apoptosis between normal murine cells and CT26 tumor cells ($p^{***} = 0.001$).

In addition to the high enzymatic activity, I have shown that the grB produced by HEK293 cells is biologically active. It specifically induces apoptosis in monolayer mouse tumor cells expressing Hsp70 on their membrane, but not in normal mouse cells that lack a membrane-Hsp70 expression.

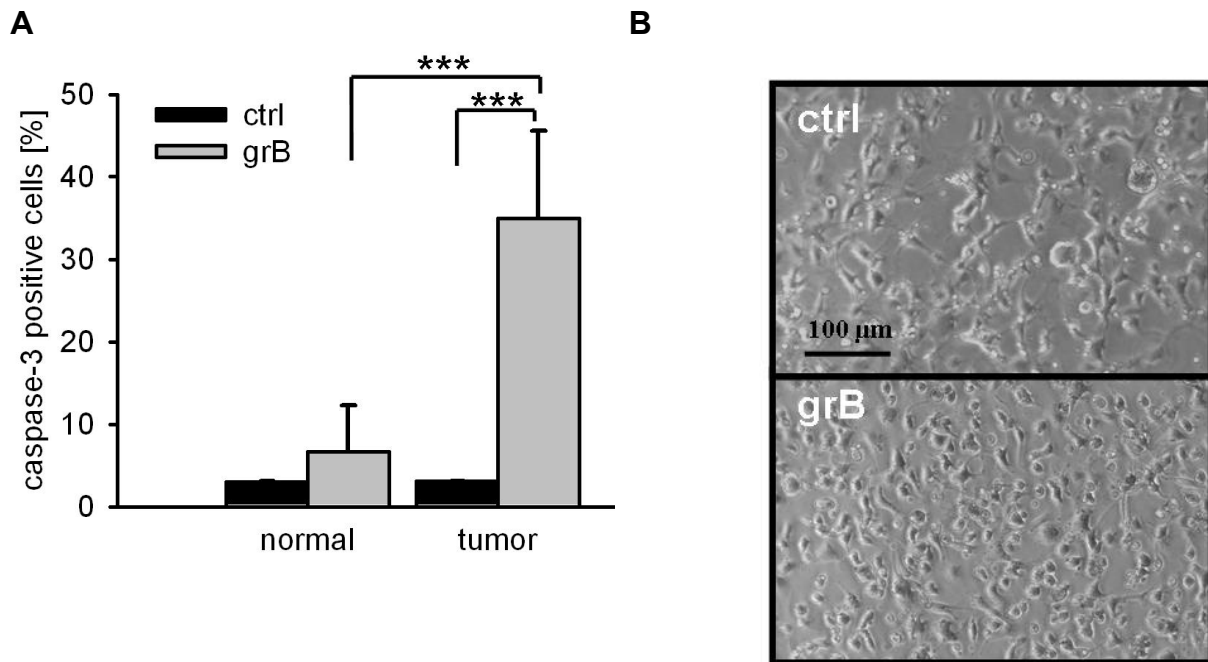


FIG. 15: Treatment of murine endothelial cells and CT26 mouse tumor cells with recombinant human grB. CD31+ cells from BALB/c mice (normal) and CT26 tumor cells (tumor) were treated with PBS as negative control and 4 μg/ml grB.

A Detached and adherent cells were collected 24 h after treatment and stained for active caspase-3 by a fluorescence labeled antibody. The fraction of cells positively stained for active caspase-3 was determined by flow cytometry. The data represent the mean from six independent experiments ± S.D. Asterisks represent significance between grB and PBS treatment of CT26 tumor cells ($p^{***} = 0.001$) and between grB treatment of normal murine cells and CT26 tumor cells ($p^{***} = 0.001$). **B** Light microscopical phase contrast analyses were shown of adherent growing CD31+ cells from BALB/c mice either treated with PBS (ctrl) or with 4 μg/ml grB for 24 h. Untreated and treated cells show regular morphology with extensions. Pictures are typical for independent experiments with similar results (n = 3, objective 20 x, scale bar 100 μm).

3.3.2 Clonogenic survival of CT26 cells after grB treatment

To address the question, whether grB influences clonogenic survival, colony forming assays (CFA) were performed (2.7.4). Contrary to apoptosis, CFA indicate the influence of grB on the long term survival of cells that do not immediately undergo apoptosis.

Only a few colonies were observed at the same concentration (4 μg/ml) used in apoptosis assays. Therefore, colony formation of grB-treated cells was monitored after treatment with concentrations ranging from 0.04 μg/ml to 4 μg/ml grB (FIG. 16, n = 2-3). Clonogenic survival of grB treated cells was largely reduced, even at lower

concentrations than used for apoptosis induction. Survival fractions of colonies after 0.6 $\mu\text{g/ml}$ ($p^* = 0.03$), 0.8 $\mu\text{g/ml}$ ($p^{**} = 0.01$), 2 $\mu\text{g/ml}$ ($p^* = 0.02$) and, 4 $\mu\text{g/ml}$ ($p^{***} = 0.00002$) were significantly different to the untreated control.

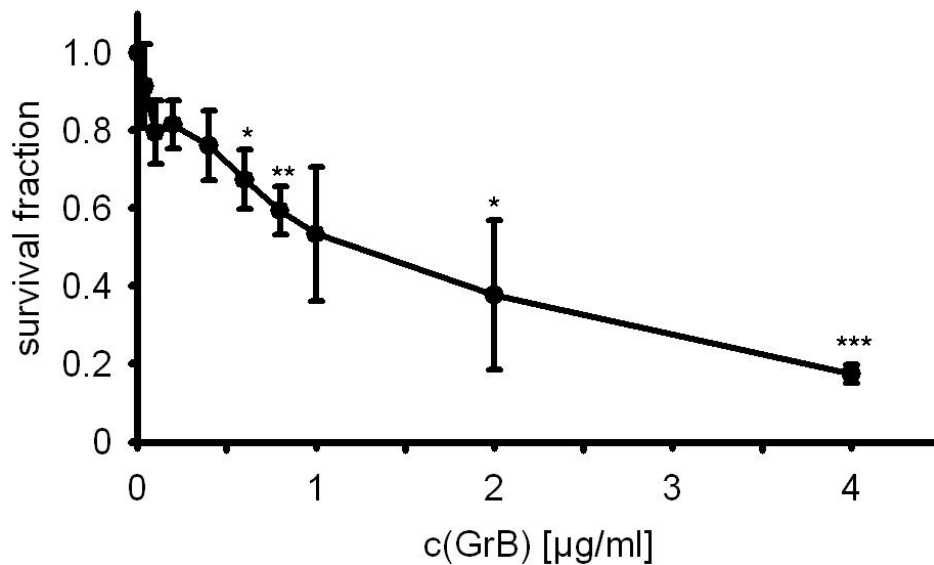


FIG. 16: Colony forming assay (CFA) showing clonogenic survival of grB-treated CT26 cells. The data represent the mean from 3 independent experiments \pm S.D. in the concentration range from 0.04 $\mu\text{g/ml}$ to 1 $\mu\text{g/ml}$ or from 2 independent experiments \pm S.D. in the concentration range from 2 $\mu\text{g/ml}$ to 4 $\mu\text{g/ml}$. Values were determined in triplet in each experiment. Plates were fixed and stained after 6 days of treatment. Asterisks represent significance between survival fraction of untreated colonies and each point of treatment (from left to the right: $p^* = 0.03$, $p^{**} = 0.01$, $p^* = 0.02$, $p^{***} = 0.00002$).

3.3.3 Escape strategies of human K562 cells

Due to its comparable membrane-Hsp70 expression levels (~50%) the human leukemic cell line K562 was chosen in addition to the CT26 mouse cell line for apoptosis assays using grB obtained from HEK293 cells. Following incubation of K562 cells with grB (4 $\mu\text{g/ml}$) for 4, 12, 24 and 48 h only $3.6 \pm 4.5\%$ apoptosis induction was measured over all timepoints ($n = 4$). A Western blot analysis revealed that in contrast to the solid tumor cell lines XF354, SAS, CX+, CX-, and SkBr3, the leukemic cell lines K562 and YT, and the lymphoma Daudi express the grB inhibitor PI-9 as determined by Western blot analysis (FIG. 17). The grB inhibitor is detected by a 42 kDa band in all three leukocyte-derived cell lines (FIG. 17; first three lanes). None of the five solid tumor cell lines showed this band (FIG.16; lanes 4-8).



FIG. 17: Western blot analysis for the grB inhibitor PI-9. 10 μ g of protein from lysed cells were analyzed for PI-9 inhibitor expression using Western blot. YT cells, which were known to produce the grB inhibitor were used as positive control. K562 and Daudi cells were checked for grB inhibitor, as well as the solid tumor cell lines XF354, SAS, CX+, CX- and SkBr3. One representative result out of three independent experiments analyzing PI-9 in YT and in K562 cells is shown.

3.4 Biological activity in multicellular spheroids

3.4.1 Growth delay and histology

To simulate a more tumor-relevant model system, the effect of grB was tested on multicellular spheroids. Spheroids grown from CT26 cells were cultured for four days, followed by a treatment period of up to 14 days. The spheroids were treated with different concentrations of grB and their diameters were analyzed by light microscopy. One representative result out of six experiments is shown (FIG. 18A). Untreated spheroids grew in a regular manner and pictures were taken on days 0, 1, 6, 7, and 14 (FIG. 18A, ctrl, left column). The spheroids were round shaped with a clearly defined border reaching their maximum size on day 6. The spheroids exposed to the same grB concentration (4 μ g/ml) used for the monolayer experiments lost their integrity 24 h after start of the treatment (FIG. 18A, second column, day 1). After 14 days of treatment, the border of the spheroids looked frazzled and the diameter started to decrease (FIG. 18A, second column, bottom panel). The effects were much more pronounced in spheroids treated with a 20 times higher grB concentration (FIG. 18A, 80 μ g/ml grB, third column). Treatment with cam results also in a decrease of spheroid diameter (FIG. 18A, right column, compare top panel with bottom panel). In comparison to the grB-treated spheroids, the surface of cam-treated spheroids stayed regular (FIG. 18A, compare right column, bottom panel with third column, bottom panel).

The diameters of the spheroids were measured on day 0, 1, 3, 6, 7, 10 and 14 (FIG. 18B). The spheroids began at similar sized diameters of 565 ± 30 μ m on day 0. No

significant changes in spheroid diameters were seen up to day 3 (see TAB.2 for *p* values corresponding to FIG. 18B). On day 6, the cam-treated spheroids differed significantly from the ctrl. From day 7 onwards, the cam-treated and the grB-treated spheroids showed a significant decrease in size (TAB.2). A comparison between day 0 and day 14 showed that the control spheroids grew from $555 \pm 27 \mu\text{m}$ to $610 \pm 48 \mu\text{m}$, the cam-treated spheroids decreased in size from $556 \pm 25 \mu\text{m}$ to $429 \pm 37 \mu\text{m}$, and the grB-treated spheroids reduced in size from $583 \pm 30 \mu\text{m}$ to $446 \pm 36 \mu\text{m}$ (FIG. 18B).

On days 0, 1, 3, 6, 7, 10, and 14, the spheroids were fixed in 3.7% PBS-buffered formalin, paraffin embedded and cut into $2.5 \mu\text{m}$ sections in order to perform hematoxylin and eosin (HE) staining. Here, spheroids are shown 3 (FIG. 18C, upper row) and 7 days (FIG. 18C, lower row) after treatment with PBS (FIG. 18C, ctrl, left column), $4 \mu\text{g/ml}$ grB, $40 \mu\text{g/ml}$ grB (FIG. 18C, two middle columns) or $4 \mu\text{g/ml}$ cam (FIG. 18C, right column). The pictures show that the grB-treated spheroids lost integrity, in contrast to cam-treated spheroids, which diminished in size. One representative result of two experiments is shown.

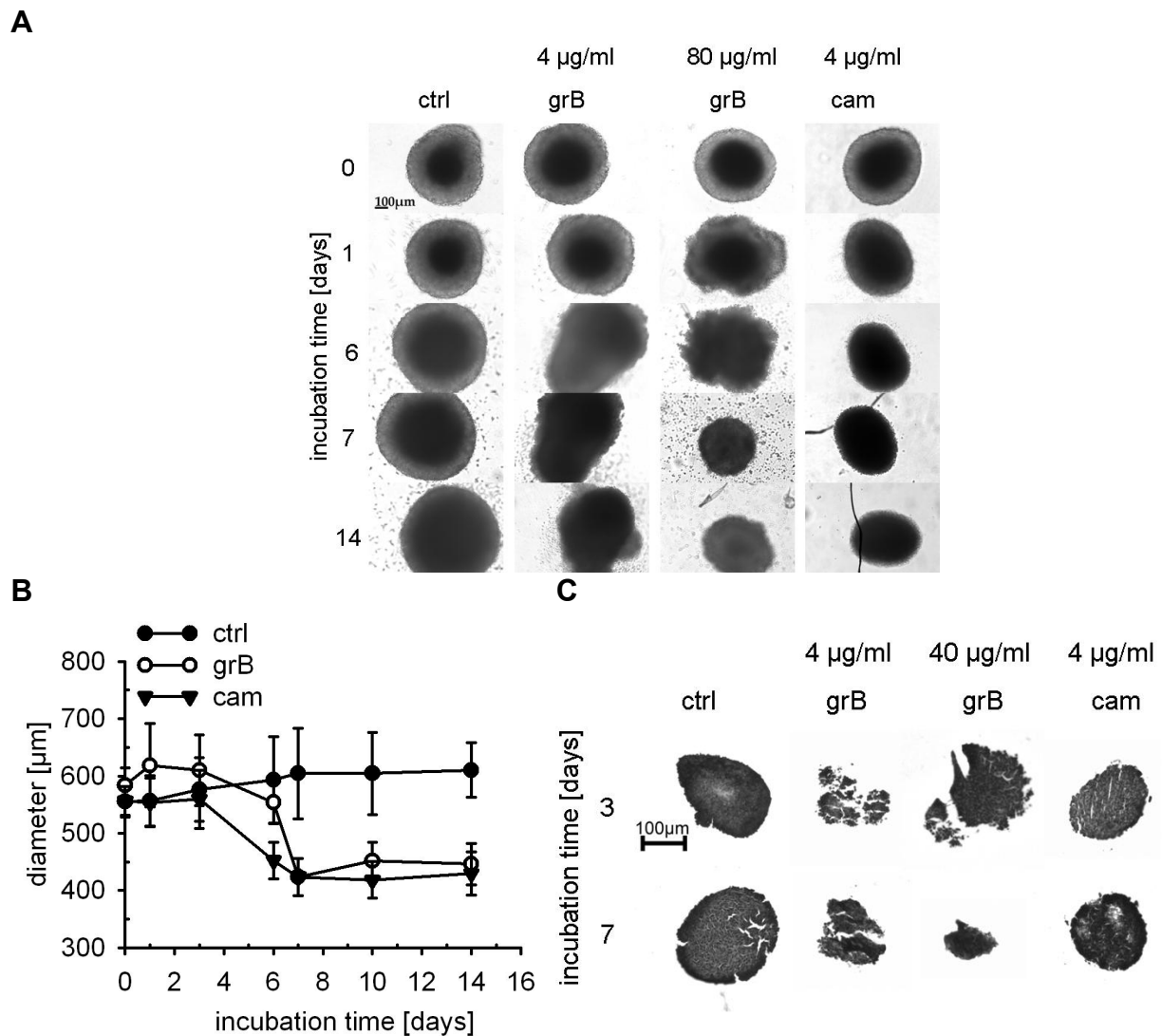


FIG. 18: Treatment of CT26 spheroids with recombinant human grB. Four day old CT26 spheroids were transferred to 96-well plates and treated for 14 days with PBS as negative control (ctrl), with 4 µg/ml grB, 80 µg/ml grB or with 4 µg/ml cam as positive control. **A** Light microscopical analyses from the multicellular spheroids were photographed at timepoints as indicated. One representative result out of six experiments is shown (objective 10 x, scale bar 100 µm). **B** Diameters of spheroids were measured up to 14 days after initial treatment. Curves are shown from spheroids treated with PBS (ctrl; black dots), 80 µg/ml grB-treated spheroids (grB; white dots) or from spheroids after 4 µg/ml cam treatment (cam; black triangles). The data represent the mean from six independent experiments \pm S.D. Starting at day seven, the diameter of grB-treated spheroids significantly differs from ctrl ($p^{**} = 0.004$), cam-treated spheroids significantly differ from ctrl ($p^{**} = 0.006$) beginning at day six. **C** CT26 spheroids were stained with hematoxylin and eosin (HE). Four day old CT26 spheroids were transferred to 96-well plates and treated with PBS as negative control (ctrl), 4 µg/ml and 40 µg/ml grB or with 4 µg/ml cam as positive control. At different timepoints, spheroids were fixed in 3.7% formalin (3 and 7 days are shown). HE staining was performed on paraffin sections on glass slides. Light microscopical analyses from the multicellular spheroids were performed. One representative result out of two experiments is shown (scale bar 100 µm, objective 10 x).

TAB.2 Statistical significance of spheroid shrinkage

This table shows the p -values and significance representing asterisks of grB-treated versus control spheroids (ctrl-grB) and of cam-treated versus control spheroids (ctrl-cam) corresponding to FIG. 18B.

	DAYS					
SIGNIFICANCE	1	3	6	7	10	14
p (ctrl-grB)				**	**	***
	0.17	0.14	0.25	0.0040	0.0063	0.00031
p (ctrl-cam)			**	**	**	**
	0.92	1.0	0.0061	0.0022	0.0019	0.0012

3.4.2 Apoptosis assay

To determine if the increase in size of the grB-treated spheroids in the first days is due to proliferation or if this phenomenon is simply due to reduced integrity and therefore more space between apoptotic cells, the spheroids were examined by apoptosis assay after a 48 h incubation period with 4, 10, 20, 40 and 80 $\mu\text{g/ml}$ grB. To compare the results with the monolayer experiments the caspase-3 assay combined with flow cytometry analysis was used. Spheroids were trypsinated and single cell suspensions were prepared. Cells were incubated with FITC-conjugated antibody against caspase-3 and the fraction of caspase-3 positive cells was analyzed by flow cytometry (FIG. 19). I found a concentration-dependent correlation between the administered grB and the percentage of caspase-3 positive cells. The amount of positive cells increased from $3 \pm 2\%$ to $8 \pm 0\%$ after incubation with 4 $\mu\text{g/ml}$ grB. High concentrations of 80 $\mu\text{g/ml}$ resulted in an increase of up to $57 \pm 3\%$ (FIG. 19). Spheroids treated with PBS as a negative control, showed no elevated apoptosis rates. The data represent the mean of 3-4 independent experiments \pm S.D. Bars represent significantly different values between ctrl and grB-treated (4 $\mu\text{g/ml}$ ($p^{***} = 0.000007$) and 80 $\mu\text{g/ml}$ ($p^{**} = 0.0003$)) cells.

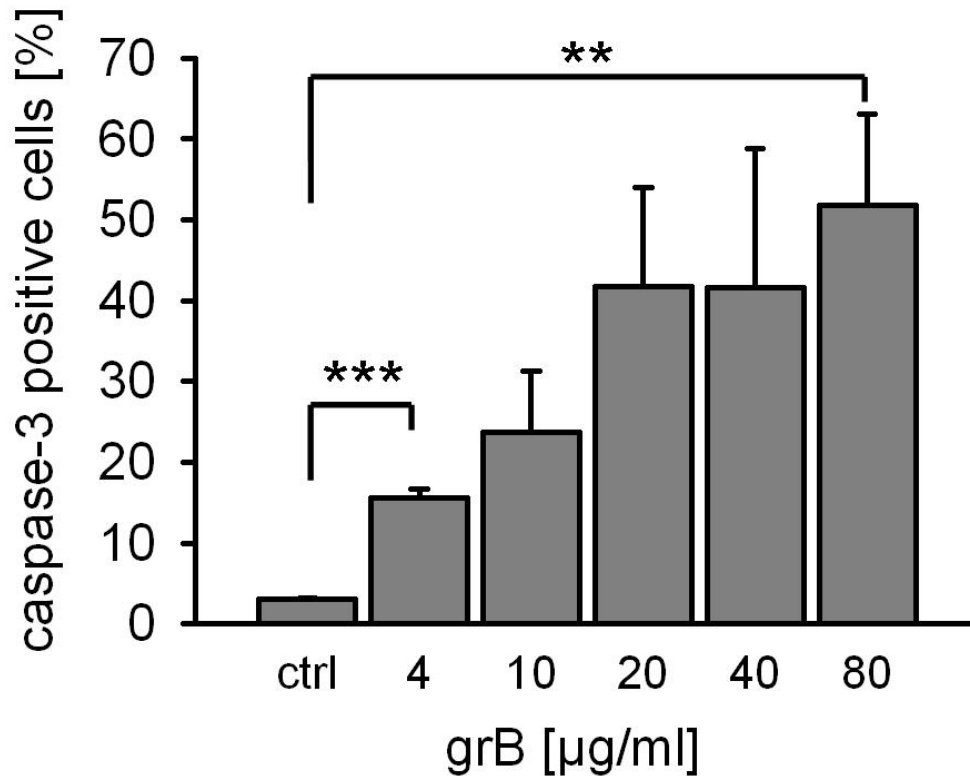


FIG. 19: Caspase-3 activation in CT26 spheroids. Spheroids were treated with PBS (ctrl) or grB at concentrations as indicated. Spheroids were trypsinated to achieve single cell suspensions, and stained for active caspase-3 with a fluorescence labeled antibody. Fractions of active caspase-3 positive cells were determined by flow cytometry analysis. The data represent the mean of 3-4 independent experiments \pm S.D. Bars represent significance between ctrl and the most important two grB concentrations of 4 $\mu\text{g/ml}$ ($p^{***} = 0.000007$) and 80 $\mu\text{g/ml}$ ($p^{**} = 0.0003$).

Here, I show that grB reduces the size of 3D spheroids, diminishes their integrity and induce apoptosis. However, in these experiments, higher grB concentrations were used to obtain comparative effects as in 2D cell culture.

3.5 grB therapy for tumor bearing mice

First mouse experiments were performed using a syngeneic BALB/c CT26 tumor mouse model. It was planned to define toxicity, the effective dose of grB, and the anti-tumoral *in vivo* activity. One CT26 spheroid grown for seven days from 5×10^3 CT26 cells, was intraperitoneally (IP) injected per mouse. Tumor-bearing mice received 20 μg of active or inactive grB (not activated by enterokinase during purification procedure) per g body weight on day 6 and day 7 after spheroid injection.

Another control group received no treatment. The time scale of this first experiment is shown in FIG. 20A. After IP injection of grB into tumor-bearing mice, the animals were monitored during the first hour after injection and then once a day. No adverse events were observed in the first group of mice. Therefore, in a second experiment grB was injected on days 6, 7, 13 and 14 with 20 μg per g body weight. The time scale of this second experiment is shown in FIG. 20B. In both experiments mice were sacrificed on day 21 and inspected for adverse effects and tumor growth reduction. Tumors and organs were resected for histological studies. Mice, whose tumor grew exponentially, started to loose weight and showed side effects. Blood was taken from the mice at the end of each experiment and the serum was tested for human grB by ELISA technique holding a sensitivity of 20 pg/ml . grB was not detectable on day 14 (first experiment) respectively day 7 (second experiment) after the last grB injection.

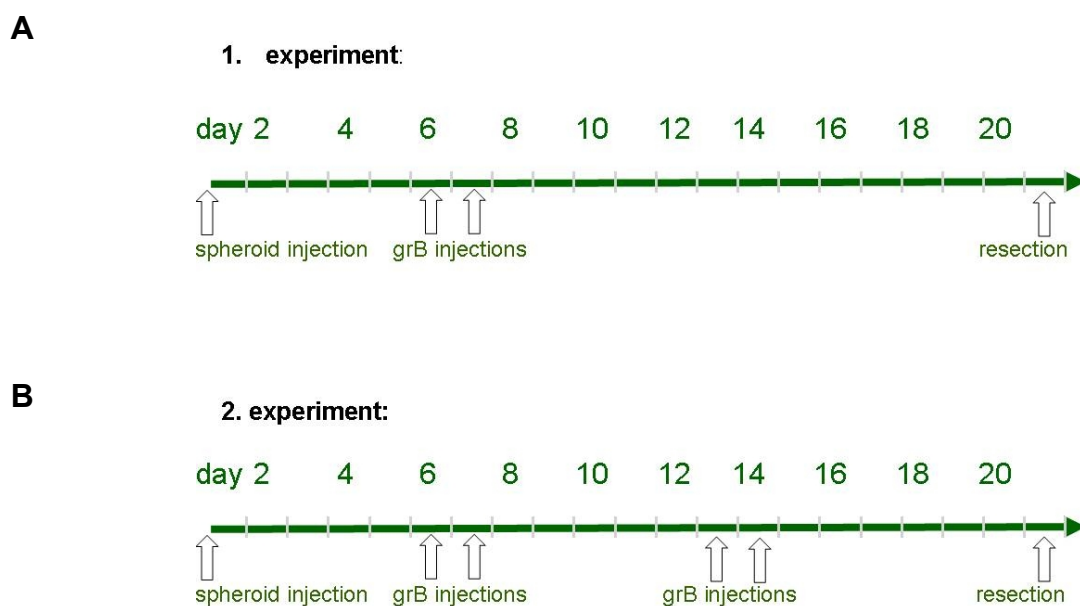


FIG. 20: Scheme of first and second mice experiments.

A Tumor-bearing BALB/c mice were injected IP with 20 μg active or inactive grB per g mouse or with PBS as negative control on days 6 and 7 after spheroid injection in the first experiment. **B** Mice were injected on days 6, 7, 13 and 14 resulting in dose doubling in the second experiment. **A+B** Both experiments were finished at day 21.

3.5.1 Tumor weight

The weight of the resected tumors was determined on day 21. Tumors below a weight of 0.1 g, which did not grow, and tumor spheroids showing a spreaded growth were excluded from the evaluation.

In the first experiment, no tumor reduction was detected by treatment at an overall dose of 40 μg per g body weight (data not shown). However, in the second experiment, a tumor reduction by grB treatment was visible at an overall dose of 80 μg per g body weight (FIG. 21). Tumors weighed 1.17 ± 0.31 g from untreated mice ($n = 2$; FIG. 21, ctrl, left balk), 0.60 ± 0.45 g from control mice treated with inactive grB ($n = 3$; FIG. 21, inact grB, middle balk) and 0.33 ± 0.12 g from active grB-treated mice ($n = 3$; FIG. 21, grB, right balk), respectively. Tumor weight decreases significantly after treatment with active grB ($p^* = 0.046$ compared to ctrl and $p^* = 0.044$ compared to inactive grB). The tumor weight difference between ctrl and inactive grB was not significantly different ($p = 0.49$). Since it was detected that inactive grB shows a small amount of activity in Ac-IEPD-pNA substrate assay, this could be an explanation for minor effects of inactive grB on the tumor size. Due to the relatively low number of mice, these results need to be confirmed in a larger experiment.

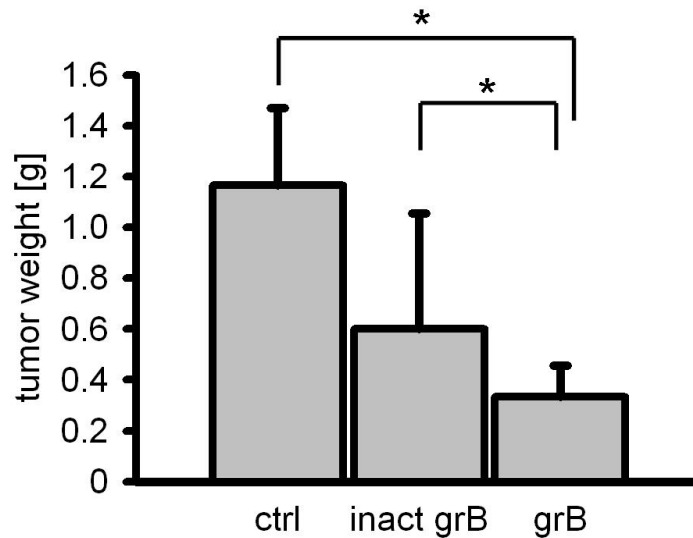


FIG. 21: grB therapy in a syngeneic mouse model (second experiment). CT26 spheroid tumor-bearing BALB/c mice were treated via IP injection for 4 times with 20 μg active grB per g body weight (grB). As negative control mice were treated with grB, which was not activated by EK digestion (inact grB) or mice were not treated at all (ctrl). For each group 5 mice were used. Tumors below a weight of 0.1 g, which did not grow, and tumor spheroids showing a spreaded growth were excluded from the evaluation. Therefore, for evaluation, 2 mice for the untreated group and 3 mice for each of the other two groups were available. The error bars represent + S.D. between tumor weights of each group. Bars represent significance between ctrl and grB-treated tumors ($p^* = 0.046$) as well as between inact grB and active grB ($p^* = 0.044$), whereas between ctrl and inact grB no significance was demonstrated ($p = 0.49$).

3.5.2 Histopathology of tumors and organs

After inspecting the tumors with respect to their sizes, histologically detectable changes resulting from the grB therapy were examined. The vitality of the tumors was estimated from HE stained sections for the amount of healthy areas, which are defined by numerous mitosis, compact tumor tissue, and random single cell apoptosis. The apoptotic/necrotic areas were recognizable by eosin staining, apoptotic bodies, bulked ECM, densed nuclei and nuclear fragmentation. No severe differences between the first and the second experiment were found, so that the following findings are valid for both experiments. The grB-treated tumors showed no worse overall vitality than untreated or inactive grB-treated control tumors. Interestingly, the necrotic/apoptotic areas were localized differently. As listed in TAB.3, the negative tumors of one out of three mice in the first experiment and both mice of the second experiment showed necrosis in the inner central area and not at the border of the tumors. In contrast, necrosis was found predominantly at the

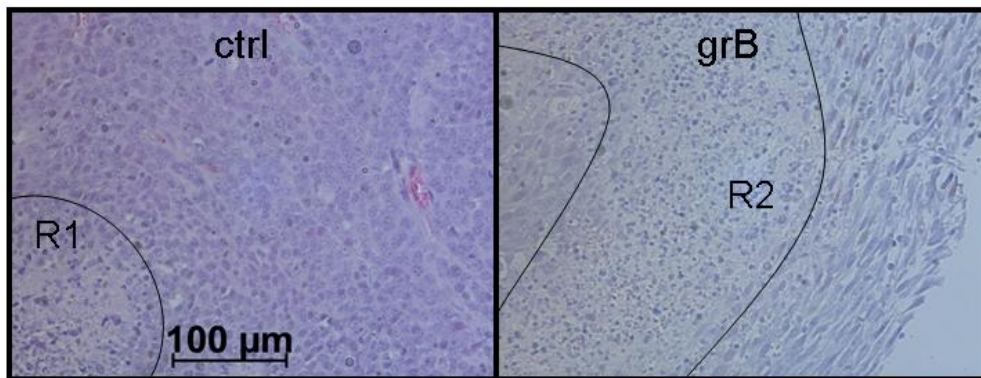
boundary area in all four tumors from grB-treated mice from the first experiment and in two of three tumors from the second experiment. Additionally, in rare cases, the area around vasculatures exhibited pathophysiological changes, which look similar to changes after radiation therapy. None of the grB-treated tumors showed necrosis in the center. Only two tumors with necrotic border areas were found in inactive grB-treated tumors (one of four tumors in the first experiment and one of three tumors in the second experiment), while central necrosis was found in one tumor from the second experiment (no tumor out of four in the first experiment and one tumor out of three in the second experiment). In FIG. 22A one exemplary tumor with necrosis in the center (R1), which was resected from an untreated mouse (FIG. 22A, ctrl), is shown compared to another exemplary tumor, showing necrosis at its border (R2), which was derived from a grB-treated mouse (FIG. 22A, grB).

TAB.3 Location of necrotic/apoptotic areas in treated and untreated tumors

experiment	treatment of mice	number of mice with necrosis in central area of tumor (%)	number of mice with necrosis in border areas of tumor (%)	overall number of evaluated mice per group
first	ctrl	1 (33 %)	0 (0 %)	3
first	inactive grB	0 (0 %)	1 (25 %)	4
first	grB	0 (0 %)	4 (100%)	4
second	ctrl	2 (100 %)	0 (0%)	2
second	inactive grB	1 (33 %)	1 (33 %)	3
second	grB	0 (0 %)	2 (67 %)	3

No obvious adverse effects occurred during the treatment. Nevertheless, HE stained paraffin sections of the vital organs (liver, kidneys, lung, heart and spleen) were analyzed for morphological abnormalities to exclude that grB could have an effect on normal tissue. The HE stained organs were examined via light microscopy for pathophysiological changes and my findings were confirmed by Dr. F. Neff, a pathologist from the Institute of Pathology of the Helmholtz Center Munich (Neuherberg, Germany). No pathophysiological changes were found in the examined organs; liver, heart, kidney, lung, heart and spleen (exemplary mice organs from one ctrl mouse and one grB-treated mouse shown in FIG. 22B). In each organ, a normal architecture, without infarcts or internal bleeding was found. Some irregularities were confirmed as artifacts.

A



B

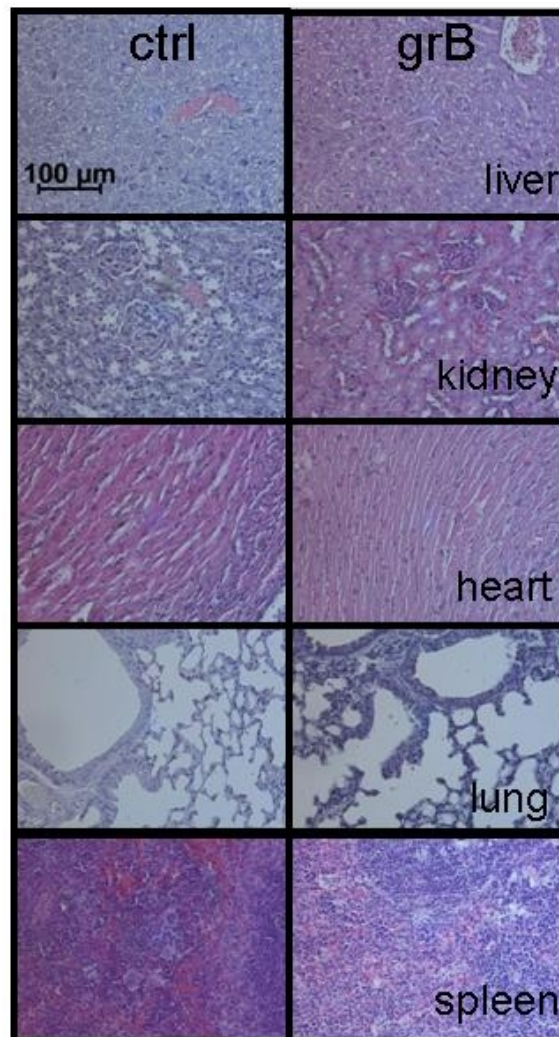


FIG. 22: HE stained sections from tumor and organs. Sections from formalin-fixed paraffin-embedded tumors and organs were stained by HE and analyzed using light microscopy (objective 20 x, indicated scale bar 100 μm). Here, tumor and organs from one exemplary untreated mouse (ctrl) and from one grB-treated mouse (grB) are shown. **A** Tumors from ctrl and from grB-treated mouse. R1 marks the necrotic/apoptotic region in the tumor center of the ctrl and R2 marks the necrotic/apoptotic region in tumor border area of the grB-treated mouse. **B** Liver, kidney, heart, lung and spleen are shown from the ctrl and from the grB-treated mouse.

4 DISCUSSION

4.1 Production of active granzyme B (grB) expressed in mammalian cells

Previously, we have demonstrated that granzyme B (grB) is able to induce perforin-independent apoptosis in membrane-Hsp70 positive tumor cells, but not in normal cells (Gross et al. 2003b). The aim of this study was to further develop the basis for a therapy in order to kill membrane-Hsp70 positive tumor cells by grB applied externally. Therefore, suitable amounts of grB were needed that show the ability to selectively induce perforin-independent apoptosis. For that reason, four different strategies to produce active grB for *in vitro* and *in vivo* experiments were tested.

Human grB isolated from cytotoxic granules of the NK cell line YT is often bound to perforin and thus shows lower enzymatic activity (Xia et al. 1998). Trapani et al. have shown that more than 50% of total cellular grB is present in the nucleus of NK cells. The advantage of grB isolated from the nucleus is the absence of perforin. Therefore, I purified grB from nuclei of the NK cell line YT (Trapani et al. 1994). The purification yielded approximately 0.8 mg grB per 2×10^8 cells (3.1.1). Unfortunately, the grB inhibitor Protease Inhibitor-9 (PI-9), which is covalently bound to grB (Sun et al. 1996) was co-purified (TAB.4; first column).

As PI-9 influences the biological activity of grB, I switched to a recombinant expression system for the production of grB. Since the grB expressed in bacteria is not glycosylated, *E. coli* is an inadequate expression system (Kurschus et al. 2005). As glycosylation seems to be important for grB uptake by target cells, I used the eukaryotic recombinant expression system *Pichia pastoris*. Using this system, the mature form of grB was expressed and secreted. grB was purified from the cell culture supernatant (Giesubel et al. 2006). This procedure resulted in the production of 0.3 mg grB per liter supernatant. This yield was significantly lower compared to results described in the literature (1-2 mg/l) (Giesubel et al. 2006; Sun et al. 1999). It should be mentioned that the grB-containing yeast culture supernatant was shipped to our laboratory. This time factor could be the reason for the low yield. The glycosylation of grB expressed in *Pichia pastoris* was higher compared to that derived from human NK or T cells. The grB purified from *Pichia pastoris* was not active in *in vitro* assays despite proven enzymatic activity (3.1.2). As proper glycosylation could be essential for the grB receptor interaction (Giesubel et al. 2006), I assumed that the proposed slightly different glycosylation by *Pichia pastoris*

influences the biological activity of grB. The glycosylation pattern could be also responsible for the lacking capacity to induce apoptosis in membrane-Hsp70 positive cells (TAB.4; second column).

In contrast to *E. coli* or yeast, insect cells are able to fulfil nearly all of the posttranslational protein modifications (including glycosylation), which are necessary for the accurate maturation of human proteins. Therefore, a Baculovirus/Sf9 insect expression system was used for the expression of grB (3.1.3). My yield of 0.3 mg grB per 3×10^7 cells was comparable or even slightly higher than that described in the literature. Previously, the Sf9/Baculovirus system was used for the production of secreted mouse grB (Xia et al. 1998). However, the induction of apoptosis by grB in membrane-Hsp70 positive tumor cells also failed (TAB 4; third column).

For this reason, I changed to a mammalian cell system to obtain all posttranslational modifications, which are necessary for the biological activity of grB. No mammalian expression system for stably producing enzymatically and biologically active grB has been published. First, I tried to directly express active grB in mammalian HEK293 cells. However, under conditions suitable for the production, active grB killed the HEK293 cells (3.1.4). Endogenous granzymes (gr) are expressed – like many other serine proteinases – as inactive zymogens that are activated by cathepsin C during packaging into granules. Therefore, they are not able to damage the producing cell line. grB was expressed in HEK293 cells in an inactive form and activation was performed after purification followed by an enterokinase (EK) cleavage. Compared to the results from Dalken et al., who purified grB from *Pichia pastoris*, the grB produced by HEK293 cells showed a higher enzymatic activity. 3 µg/ml of my grB was able to process 200 µM Ac-IETD-pNA substrate completely during the first hour. In comparison to HEK293-derived grB, at least 6 µg/ml of grB expressed in *Pichia pastoris* are needed to reach saturation in an Ac-IETD-pNA substrate assay performed in the same manner (Dalken et al. 2006). The grB produced from HEK293 cells was able to induce apoptosis in human cancer cells and therefore was chosen for further experiments (TAB.4; fourth column). It should be emphasized that it is very important for the purposes of my work to use the mammalian expressed, fully active and inhibitor-free grB. Inaccurately modified grB is not able to induce apoptosis in membrane-Hsp70 positive tumor cells in a perforin-independent pathway. Other laboratories who are using *E. coli* or *Pichia pastoris*-derived grB or grB purified from YT cells have not investigated the apoptotic action in a perforin-independent manner.

In these assays proper glycosylation was not important for their apoptosis experiments, especially if lytic agents were used to perform grB's uptake into the target cells.

TAB.4 Comparison of the different production methods of grB

expression system	NK cell line YT	<i>Pichia pastoris</i>	Sf9/Baculovirus transfection	mammalian cell system HEK293
problem	grB inhibitor; low biological activity	low biological activity; low yield; too much glycosylation	low biological activity	–
publication	Trapani et al. 1994	Giesubel et al. 2006; Sun et al. 1999	Xia et al. 1998 (mouse grB)	publication of my work <i>in preparation</i>

4.2 Membrane-Hsp70 mediates perforin (PFN)-independent apoptosis of human grB in mouse cells

Gross et al. (2003b) previously showed that cell surface-bound Hsp70 mediates perforin-independent apoptosis by specific binding and uptake of grB. This specific binding and uptake could be blocked by the Hsp70 specific antibody cmHsp70.1. In our laboratory, the human colon carcinoma cell line CX-2 was sorted for sublines with a high and a low membrane-Hsp70 status. The resulting sublines CX+ (high; > 80%) and CX- (low; < 30%) show membrane-Hsp70-dependent sensibility towards grB (Gross et al. 2003b).

Herein, it was shown that human grB also induces perforin-independent apoptosis in membrane-Hsp70 positive mouse tumor cells (3.3.1.1), whereas it has no effect on normal mouse cells lacking Hsp70 on their membrane (3.3.1.2). These data are a prerequisite for future analysis in a tumor mouse model. Perforin-independent apoptosis was tested 12, 24 and 48 h after treatment. I detected early apoptotic cells by an annexin-V assay (FIG. 6), and determined the amount of cells, which were apoptotic without the possibility to recover, by caspase-3 assay (FIG. 13A+C). This “point of no return” represents the activation of the effector caspases. Nucleus fragmentation was measured by DAPI staining as an additional endpoint of apoptosis

(FIG. 13C). All three assays revealed a time-dependent increase in apoptosis after grB treatment for 12 to 48 h.

Normally, the perforin-dependent grB pathway is investigated in combination with perforin or with other lytic agents (e.g. by the cationic lipid formulation Bioporter®, Gene Therapy Systems Inc., San Diego, CA, USA; (Azuma et al. 2007)). Typically, timepoints between 4 and 48 h have been used to measure apoptosis induction. 12 h was determined as the maximum level for cell surface exposure of phosphatidylserine, representing early apoptosis. Often, grB concentrations between 10 ng/ml-10 µg/ml (tending towards concentrations in the range of [µg/ml]) have been used and a dose-dependent induction was detected and reached a plateau around 2 µg/ml in one experimental approach (Azuma et al. 2007; Giesubel et al. 2006; Gross et al. 2003b; Kurschus et al. 2004). Comparing these results from the literature with my results, no great difference between the perforin-dependent and perforin-independent induction of apoptosis with respect to the required time period and the concentration range can be assumed. Also I observed no evident differences between human and mouse cell lines concerning the perforin-independent pathway were observed.

Additionally, a time-dependent increase detectable in the percentage of late-apoptotic and necrotic, PI-positive cells was shown (FIG. 14A). This effect was stronger in cam-treated cells than in grB-treated cells (FIG. 14A). In contrast, apoptosis induction measured by caspase-3 was stronger in grB-treated cells than in cam-treated cells (FIG. 13A). Photos illustrate that 48 h after treatment (either with cam or grB), caspase-3-stained cells had condensed and often fragmented nuclei. This confirms that 48 h represents a suitable timepoint to measure late apoptosis (FIG. 13). These experiments suggest that the induction of perforin-independent apoptosis is as fast as the induction by perforin-dependent apoptosis. In contrast, the induction of apoptosis by cam treatment was faster. This indicates that initiation of apoptosis by grB and cam might be mediated by different routes. Furthermore, the previously detected difference in apoptosis induction in membrane-Hsp70 positive human cells and in negative cells could be confirmed for mouse cells and is found only after treatment with grB, but not with cam (3.3.1) (Gross et al. 2003b). The alkaloid cam inhibits DNA topoisomerase I by stabilizing the cleavable complex and thereby causes apoptosis. While grB is able to induce apoptosis through

mitochondrial leakage and the caspase cascade (Boivin et al. 2009), cam does not significantly affect the mitochondrial apoptosis pathway (Bredholt et al. 2009).

Moreover, anoikis, a special form of apoptosis, which is induced by the detachment of cells from extracellular matrices (ECM) could also contribute to apoptosis induced by grB (Buzza et al. 2005; Pardo et al. 2007). However, grB does not induce significant apoptosis in normal, membrane-Hsp70 negative mouse cells (FIG. 15). This contradicts the assumption that anoikis, which would be a membrane-Hsp70 independent phenomenon, plays a role in grB-mediated, perforin-independent apoptosis.

Apoptosis induction in a specific population of tumor cells may not result in the kill of all tumor cells. Therefore, clonogenic survival was measured by a colony forming assay (CFA; 3.3.2). The CFA serves as a validated endpoint to study the efficacy of drugs and radiotherapy. Clonogenicity was reduced to approximately 20% using 4 µg/ml grB (FIG. 16). This indicates that lower grB concentrations are sufficient to reduce clonogenicity as compared to the induction of *in vitro* apoptosis. These results are in agreement with data from the literature. Different concentrations of cam were used for CFA and apoptosis induction, due to the stronger effects in the CFA assays (Havelka et al. 2007).

4.3 Biological activity in multicellular spheroids consisting of mouse tumor cells

To test the putative value of grB therapy not only on cells cultured as monolayer, but also in a system, which better reflects tumors *in vivo*, experiments were performed using multicellular tumor spheroids (3.4). Spheroids represent an established model for *in vitro* 3D tissue structures that mimic *in vivo* tumor tissue organization including cellular and organotypic histomorphological features (Dertinger and Hulser 1984; Friedrich et al. 2007; Sutherland 1988). Tumor spheroids have been established for testing anti-tumor drugs to improve pre-animal and pre-clinical selection (Friedrich et al. 2009; Lin and Chang 2008). My results consistently show that much higher concentrations of grB (approximately 80 µg/ml) are necessary to obtain levels of apoptosis comparable to the monolayer culture (4 µg/ml grB; 3.4.2). Using low grB concentrations (4 µg/ml) only a slight loss of spheroid integrity was observed and

apoptosis occurred only in a small amount of cells, probably in the outer cell layer of the spheroids (FIG. 18A+19). This result was expected because cells in a spheroid formation are less accessible to drugs than cells in a monolayer formation. Many drugs show reduced efficacy in the 3D pathophysiological environment compared to 2D (Hirschhaeuser et al. 2010).

The difference in induction of apoptosis of cam and grB is observable in 3D spheroids, additionally to the mentioned 2D induction divergence. Whereas, in cam-treated spheroids a gradual loss of size is detectable, grB first disturbs the spheroid's integrity. This is another interesting hint for the utilized different apoptosis pathways (discussed in 4.2).

The results gained from the spheroid experiments serve as an estimation for future *in vivo* anti-tumor dose ranges and for the design of treatment modalities (Kunz-Schughart 1999). Therefore, a dose in a similar order of magnitude was converted for *in vivo* studies from $\mu\text{g}/\text{ml}$ to μg per g body weight.

4.4 Syngeneic tumor mouse model

For pilot animal studies a syngeneic BALB/c CT26 tumor mouse model was established based on the finding that human grB acts on tumor mouse cells and therefore, putative side effects on normal mouse cells could be analyzed. The results gained from the first two experiments were quite promising (3.5). Safety and tolerability were proven by observation of mice and histochemistry. No irregularities or pathophysiological changes were found in liver, kidney, lung, heart and spleen (3.5.2).

The tumor weight of grB-treated mice (overall dose of $80 \mu\text{g}$ per g body weight) was significantly less than that of mice treated with inactive grB or untreated mice (FIG. 21). Additionally, higher overall doses could be tested in future experiments since multiple doses of $20 \mu\text{g}$ per g body weight were found to be safe.

Very interesting is the finding that apoptotic/necrotic regions were located mainly in peripheral areas of the grB-treated tumors. This indicates that the intraperitoneally (IP)-administered grB enters the tumor from the surrounding (3.5.2). It was not assumed that grB that was injected IP enters the blood circulation. However, I observed increased necrotic/apoptotic areas close to vessels in individual cases.

Although, mouse and human grB have distinct structural and functional characteristics (Kaiserman et al. 2006), and despite the fact that there are differences in the substrate specificity, human grB is able to induce cell death in mouse tumors. It is known that human grB is inhibited 20 times better by the human inhibitor PI-9 than by the mouse inhibitor SPI-6 (Sun et al. 1997). Therefore, possible escape mechanisms could not be simulated in this syngeneic model system. The relevance of escape mechanisms will be further enlightened below (4.5). It was shown by *in vitro* experiments that procaspase-3 was as well activated by human grB as by mouse grB. In contrast, Bid, whose cleavage results in release of cytochrom c from mitochondria, was not processed as efficiently by mouse grB as by human grB (Bell et al. 2003). Moreover, mouse grB is 30 times less cytotoxic than human grB when applied to mice (Kaiserman et al. 2006). It is known that the caspase cascade pathway is favored in mice compared to the mitochondrial pathway (Cullen et al. 2010). Whereas in humans, the influence of both pathways (caspase cascade and mitochondrial pathway) has not been clarified completely. There is evidence that supports an intensified mitochondrial pathway in humans (Boivin et al. 2009; Chavez-Galan et al. 2009; MacDonald et al. 1999).

Nevertheless, it could not be concluded that using human grB in mice induces naturally occurring apoptosis pathways. Therefore, I assume that the doses used in animal experiments have to be altered for humans. Nevertheless, these and the following animal experiments provide an important tool to demonstrate *in vivo* efficacy of human grB.

4.5 Future prospects: grB as therapy

Membrane-Hsp70-bearing tumors comprise 40-80% of various tumor entities in humans. Therefore, Hsp70 constitutes a common object for targeted therapy. Three strategies of therapy against membrane-Hsp70 positive tumors are being pursued by our group. In NK cell therapy, patient's NK cells get stimulated *ex vivo* against membrane-Hsp70 on tumor cells (with IL-2/TKD) (Krause et al. 2004). In the second strategy, a therapeutical monoclonal antibody targets membrane-Hsp70 on tumor cells directly and leads to an antibody-dependent cellular cytotoxicity (ADCC) (Stangl et al.; *in preparation*). The strategy in my project is to develop a therapy based on the

apoptosis-inducing protein grB, which specifically induces apoptosis in membrane-Hsp70 positive tumor cells. The proposed therapy in the future will consist of IV injections of active grB. Results gained from *in vitro* and preliminary animal experiments propose an application for grB administration as a novel therapeutic concept. grB therapy for human cancer patients is supposed to increase the level of the cytotoxic lymphocyte protease grB in blood circulation.

As previously mentioned, I applied grB concentrations similar to those used in published *in vitro* studies for perforin-dependent apoptosis (see 4.2). These concentrations exceed normal healthy patients serum levels of up to 15-40 pg/ml (very large variability) and also exceed the elevated levels found in various disease states (e.g. 250 pg/ml during severe meningitis), which elicit a cytotoxic lymphocyte-mediated immune response. grB concentrations of up to 5.6 ng/ml have been found in synovial fluid of reactive arthritis disease states (Balkow et al. 2001; Boivin et al. 2009; Buzza and Bird 2006). Nevertheless, the effective dose for therapy purposes is considerably higher than the physiological or pathophysiological concentrations found in the serum. This is due to the efficient, probably high concentrations present in an immunological synapse (IS). Even though I used quite high concentrations of grB (4 µg/ml in monolayer experiments and 80 µg/ml in spheroid experiments), no conclusions could be drawn from the literature that such elevated levels in the serum would induce adverse effects *in vivo*. Since grB is present naturally in body fluids, humans should have a strong immunological tolerance, so that immune responses against grB are not expected. Additionally, my recombinantly produced grB is derived from a human expression system, which minimizes the risk of cellular or humoral immune responses. Also, the finding that the grB-PFN-pathway is more relevant for the graft versus leukemia effect than for the graft versus host effect, encounters for a safe treatment procedure with supportive but not overreactive immune responses (Hsieh et al. 2000). For this reason, the benefits of grB therapy should greatly outweigh hazards by putative side effects.

Irradiation increases membrane-Hsp70 expression on surviving tumor cells (Gehrmann et al. 2005) and consequently sensitizes remaining cells for grB attack. Therefore, grB therapy could be applied especially as an adjuvant therapy following radiotherapy. Another putative application of grB therapy is to target metastases that often show a higher expression density of Hsp70 than the primary tumor (Ciocca and Calderwood 2005). Therefore, a megacolony model system will be established as

another 3D cell culture system for measuring the combined effects of irradiation and grB in cooperation with PD Dr. J. Kummermehr (Radiation Biology, LMU Munich, Germany) (Kummermehr et al. 2001; Tarnawski et al. 1998). In preliminary experiments, we already could show that CT26 cells are able to form multilayered megacolonies and show regrowth after irradiation. Additionally, further CFA experiments and *in vivo* experiments will be performed combining radiation and grB treatment to gain more knowledge about grB effects after radiation therapy.

It is known that often leukemia cells and only occasionally some solid tumors including melanoma, breast, cervical and colon carcinoma, are able to escape from grB-mediated apoptosis induction by producing serpin grB inhibitors and that a number of mouse tumors express SPI-6, the mouse homologue of the human grB inhibitor PI-9 (Medema et al. 2001). My findings that all tested human leukemia cell lines, including K562 cells, but none of the solid tumors express PI-9, confirm this tendency described in the literature (3.3.3). Immune escape via expressing a grB inhibitor could be a reason for tumors not responding to this treatment. Therefore, grB therapy is recommended only for solid tumors, which are not expressing a grB inhibitor. Although leukemia cells are very well accessible by IV injection of grB, they should be excluded due to their high expression levels of grB inhibitor. Since grB acts on different apoptosis pathways (FIG. 3) escape mechanisms targeting one pathway are not able to block the whole action of grB (Dalken et al. 2006). To exclude escape mechanisms by inhibitor expression, a combination therapy together with grM could be considered. grM is known as a regulatory protease that might inactivate PI-9 (Mahrus et al. 2004).

A major point that needs to be improved for therapy development is definitively the stability of grB in the blood circulation. grB's half-time life is approximately seven days at 37°C under cell culture conditions (3.2). Due to my finding that no grB is detectable *in vivo* after seven days, it is possible that the stability of exogenously applied grB in the blood circulation is lower than in cell culture. The half-life times of proteins in plasma are often in the range of minutes to hours. On the other hand, grB is described to show intrinsic stability in extracellular body fluids due to its natural occurrence. grB therapy can only be successful, if grB is able to reach the tumor. This could be achieved by high concentrations in repeated single doses or modifications of the grB structure that optimize the pharmacokinetic properties. Modifications of grB, such as substitutions, acylation and PEGylation (covalent

attachment of polyethylene glycol polymer chains) could lead to prolonged plasma half-life times (Werle and Bernkop-Schnurch 2006) and thus could reduce the amounts which are injected.

In summary, the combination of grB with radiation therapy needs to be tested *in vitro* and *in vivo*. The data that I present here strongly recommend further development of this innovative molecular therapy. The idea of targeting membrane-Hsp70 positive tumors should be approved in further mouse experiments using a higher number of animals.

5 APPENDIX

```

>.....GZMB.....>
p h p a y n p k n f s n d i m l l q l e r k a k r t r
401 ctgtgcagcc cctcaggcta cctagcaaca aggccaggt gaagccaggg cagacatgca gtgtggccgg ctggggggcag
  a v q p l r l p s n k a q v k p g q t c s v a g w g q
>.....GZMB.....>
  a v q p l r l p s n k a q v k p g q t c s v a g w g q
481 acggccccc tgggaaaaca ctacacacaca ctacaagagg tgaagatgac agtgcaggaa gatcgaaagt gccaatctga
  t a p l g k h s h t l q e v k m t v q e d r k c e s
>.....GZMB.....>
  t a p l g k h s h t l q e v k m t v q e d r k c e s
561 cttacgccat tattacgaca gtaccattga gttgtgcgtg ggggaccag agattaataaa gacttccttt aagggggact
  d l r h y y d s t i e l c v g d p e i k k t s f k g d
>.....GZMB.....>
  d l r h y y d s t i e l c v g d p e i k k t s f k g d
641 ctggaggccc tcttgtgtgt aacaagggtg cccagggcat tgtctcctat ggacgaaaca atggcatgcc tccacgagcc
  s g g p l v c n k v a q g i v s y g r n n g m p p r a
>.....GZMB.....>
  s g g p l v c n k v a q g i v s y g r n n g m p p r a
                                     EcoRI
                                     -+----
721 tgcaccaaag tctcaagcct tgtacactgg ataaagaaaa ccatgaaacg ctactaagaa ttctgcagat atccagcaca
  c t k v s s f v h w i k k t m k r y - e f c r y p a
>.....GZMB.....>
  c t k v s s f v h w i k k t m k r y
801 gtggcgcccg cccaccatca tcaccatcac taatctagag ggccgaaaca aaaactcadc tcagaagagg atctgaaatag
  q w r p p t i i t i t n l e g p n k n s s q k r i - i
881 cgccgtcgac catcatcadc atcatcattg agtttaaacc cgctgatcag cctcgactgt gccttctagt tgccagccat
  a p s t i i i i i e f k p a d q p r l c l l v a s h
                                     pSec-Seq2
961 ctgttgcttg cccctcccc gtgccttccet tgaccctgga aggtgccact cccactgtcc tttcctaata aaatgaggaa
  l l f a p p p c l p - p w k v p l p l s f p n k m r
1041 attgcatcgc attgtctgag taggtgtcat tctattctgg ggggtggggg ggggcaggac agcaaggggg aggattggga
  k l h r i v - v g v i l f w g v g w g r t a r g r i g
1121 agacaatagc aggcattgct gggatgctgt gggctctatg gcttctgagg cggaaagaac cagctggggc tctagggggg
  k t i a g m l g m r w a l w l l r r k e p a g a l g g
1201 atccccacgc gccctgtagc ggcgcattaa ggcggcgggg tgtggtggtt acgcgagcgc tgaccgctac acttgccagc
  i p t r p v a a h - a r r v w w l r a a - p l h l p
1281 gccctagcgc ccgctccttt cgctttcttc ccttccttcc tcgccacggt cgccggcttt ccccgtaag ctctaaatcg
  a p - r p l l s l s s l p f s p r s p a f p v k l - i
1361 gggcatccct ttaggttcc gatttagtgc tttacggcac ctcgaccca aaaacttga ttaggtgat ggttcacgta
  g a s l - g s d l v l y g t s t p k n l i r v m v h v
1441 gtgggccatc gccctgatag acggttttcc gccctttgac gttggagtcc acgttcttta atagtggact cttgttccaa
  v g h r p d r r f f a l - r w s p r s l i v d s c s
1521 actggaacaa cactcaacc tatctcgttc tattcttttg attataagg gattttgggg atttcggcct attggttaaa
  k l e q h s t l s r s i l l i y k g f w g f r p i g -
1601 aaatgagctg atttaacaaa aatttaacgc gaattaatc tgtggaatg gtgtcagtta ggggtgtgaa agtccccagg
  k m s - f n k n l t r i n s v e c v s v r v w k v p r
1681 ctccccagca ggcagaagta tgcaagcat gcactcfaat tagtcagcaa ccagggtgtg aaagtcccc ggtccccag
  l p s r q k y a k h a s q l v s n q v w k v p r l p
1761 caggcagaag tatgcaaagc atgcatctca attagtcagc aaccatagtc ccgccctaa ctccgccat cccgcccta
  s r q k y a k h a s q l v s n h s p a p n s a h p a p
1841 actccgccca gttccgccca ttctccgcc catggtgac taatttttt ttttatgca gaggccagg ccgctctgc
  n s a q f r p f s a p w l t n f f y l c r g r g r l c
1921 ctctgagcta ttccagaagt agtgaggagg cttttttgga ggctaggct tttgcaaaaa gtccccgga gcttgtatat
  l - a i p e v v r r l f w r p r l l q k a p g s l y
2001 ccattttcgg atctgatcag cacgtgttga caattaatca tcggcatagt atatcggcat agtataatac gacaaggtga
  i h f r i - s a r v d n - s s a - y i g i v - y d k v

```

5 APPENDIX

2081 ggaactaac catggccaag ttgaccagt cgttccggt gtcaccgcg cgcgacgtc cggagcggg cgagttctgg
 r n - t m a k l t s a v p v l t a r d v a g a v e f w

2161 accgaccggc tcgggttctc ccgggacttc gtggaggacg acttcgccgg tgtgggtccg gacgacgtga ccctgttcat
 t d r l g f s r d f v e d d f a g v v r d d v t l f

2241 cagcgcggtc caggaccagg tgggtccgga caacaccctg gcctgggtgt gggtgccggg cctggacgag ctgtacccg
 i s a v q d q v v p d n t l a w v w v r g l d e l y a

2321 agtggtcgga ggtcgtgtcc acgaacttcc gggacgcctc cgggccggcc atgaccgaga tcggcgagca gccgtggggg
 e w s e v v s t n f r d a s g p a m t e i g e q p w g

2401 cgggagttcg ccctgcgcca cccggccggc aactgcgtgc acttcgtggc cgaggagcag gactgacacg tgctacgaga
 r e f a l r d p a g n c v h f v a e e q d - h v l r

2481 tttcgattcc accgcgcct tctatgaaag gttgggcttc ggaatcgttt tccgggacgc cggtggatg atcctccagc
 d f d s t a a f y e r l g f g i v f r d a g w m i l q

2561 gcggggatct catgctggag ttcttgccc accccaactt gtttattgca gcttataatg gttacaataa aagcaatagc
 r g d l m l e f f a h p n l f i a a y n g y k - s n s

2641 atcacaatt tcacaataa agcatttttt tcactgcatt ctagtgtggg ttgtccaaa ctcatcaatg tatcttatca
 i t n f t n k a f f s l h s s c g l s k l i n v s y

2721 tgtctgtata ccgtcgacct ctactagag cttggcgtaa tcatggtcat agctgtttcc tgtgtgaaat tgttatccgc
 h v c i p s t s s - s l a - s w s - l f p v - n c y p

2801 tcacaattcc acacaacata cgagccggaa gcataaagt taaagcctgg ggtgcctaat gactgagcta actcacatta
 l t i p h n i r a g s i k c k a w g a - - v s - l t l

2881 attgcgttgc gctcactgcc cgctttccag tcgggaaacc tgcgtgcca gctgcattaa tgaatcgcc aacgcggggg
 i a l r s l p a f q s g n l s c q l h - - i g q r a

2961 gagagcggg ttgcgtattg ggcgtcttc cgcttctcgc ctactgact cgctgcgctc ggtcgttcgg ctgcggcgag
 g r g g l r i g r s s a s s l t d s l r s v v r l r r

3041 cggatcagc tcaactcaag gcgtaatac ggttatccac agaatcaggg gataacgag gaaagaacat gtgagcaaaa
 a v s a h s k a v i r l s t e s g d n a g k n m - a k

3121 ggccagcaaa aggccaggaa ccgtaaaaag gccgcgttgc tggcgttttt ccataggctc cgccccctg acgagcatca
 g q q k a r n r k k a a l l a f f h r l r p p d e h

3201 caaaaaatga cgctcaagtc agaggtggcg aaaccgaca ggactataaa gataaccaggc gtttccccct ggaagctccc
 h k n r r s s q r w r n p t g l - r y q a f p p g s s

3281 tcgtgcgctc tcctgttccg accctgccgc ttaccggata cctgtccgcc tttctccctt cgggaagcgt ggcgttttct
 l v r s p v p t l p l t g y l s a f l p s g s v a l s

3361 caatgctcac gctgtaggta tctcagttcg gtgtaggctg ttgcctcaa gctgggctgt gtgcacgaac cccccgttca
 q c s r c r y l s s v - v v r s k l g c v h e p p v

3441 gcccgaccgc tgcgccttat ccgtaacta tcgtcttgag tccaaccggg taagacagca ctatcgcca ctggcagcag
 q p d r c a l s g n y r l e s n p v r h d l s p l a a

3521 ccaactgtaa caggattagc agagcgaggt atgtaggcgg tgctacagag ttcttgaagt ggtggcctaa ctacggctac
 a t g n r i s r a r y v g g a t e f l k w w p n y g y

3601 actagaagga cagtatttgg tatctgcgct ctgctgaagc cagttacctt cgaaaaaga gttggtagct ctgcatccgg
 t r r t v f g i c a l l k p v t f g k r v g s s - s

3681 caaacaacc accgctgcta gcggtggttt tttgtttgc aagcagcaga ttacgcgag aaaaaagga tctcaagaag
 g k q t t a g s g g f f v c k q q i t r r k k g s q e

3761 atcctttgat ctttctacg gggctgacg ctactggaa cgaaaactca cgtaaggga ttttggtcat gagattatca
 d p l i f s t g s d a q w n e n s r - g i l v m r l s

3841 aaaagatct tcacctagat ctttttaaat taaaaatgaa gtttttaatc aatctaaagt atatatgagt aaacttggtc
 k r i f t - i l l n - k - s f k s i - s i y e - t w

3921 tgacagttac caatgcttaa tcagtgggc acctatctca gcgatctgtc tatttcgttc atccatagtt gctgactcc
 s d s y q c l i s e a p i s a i c l f r s s i v a - l

4001 ccgtcgtgta gataactacg atacgggag gcttaccatc tggccccagt gctgcaatga taccgcgaga cccacgctca
 p v v - i t t i r e g l p s g p s a a m i p r d p r s

4081 ccggtccag atttatcagc aataaaccag ccagccggaa gggccgagcg cagaagtggg cctgcaactt tatccgcctc
 p a p d l s a i n q p a g r a e r r s g p a t l s a

5 APPENDIX

4161 catccagtct attaattggt gccgggaagc tagagtaagt agttcgccag ttaatagttt gcgcaacggt gttgccattg
 s i q s i n c c r e a r v s s s p v n s l r n v v a i

4241 ctacagggcat cgtgggtgtca cgctcgtcgt ttggatggc ttcatcagc tccggttccc aacgatcaag gcgagttaca
 a t g i v v s r s s f g m a s f s s g s q r s r r v t

4321 tgatccccca tgttggtgcaa aaaagcgggt agtcctctcg gtctcctgat cgttgtcaga agtaagttgg ccgcagtggt
 - s p m l c k k a v s s f g p p i v v r s k l a a v

4401 atcaactcatg gttatggcag cactgcataa ttctcttact gtcatgccat ccgtaagatg cttttctgtg actggtgagt
 l s l m v m a a l h n s l t v m p s v r c f s v t g e

4481 actcaaccaa gtcattctga gaatagtgta tgcggcgacc gagttgctct tgcccggcgt caatacggga taataccgg
 y s t k s f - e - c m r r p s c s c p a s i r d n t a

4561 ccacatagca gaactttaaa agtgctcatc attgaaaac gttcttcggg gcgaaaactc tcaaggatct taccgtggt
 p h s r t l k v l i i g k r s s g r k l s r i l p l

4641 gagatccagt tcgatgtaac ccaactgtgc acccaactga tcttcagcat cttttacttt caccagcgtt tctgggtgag
 l r s s s m - p t r a p n - s s a s f t f t s v s g -

4721 caaaaaacagg aaggcaaaat gccgcaaaaa agggaataag ggcgacacgg aaatggtgaa tactcatact cttcctttt
 a k t g r q n a a k k g i r a t r k c - i l l i l f l f

4801 caatattatt gaagcattta tcagggttat tgtctcatga gcggatacat atttgaatgt atttagaaaa ataaacaaat
 q y y - s i y q g y c l m s g y i f e c i - k n k q

4881 aggggttccg cgcacatttc cccgaaaagt gccacctgac gtgcacggat cgggagatct cccgatcccc tatggtcgac
 i g v p r t f p r k v p p d v d g s g d l p i p y g r

4961 tctcagtaca atctgctctg atgccgcata gttaaagccag tatctgctcc ctgcttgtg gttggaggtc gctgagtagt
 l s v q s a l m p h s - a s i c s l l v c w r s l s s

5041 gcgcgagcaa aatttaagct acaacaaggc aaggcttgac cgacaattgc atgaagaatc tgcttagggt taggcgtttt
 a r a k f k l q q g k a - p t i a - r i c l g l g v

5121 gcgctgcttc gcgatgtacg ggccagatat acgcgttgac attgattatt gactagttat taatagtaat caattacggg
 l r c f a m y g p d i r v d i d y - l v i n s n q l r

5201 gtcattagtt catagcccat atatggagtt ccgcgttaca taacttacgg taaatggccc gcctggctga ccgcccacg
 g h - f i a h i w s s a l h n l r - m a r l a d r p t

5281 acccccgcc attgacgtca ataatgacgt atgttcccat agtaacgcca atagggactt tccattgacg tcaatgggtg
 t p a h - r q - - r m f p - - r q - g l s i d v n g

5361 gactatttac ggtaaactgc ccaactggca gtacatcaag tgtatcatat gccaaagtacg cccctattg acgtcaatga
 w t i y g k l p t w q y i k c i i c q v r p l l t s m

5441 cggtaaatgg cccgcctggc attatgcca gtacatgacc ttatgggact ttctacttg gcagtacatc tacgtattag
 t v n g p p g i m p s t - p y g t f l l g s t s t y -

5521 tcatcgctat taccatgggt atgcggtttt ggcagtacat caatgggctg ggatagcgtt ttgactcagc gggatttcca
 s s l l p w - c g f g s t s m g v d s g l t h g d f

5601 agtctccacc ccattgacgt caatgggagt ttgttttggc accaaaatca acgggacttt ccaaaatgct gtaacaactc
 q v s t p l t s m g v c f g t k i n g t f q n v v t t

5681 cgccccattg acgcaaatgg gcggtaggcg tgtacggtgg gaggtctata taagcagagc tctctggcta actagagaac
 p p h - r k w a v g v y g g r s i - a e l s g - l e n

5761 ccactgctta ctggcttacc gaaat**taata cgactcacta tagggagacc** caagctggct agccacc
 p l l t g l s k l i r l t i g r p k l a s h

6 ACKNOWLEDGEMENTS

At this point, I would like to thank all the people who supported me in my work:

- First of all, I wish to thank Prof. Dr. Gabriele Multhoff, for assigning me this interesting research project, for her support and discussions, and last but not least for giving me the opportunity to publish my work.
- I am thankful to my first reviewer Prof. Dr. Friederike Eckardt-Schupp for her support, comments, and constructive suggestions concerning this work, during the last three years.
- I am grateful to my second reviewer Prof. Dr. Elisabeth Weiss and to the professors who reviewed this work.
- Moreover, I would like to thank Prof. Dr. Michael Molls for giving me the opportunity to work in the facilities of the Department of Radiotherapy of the Clinic and Policlinic for Radiotherapy and Radiooncology at the *University Hospital rechts der Isar of the Munich Technical University, Munich, Germany*.
- Additionally, I would like to thank all former and present members of the group of Gabriele Multhoff for supporting me in my project and for providing a stimulating research environment, especially for the constructive discussions in the lab meetings. Namely, I want to thank Dr. Daniela Schilling and Christine Bayer, PhD, for always having an open ear during my doctoral thesis, their good advice and their ideas on problem solving. Dr. Mathias Gehrmann I wish to thank for his support at the beginning of my work, and for his guidance with flow cytometry, fluorescence microscopy and paper writing. I want to thank Eva Kriehuber for her suggestions and ideas concerning these studies. I wish to thank Stefan Stangl and Anna Marwedel for their assistance doing the mouse experiments. Moreover, I want to thank Wolfgang Sievert, who provided CD31 epithelial cells as control. I want to thank Kristin Kuhs for teaching me her expertise in performing paraffin sections. Thank you all, for a great time in such a marvelous team!

6 ACKNOWLEDGEMENTS

- I wish to thank Prof. Graham Pockley for his suggestions during the time he joined our working group. I also want to thank him for the interesting data concerning my grB project, which are being generated by his lab member Gemma Foulds.
- I wish to thank Prof. Dr. Roland Kontermann from the Institute of Cell Biology and Immunology of the University of Stuttgart and his lab members for the cooperation. Especially, I want to thank Kirstin Zettlitz who cloned the *Pichia pastoris*-derived grB. I joined their lab twice for some time to do the cloning and transfection of the HEK293 expression system.
- I am grateful to Dr. Frauke Neff from the Institute of Pathology (Helmholtz Center, Munich, Germany), who invested a lot of time looking over my HE-stained sections and explaining their pathohistology to me.
- I want to thank PD Dr. Johann Kummermehr from the Institute for Radiation Biology of the LMU Munich for his impetus to develop a megacolony model suitable to test grB treatment after radiotherapy.
- Financial support from Helmholtz Center Munich is gratefully acknowledged.
- I am grateful to my parents, siblings, relatives and friends for their belief in me and for their support during my studies.
- Last but not least, I want to thank Dominik for his love and support, also during the ups and downs of this work!

7 CURRICULUM VITAE

Personal Data

Name: Brigitte Tina Maria Doß
Date of birth: July, 12th 1981
Place of birth: Regensburg, Germany

Education

02/07- 06/10

Doctoral student at the Faculty of Biology at the *Ludwig-Maximilians-University, Munich, Germany* (Subject: Generation of an expression system for human granzyme B and analysis of the *in vitro* and *in vivo* efficiency); supervised by Prof. F. Eckardt-Schupp and accomplished at the group of Prof. G. Multhoff (leader of the Clinical Cooperation Group “Innate Immunity in Tumor Biology”, *Helmholtz Center Munich, Neuherberg, Germany* and professor for “Experimental Radiotherapy and Radiobiology”, *University Hospital rechts der Isar of the Technical University, Munich, Germany*).

12/05-09/06

Thesis for Diploma at the *University of Regensburg* (Subject: Proteoglycans in *Hydra vulgaris*); supervised by Prof. R. Deutzmann (Institute for Biochemistry I)

10/01- 09/06

Diploma of biochemistry from the *University of Regensburg*

01/05 - 05/05

Visiting scholar at the *University of Michigan, Ann Arbor, MI, USA*

06/01

„Abitur“ at the *Werner-von-Siemens-Gymnasium Regensburg*

Trainings and Congresses

11/09

Doctoral Students Day, Helmholtz Center Munich, *Neuherberg*

05/09

Women in Radiation Sciences – a Century after Marie Curie, *Neuherberg*

06/09

Seminar “Making Effective Scientific Presentations in English”, *TU Munich, Weihenstephan*

11/08

Doctoral Students Day, Helmholtz Center Munich, *Neuherberg*

03/07

Cellular Therapy, *Regensburg*

01/05

10th Annual Midwest Stress Response and Molecular Chaperone Meeting, *Chicago, IL, USA*

Publications

Doss B.T., Marwedel A.L., Sievert W., Foulds G., Zettlitz K.A., Gehrman M., Kontermann R.E., Pockley A.G., Eckardt-Schupp F. and Multhoff G. The efficiency of human granzyme B in a murine tumor model. *In preparation* (2010)

8 REFERENCES

1. Andoniou, C. E., Coudert, J. D., and Degli-Esposti, M. A. Killers and beyond: NK-cell-mediated control of immune responses. *Eur.J.Immunol.* **38**, 2938-2942 (2008)
2. Arispe, N. and De Maio, A. ATP and ADP modulate a cation channel formed by Hsc70 in acidic phospholipid membranes. *J.Biol.Chem.* **275**, 30839-30843 (2000)
3. Arispe, N., Doh, M., and De Maio, A. Lipid interaction differentiates the constitutive and stress-induced heat shock proteins Hsc70 and Hsp70. *Cell Stress.Chaperones.* **7**, 330-338 (2002)
4. Azuma, Y., Kurusu, Y., Sato, H., Higai, K., and Matsumoto, K. Increased expression of Lewis X and Y antigens on the cell surface and FUT 4 mRNA during granzyme B-induced Jurkat cell apoptosis. *Biol.Pharm.Bull.* **30**, 655-660 (2007)
5. Balkow, S., Kersten, A., Tran, T. T., Stehle, T., Grosse, P., Museteanu, C., Utermohlen, O., Pircher, H., von, W. F., Wallich, R., Mullbacher, A., and Simon, M. M. Concerted action of the FasL/Fas and perforin/granzyme A and B pathways is mandatory for the development of early viral hepatitis but not for recovery from viral infection. *J.Virol.* **75**, 8781-8791 (2001)
6. Barreto, A., Gonzalez, J. M., Kabingu, E., Asea, A., and Fiorentino, S. Stress-induced release of HSC70 from human tumors. *Cell Immunol.* **222**, 97-104 (2003)
7. Bell, J. K., Goetz, D. H., Mahrus, S., Harris, J. L., Fletterick, R. J., and Craik, C. S. The oligomeric structure of human granzyme A is a determinant of its extended substrate specificity. *Nat.Struct.Biol.* **10**, 527-534 (2003)
8. Bird, C. H., Sun, J., Ung, K., Karambalis, D., Whisstock, J. C., Trapani, J. A., and Bird, P. I. Cationic sites on granzyme B contribute to cytotoxicity by promoting its uptake into target cells. *Mol.Cell Biol.* **25**, 7854-7867 (2005)
9. Boivin, W. A., Cooper, D. M., Hiebert, P. R., and Granville, D. J. Intracellular versus extracellular granzyme B in immunity and disease: challenging the dogma. *Lab Invest* **89**, 1195-1220 (2009)
10. Botzler, C., Issels, R., and Multhoff, G. Heat-shock protein 72 cell-surface expression on human lung carcinoma cells is associated with an increased sensitivity to lysis mediated by adherent natural killer cells. *Cancer Immunol.Immunother.* **43**, 226-230 (1996)
11. Botzler, C., Schmidt, J., Luz, A., Jennen, L., Issels, R., and Multhoff, G. Differential Hsp70 plasma-membrane expression on primary human tumors and metastases in mice with severe combined immunodeficiency. *Int.J.Cancer* **77**, 942-948 (1998)
12. Bredholt, T., Dimba, E. A., Hagland, H. R., Wergeland, L., Skavland, J., Fossan, K. O., Tronstad, K. J., Johannessen, A. C., Vintermyr, O. K., and

- Gjertsen, B. T. Camptothecin and khat (*Catha edulis* Forsk.) induced distinct cell death phenotypes involving modulation of c-FLIPL, Mcl-1, procaspase-8 and mitochondrial function in acute myeloid leukemia cell lines. *Mol.Cancer* **8**, 101-(2009)
13. Brocchieri, L., Conway de Macario, E., and Macario, A. hsp70 genes in the human genome: Conservation and differentiation patterns predict a wide array of overlapping and specialized functions. *BMC Evolutionary Biology* **8**, 19-(2008)
 14. Buzza, M. S. and Bird, P. I. Extracellular granzymes: current perspectives. *Biol.Chem.* **387**, 827-837 (2006)
 15. Buzza, M. S., Zamurs, L., Sun, J., Bird, C. H., Smith, A. I., Trapani, J. A., Froelich, C. J., Nice, E. C., and Bird, P. I. Extracellular matrix remodeling by human granzyme B via cleavage of vitronectin, fibronectin, and laminin. *J.Biol.Chem.* **280**, 23549-23558 (2005)
 16. Caputo, A., Parrish, J. C., James, M. N., Powers, J. C., and Bleackley, R. C. Electrostatic reversal of serine proteinase substrate specificity. *Proteins* **35**, 415-424 (1999)
 17. Chang, C. C., Campoli, M., and Ferrone, S. Classical and nonclassical HLA class I antigen and NK Cell-activating ligand changes in malignant cells: current challenges and future directions. *Adv.Cancer Res.* **93**, 189-234 (2005)
 18. Chavez-Galan, L., Arenas-Del Angel, M. C., Zenteno, E., Chavez, R., and Lascurain, R. Cell death mechanisms induced by cytotoxic lymphocytes. *Cell Mol.Immunol.* **6**, 15-25 (2009)
 19. Chowdhury, D. and Lieberman, J. Death by a thousand cuts: granzyme pathways of programmed cell death. *Annu.Rev.Immunol.* **26**, 389-420 (2008)
 20. Ciocca, D. R. and Calderwood, S. K. Heat shock proteins in cancer: diagnostic, prognostic, predictive, and treatment implications. *Cell Stress.Chaperones.* **10**, 86-103 (2005)
 21. Coca, S., Perez-Piqueras, J., Martinez, D., Colmenarejo, A., Saez, M. A., Vallejo, C., Martos, J. A., and Moreno, M. The prognostic significance of intratumoral natural killer cells in patients with colorectal carcinoma. *Cancer* **79**, 2320-2328 (1997)
 22. Cullen, S. P., Brunet, M., and Martin, S. J. Granzymes in cancer and immunity. *Cell Death.Differ.* **17**, 616-623 (2010)
 23. Dalken, B., Giesubel, U., Knauer, S. K., and Wels, W. S. Targeted induction of apoptosis by chimeric granzyme B fusion proteins carrying antibody and growth factor domains for cell recognition. *Cell Death.Differ.* **13**, 576-585 (2006)

24. DeNagel, D. C. and Pierce, S. K. A case for chaperones in antigen processing. *Immunol.Today* **13**, 86-89 (1992)
25. Dertinger, H. and Hulser, D. F. Intercellular communication in spheroids. *Recent Results Cancer Res.* **95**, 67-83 (1984)
26. Dressel, R., Raja, S. M., Honing, S., Seidler, T., Froelich, C. J., von, F. K., and Gunther, E. Granzyme-mediated cytotoxicity does not involve the mannose 6-phosphate receptors on target cells. *J.Biol.Chem.* **279**, 20200-20210 (2004)
27. Falguieres, T., Maak, M., von, W. C., Sarr, M., Sastre, X., Poupon, M. F., Robine, S., Johannes, L., and Janssen, K. P. Human colorectal tumors and metastases express Gb3 and can be targeted by an intestinal pathogen-based delivery tool. *Mol.Cancer Ther.* **7**, 2498-2508 (2008)
28. Farkas, B., Hantschel, M., Magyarlaki, M., Becker, B., Scherer, K., Landthaler, M., Pfister, K., Gehrmann, M., Gross, C., Mackensen, A., and Multhoff, G. Heat shock protein 70 membrane expression and melanoma-associated marker phenotype in primary and metastatic melanoma. *Melanoma Res.* **13**, 147-152 (2003)
29. Ferrarini, M., Heltai, S., Zocchi, M. R., and Rugarli, C. Unusual expression and localization of heat-shock proteins in human tumor cells. *Int.J.Cancer* **51**, 613-619 (1992)
30. Friedrich, J., Ebner, R., and Kunz-Schughart, L. A. Experimental anti-tumor therapy in 3-D: spheroids--old hat or new challenge? *Int.J.Radiat.Biol.* **83**, 849-871 (2007)
31. Friedrich, J., Seidel, C., Ebner, R., and Kunz-Schughart, L. A. Spheroid-based drug screen: considerations and practical approach. *Nat.Protoc.* **4**, 309-324 (2009)
32. Froelich, C. J., Orth, K., and Turbov, J. New paradigm for lymphocyte granule-mediated cytotoxicity. Target cells bind and internalize granzyme B, but an endosomolytic agent is necessary for cytosolic delivery and subsequent apoptosis. *J Biol Chem* **271**, 29073-29079 (1996)
33. Gasser, S., Orsulic, S., Brown, E. J., and Raulet, D. H. The DNA damage pathway regulates innate immune system ligands of the NKG2D receptor. *Nature* **436**, 1186-1190 (2005)
34. Gastpar, R., Gross, C., Roszbacher, L., Ellwart, J., Riegger, J., and Multhoff, G. The cell surface-localized heat shock protein 70 epitope TKD induces migration and cytolytic activity selectively in human NK cells. *J.Immunol.* **172**, 972-980 (2004)
35. Gehrmann, M., Liebisch, G., Schmitz, G., Anderson, R., Steinem, C., De, M. A., Pockley, G., and Multhoff, G. Tumor-specific Hsp70 plasma membrane localization is enabled by the glycosphingolipid Gb3. *PLoS.ONE.* **3**, e1925-(2008a)

36. Gehrman, M., Marienhagen, J., Eichholtz-Wirth, H., Fritz, E., Ellwart, J., Jaattela, M., Zilch, T., and Multhoff, G. Dual function of membrane-bound heat shock protein 70 (Hsp70), Bag-4, and Hsp40: protection against radiation-induced effects and target structure for natural killer cells. *Cell Death.Differ.* **12**, 38-51 (2005)
37. Gehrman, M., Pfister, K., Hutzler, P., Gastpar, R., Margulis, B., and Multhoff, G. Effects of antineoplastic agents on cytoplasmic and membrane-bound heat shock protein 70 (Hsp70) levels. *Biol.Chem.* **383**, 1715-1725 (2002)
38. Gehrman, M., Radons, J., Molls, M., and Multhoff, G. The therapeutic implications of clinically applied modifiers of heat shock protein 70 (Hsp70) expression by tumor cells. *Cell Stress.Chaperones.* **13**, 1-10 (2008b)
39. Giesubel, U., Dalen, B., Mahmud, H., and Wels, W. S. Cell binding, internalization and cytotoxic activity of human granzyme B expressed in the yeast *Pichia pastoris*. *Biochem.J.* **394**, 563-573 (2006)
40. Gross, C., Hansch, D., Gastpar, R., and Multhoff, G. Interaction of heat shock protein 70 peptide with NK cells involves the NK receptor CD94. *Biol.Chem.* **384**, 267-279 (2003a)
41. Gross, C., Koelch, W., and DeMaio, A. Cell surface-bound heat shock protein 70 (Hsp70) mediates perforin-independent apoptosis by specific binding and uptake of granzyme B. *J Biol Chem* **278**, 41173-41181 (2003b)
42. Grujic, M., Braga, T., and Lukinius, A. Serglycin-deficient cytotoxic T lymphocytes display defective secretory granule maturation and granzyme B storage. *J Biol Chem* **280**, 33411-33418 (2005)
43. Hagn, M., Schwesinger, E., Ebel, V., Sontheimer, K., Maier, J., Beyer, T., Syrovets, T., Laumonnier, Y., Fabricius, D., Simmet, T., and Jahrsdorfer, B. Human B cells secrete granzyme B when recognizing viral antigens in the context of the acute phase cytokine IL-21. *J.Immunol.* **183**, 1838-1845 (2009)
44. Hantschel, M., Pfister, K., Jordan, A., Scholz, R., Andreessen, R., Schmitz, G., Schmetzer, H., Hiddemann, W., and Multhoff, G. Hsp70 plasma membrane expression on primary tumor biopsy material and bone marrow of leukemic patients. *Cell Stress.Chaperones.* **5**, 438-442 (2000)
45. Hartl, F. U. Molecular chaperones in cellular protein folding. *Nature* **381**, 571-579 (1996)
46. Havelka, A. M., Berndtsson, M., Olofsson, M. H., Shoshan, M. C., and Linder, S. Mechanisms of action of DNA-damaging anticancer drugs in treatment of carcinomas: is acute apoptosis an "off-target" effect? *Mini.Rev.Med.Chem.* **7**, 1035-1039 (2007)
47. Hirschhaeuser, F., Menne, H., Dittfeld, C., West, J., Mueller-Klieser, W., and Kunz-Schughart, L. A. Multicellular tumor spheroids: An underestimated tool is catching up again. *J.Biotechnol.*(2010)

48. Hoves, S., Trapani, J. A., and Voskoboinik, I. The battlefield of perforin/granzyme cell death pathways. *J.Leukoc.Biol.* **87**, 237-243 (2010)
49. Hsieh, M. H., Patterson, A. E., and Korngold, R. T-cell subsets mediate graft-versus-myeloid leukemia responses via different cytotoxic mechanisms. *Biol.Blood Marrow Transplant.* **6**, 231-240 (2000)
50. Kaiserman, D., Bird, C. H., Sun, J., Matthews, A., Ung, K., Whisstock, J. C., Thompson, P. E., Trapani, J. A., and Bird, P. I. The major human and mouse granzymes are structurally and functionally divergent. *J.Cell Biol.* **175**, 619-630 (2006)
51. Kampinga, H. H., Hageman, J., Vos, M. J., Kubota, H., Tanguay, R. M., Bruford, E. A., Cheetham, M. E., Chen, B., and Hightower, L. E. Guidelines for the nomenclature of the human heat shock proteins. *Cell Stress.Chaperones.* **14**, 105-111 (2009)
52. Keefe, D., Shi, L., and Feske, S. Perforin triggers a plasma membrane-repair response that facilitates CTL induction of apoptosis. *Immunity* **23**, 249-262 (2005)
53. Kiessling, R., Klein, E., Pross, H., and Wigzell, H. "Natural" killer cells in the mouse. II. Cytotoxic cells with specificity for mouse Moloney leukemia cells. Characteristics of the killer cell. *Eur.J.Immunol.* **5**, 117-121 (1975a)
54. Kiessling, R., Klein, E., and Wigzell, H. "Natural" killer cells in the mouse. I. Cytotoxic cells with specificity for mouse Moloney leukemia cells. Specificity and distribution according to genotype. *Eur.J.Immunol.* **5**, 112-117 (1975b)
55. Krause, S. W., Gastpar, R., Andreesen, R., Gross, C., Ullrich, H., Thonigs, G., Pfister, K., and Multhoff, G. Treatment of colon and lung cancer patients with ex vivo heat shock protein 70-peptide-activated, autologous natural killer cells: a clinical phase i trial. *Clin.Cancer Res.* **10**, 3699-3707 (2004)
56. Kummermehr, J., Malinen, E., Freykowski, S., Sund, M., and Trott, K. R. The influence of autologous tumor fibroblasts on the radiosensitivity of squamous cell carcinoma megacolonies. *Int.J.Radiat.Oncol.Biol.Phys.* **50**, 229-237 (2001)
57. Kunz-Schughart, L. A. Multicellular tumor spheroids: intermediates between monolayer culture and in vivo tumor. *Cell Biol.Int.* **23**, 157-161 (1999)
58. Kurschus, F. C., Bruno, R., Fellows, E., Falk, C. S., and Jenne, D. E. Membrane receptors are not required to deliver granzyme B during killer cell attack. *Blood* **105**, 2049-2058 (2005)
59. Kurschus, F. C., Kleinschmidt, M., Fellows, E., Dornmair, K., Rudolph, R., Lilie, H., and Jenne, D. E. Killing of target cells by redirected granzyme B in the absence of perforin. *FEBS Lett.* **562**, 87-92 (2004)

60. Laemmli, U. K. Cleavage of structural proteins during the assembly of the head of bacteriophage T4. *Nature* **227**, 680-685 (1970)
61. Lanier, L. L. Up on the tightrope: natural killer cell activation and inhibition. *Nat.Immunol.* **9**, 495-502 (2008)
62. Lin, R. Z. and Chang, H. Y. Recent advances in three-dimensional multicellular spheroid culture for biomedical research. *Biotechnol.J.* **3**, 1172-1184 (2008)
63. Ljunggren, H. G. and Karre, K. In search of the 'missing self': MHC molecules and NK cell recognition. *Immunol.Today* **11**, 237-244 (1990)
64. Loeb, C. R., Harris, J. L., and Craik, C. S. Granzyme B proteolyzes receptors important to proliferation and survival, tipping the balance toward apoptosis. *J Biol Chem* **281**, 28326-28335 (2006)
65. MacDonald, G., Shi, L., Vande, V. C., Lieberman, J., and Greenberg, A. H. Mitochondria-dependent and -independent regulation of Granzyme B-induced apoptosis. *J.Exp.Med.* **189**, 131-144 (1999)
66. Mahrus, S., Kisiel, W., and Craik, C. S. Granzyme M is a regulatory protease that inactivates proteinase inhibitor 9, an endogenous inhibitor of granzyme B. *J Biol Chem* **279**, 54275-54282 (2004)
67. Mambula, S. S. and Calderwood, S. K. Heat shock protein 70 is secreted from tumor cells by a nonclassical pathway involving lysosomal endosomes. *J.Immunol.* **177**, 7849-7857 (2006)
68. Medema, J. P., de, J. J., Peltenburg, L. T., Verdegaal, E. M., Gorter, A., Bres, S. A., Franken, K. L., Hahne, M., Albar, J. P., Melief, C. J., and Offringa, R. Blockade of the granzyme B/perforin pathway through overexpression of the serine protease inhibitor PI-9/SPI-6 constitutes a mechanism for immune escape by tumors. *Proc.Natl.Acad.Sci.U.S.A* **98**, 11515-11520 (2001)
69. Metkar, S. S., Mena, C., Pardo, J., Wang, B., Wallich, R., Freudenberg, M., Kim, S., Raja, S. M., Shi, L., Simon, M. M., and Froelich, C. J. Human and mouse granzyme A induce a proinflammatory cytokine response. *Immunity.* **29**, 720-733 (2008)
70. Motyka, B., Korbitt, G., Pinkoski, M. J., Heibei, J. A., Caputo, A., Hobman, M., Barry, M., Shostak, I., Sawchuk, T., Holmes, C. F., Gauldie, J., and Bleackley, R. C. Mannose 6-phosphate/insulin-like growth factor II receptor is a death receptor for granzyme B during cytotoxic T cell-induced apoptosis. *Cell* **103**, 491-500 (2000)
71. Multhoff, G. Heat shock protein 72 (HSP72), a hyperthermia-inducible immunogenic determinant on leukemic K562 and Ewing's sarcoma cells. *Int.J.Hyperthermia* **13**, 39-48 (1997)

72. Multhoff, G., Botzler, C., Jennen, L., Schmidt, J., Ellwart, J., and Issels, R. Heat shock protein 72 on tumor cells: a recognition structure for natural killer cells. *J.Immunol.* **158**, 4341-4350 (1997)
73. Multhoff, G., Botzler, C., Wiesnet, M., Eissner, G., and Issels, R. CD3- large granular lymphocytes recognize a heat-inducible immunogenic determinant associated with the 72-kD heat shock protein on human sarcoma cells. *Blood* **86**, 1374-1382 (1995a)
74. Multhoff, G., Botzler, C., Wiesnet, M., Muller, E., Meier, T., Wilmanns, W., and Issels, R. D. A stress-inducible 72-kDa heat-shock protein (HSP72) is expressed on the surface of human tumor cells, but not on normal cells. *Int.J.Cancer* **61**, 272-279 (1995b)
75. Multhoff, G., Mizzen, L., Winchester, C. C., Milner, C. M., Wenk, S., Eissner, G., Kampinga, H. H., Laumbacher, B., and Johnson, J. Heat shock protein 70 (Hsp70) stimulates proliferation and cytolytic activity of natural killer cells. *Exp.Hematol.* **27**, 1627-1636 (1999)
76. Ovejera, A. A., Houchens, D. P., and Barker, A. D. Chemotherapy of human tumor xenografts in genetically athymic mice. *Ann.Clin.Lab Sci.* **8**, 50-56 (1978)
77. Pardo, J., Aguilo, J. I., Anel, A., Martin, P., Joeckel, L., Borner, C., Wallich, R., Mullbacher, A., Froelich, C. J., and Simon, M. M. The biology of cytotoxic cell granule exocytosis pathway: granzymes have evolved to induce cell death and inflammation. *Microbes.Infect.* **11**, 452-459 (2009)
78. Pardo, J., Wallich, R., Ebnet, K., Iden, S., Zentgraf, H., Martin, P., Ekiciler, A., Prins, A., Mullbacher, A., Huber, M., and Simon, M. M. Granzyme B is expressed in mouse mast cells in vivo and in vitro and causes delayed cell death independent of perforin. *Cell Death.Differ.* **14**, 1768-1779 (2007)
79. Patury, S., Miyata, Y., and Gestwicki, J. E. Pharmacological targeting of the Hsp70 chaperone. *Curr.Top.Med.Chem.* **9**, 1337-1351 (2009)
80. Pinkoski, M. J., Hobman, M., Heibein, J. A., Tomaselli, K., Li, F., Seth, P., Froelich, C. J., and Bleackley, R. C. Entry and trafficking of granzyme B in target cells during granzyme B-perforin-mediated apoptosis. *Blood* **92**, 1044-1054 (1998)
81. Pipkin, M. E. and Lieberman, J. Delivering the kiss of death: progress on understanding how perforin works. *Curr Opin Immunol* **19**, 301-308 (2007)
82. Poli, A., Michel, T., Theresine, M., Andres, E., Hentges, F., and Zimmer, J. CD56bright natural killer (NK) cells: an important NK cell subset. *Immunology* **126**, 458-465 (2009)
83. Prakash, M. D., Bird, C. H., and Bird, P. I. Active and zymogen forms of granzyme B are constitutively released from cytotoxic lymphocytes in the

- absence of target cell engagement. *Immunol.Cell Biol.* **87**, 249-254 (2009)
84. Ritossa, F. M. A new puffing pattern induced by temperature shock and DNP in *Drosophila*. *Experientia* **18**, 571-573 (1962)
 85. Robertson, M. J. and Ritz, J. Biology and clinical relevance of human natural killer cells. *Blood* **76**, 2421-2438 (1990)
 86. Sauer, H., Pratsch, L., and Tschopp, J. Functional size of complement and perforin pores compared by confocal laser scanning microscopy and fluorescence microphotolysis. *Biochim Biophys Acta* **1063**, 137-146 (1991)
 87. Schilling, D., Gehrman, M., Steinem, C., De, M. A., Pockley, A. G., Abend, M., Molls, M., and Multhoff, G. Binding of heat shock protein 70 to extracellular phosphatidylserine promotes killing of normoxic and hypoxic tumor cells. *FASEB J.* **23**, 2467-2477 (2009)
 88. Shi, L., Keefe, D., Durand, E., Feng, H., Zhang, D., and Lieberman, J. Granzyme B binds to target cells mostly by charge and must be added at the same time as perforin to trigger apoptosis. *J.Immunol.* **174**, 5456-5461 (2005)
 89. Spaeny-Dekking, E. H., Hanna, W. L., and Wolbink, A. M. Extracellular granzymes A and B in humans: detection of native species during CTL responses in vitro and in vivo. *J Immunol* **160**, 3610-3616 (1998)
 90. Sun, J., Bird, C. H., Buzza, M. S., McKee, K. E., Whisstock, J. C., and Bird, P. I. Expression and purification of recombinant human granzyme B from *Pichia pastoris*. *Biochem.Biophys.Res.Comm.* **261**, 251-255 (1999)
 91. Sun, J., Bird, C. H., and Sutton, V. A cytosolic granzyme B inhibitor related to the viral apoptotic regulator cytokine response modifier A is present in cytotoxic lymphocytes. *J Biol Chem* **271**, 27802-27809 (1996)
 92. Sun, J., Ooms, L., Bird, C. H., Sutton, V. R., Trapani, J. A., and Bird, P. I. A new family of 10 murine ovalbumin serpins includes two homologs of proteinase inhibitor 8 and two homologs of the granzyme B inhibitor (proteinase inhibitor 9). *J.Biol.Chem.* **272**, 15434-15441 (1997)
 93. Sun, J. C., Beilke, J. N., and Lanier, L. L. Adaptive immune features of natural killer cells. *Nature* **457**, 557-561 (2009)
 94. Sutherland, R. M. Cell and environment interactions in tumor microregions: the multicell spheroid model. *Science* **240**, 177-184 (1988)
 95. Tamura, Y., Tsuboi, N., Sato, N., and Kikuchi, K. 70 kDa heat shock cognate protein is a transformation-associated antigen and a possible target for the host's anti-tumor immunity. *J.Immunol.* **151**, 5516-5524 (1993)

96. Tarnawski, R., Kummermehr, J., and Trott, K. R. The radiosensitivity of recurrent clones of an irradiated murine squamous cell carcinoma in the in vitro megacolony system. *Radiother.Oncol.* **46**, 209-214 (1998)
97. Trapani, J. A., Browne, K. A., Smyth, M. J., and Jans, D. A. Localization of granzyme B in the nucleus. A putative role in the mechanism of cytotoxic lymphocyte-mediated apoptosis. *J.Biol.Chem.* **271**, 4127-4133 (1996)
98. Trapani, J. A., Klein, J. L., White, P. C., and Dupont, B. Molecular cloning of an inducible serine esterase gene from human cytotoxic lymphocytes. *Proc.Natl.Acad.Sci.U.S.A* **85**, 6924-6928 (1988)
99. Trapani, J. A., Smyth, M. J., Apostolidis, V. A., Dawson, M., and Browne, K. A. Granule serine proteases are normal nuclear constituents of natural killer cells. *J.Biol.Chem.* **269**, 18359-18365 (1994)
100. Tschopp, J., Masson, D., and Schafer, S. Inhibition of the lytic activity of perforin by lipoproteins. *J Immunol* **137**, 1950-1953 (1986)
101. Veugelers, K., Motyka, B., and Goping, I. S. Granule-mediated killing by granzyme B and perforin requires a mannose 6-phosphate receptor and is augmented by cell surface heparan sulfate. *Mol Biol Cell* **17**, 623-633 (2006)
102. Vivier, E., Tomasello, E., Baratin, M., Walzer, T., and Ugolini, S. Functions of natural killer cells. *Nat.Immunol.* **9**, 503-510 (2008)
103. Wang, M., Bronte, V., Chen, P. W., Gritz, L., Panicali, D., Rosenberg, S. A., and Restifo, N. P. Active immunotherapy of cancer with a nonreplicating recombinant fowlpox virus encoding a model tumor-associated antigen. *J.Immunol.* **154**, 4685-4692 (1995)
104. Werle, M. and Bernkop-Schnurch, A. Strategies to improve plasma half life time of peptide and protein drugs. *Amino.Acids* **30**, 351-367 (2006)
105. Xia, Z., Kam, C. M., Huang, C., Powers, J. C., Mandle, R. J., Stevens, R. L., and Lieberman, J. Expression and purification of enzymatically active recombinant granzyme B in a baculovirus system. *Biochem.Biophys.Res.Commun.* **243**, 384-389 (1998)
106. Yodoi, J., Teshigawara, K., Nikaido, T., Fukui, K., Noma, T., Honjo, T., Takigawa, M., Sasaki, M., Minato, N., Tsudo, M., and . TCGF (IL 2)-receptor inducing factor(s). I. Regulation of IL 2 receptor on a natural killer-like cell line (YT cells). *J.Immunol.* **134**, 1623-1630 (1985)